UNIFORMED SERVICES UNIVERSITY OF THE HEALTH SCIENCES
F. EDWARD HÉBERT SCHOOL OF MEDICINE
4301 JONES BRIDGE ROAD
BETHESDA, MARYLAND 20814-4799

December 11, 2006

BIOMEDICAL GRADUATE PROGRAMS

Ph.D. Degrees

Interdisciplinary
-Emerging Infectious Diseases
-Molecular & Cell Biology
-Neuroscience

Departmental
-Clinical Psychology
-Environmental Health Sciences
-Medical Psychology
-Medical Zoology
-Pathology

Doctor of Public Health (Dr.P.H.)

Physician Scientist (MD/Ph.D.)

Master of Science Degrees

-Molecular & Cell Biology
-Public Health

Masters Degrees

-Comparative Medicine
-Military Medical History
-Public Health
-Tropical Medicine & Hygiene

Graduate Education Office
Dr. Eleanor S. Metcalf, Associate Dean
Janet Anastasi, Program Coordinator
Tanice Acevedo, Education Technician

Web Site
www.usuhs.mil/geo/gradpgm_index.html

E-mail Address
graduateprogram@usuhs.mil

Phone Numbers
Commercial: 301-295-9474
Toll Free: 800-772-1747
DSN: 295-9474
FAX: 301-295-6772

APPROVAL SHEET

Title of Dissertation: "Identification of the Regions of Cytotoxic Necrotizing Factor Type 1 Responsible for Receptor Binding and Enzymatic Activity"

Name of Candidate: Beth McNichol
Doctor of Philosophy Degree
5 February 2007

Dissertation and Abstract Approved:

Ann Jerse — 2/5/07
Ann Jerse, Ph.D. — Date
Department of Microbiology & Immunology
Committee Chairperson

Alison O'Brien — 2/5/07
Alison O'Brien, Ph.D. — Date
Department of Microbiology & Immunology
Committee Member

Theresa M Dunn — 2/5/07
Theresa Dunn, Ph.D. — Date
Department of Biochemistry
Committee Member

Guangong Ji — 2/5/07
Guangong Ji, Ph.D. — Date
Department of Microbiology & Immunology
Committee Member

Drusilla Burns — 2/5/07
Drusilla Burns, Ph.D. — Date
FDA/CBER
Committee Member

UNIFORMED SERVICES UNIVERSITY OF THE HEALTH SCIENCES
F. EDWARD HÉBERT SCHOOL OF MEDICINE
4301 JONES BRIDGE ROAD
BETHESDA, MARYLAND 20814-4799

December 11, 2006

BIOMEDICAL GRADUATE PROGRAMS

Ph.D. Degrees

Interdisciplinary
-Emerging Infectious Diseases
-Molecular & Cell Biology
-Neuroscience

Departmental
-Clinical Psychology
-Environmental Health Sciences
-Medical Psychology
-Medical Zoology
-Pathology

Doctor of Public Health (Dr.P.H.)

Physician Scientist (MD/Ph.D.)

Master of Science Degrees

-Molecular & Cell Biology
-Public Health

Masters Degrees

-Comparative Medicine
-Military Medical History
-Public Health
-Tropical Medicine & Hygiene

Graduate Education Office
Dr. Eleanor S. Metcalf, Associate Dean
Janet Anastasi, Program Coordinator
Tanice Acevedo, Education Technician

Web Site
www.usuhs.mil/geo/gradpgm_index.html

E-mail Address
graduateprogram@usuhs.mil

Phone Numbers
Commercial: 301-295-9474
Toll Free: 800-772-1747
DSN: 295-9474
FAX: 301-295-6772

FINAL EXAMINATION FOR THE DEGREE
OF DOCTOR OF PHILOSOPHY

Name of Student: Beth McNichol

Date of Examination: 5 February 2007

Time: 10:00

Place: Lecture Room E

DECISION OF EXAMINATION COMMITTEE MEMBERS:

	PASS	FAIL
Ann Jerse, Ph.D. Department of Microbiology & Immunology Chairperson	X	___
Alison O'Brien, Ph.D. Department of Microbiology & Immunology Major Advisor	X	___
Teresa Dunn, Ph.D. Department of Biochemisry Member	X	___
Guangyong Ji, Ph.D. Department of Microbiology & Immunology Member	X	___
Drusilla Burns, Ph.D. FDA/CBER Member	X	___

The author hereby certifies that the use of any copyrighted material in the thesis manuscript entitled:

"Identification of the Regions of Cytotoxic Necrotizing Factor Type 1 Responsible for Receptor Binding and Enzymatic Activity"

beyond brief excerpts is with permission of the copyright owner, and will save and hold harmless the Uniformed Services University of the Health Sciences from any damage which may arise from such copyright violations.

Beth Ann McNichol

Department of Microbiology and Immunology

Uniformed Services University of the Health Sciences

Abstract

Title of Dissertation:

Identification of the Regions of Cytotoxic Necrotizing Factor Type 1 Responsible for Receptor Binding and Enzymatic Activity

Beth Ann McNichol

Doctor of Philosophy, 2007

Thesis directed by:

Alison D. O'Brien, Ph.D.

Professor and Chair, Department of Microbiology and Immunology

Uropathogenic *Escherichia coli* (UPEC) cause the majority of uncomplicated urinary tract infections (UTIs) in the United States. UPEC express a number of virulence factors, including type 1 and P fimbriae, hemolysin, and Cytotoxic Necrotizing Factor type 1 (CNF1) that are associated with the capacity of the organism to colonize the human urinary tract and cause cystitis and/or pyelonephritis. CNF1 is a cytoplasmic polypeptide toxin that is composed of a reputed N-terminal binding domain and a C-terminal enzymatic domain. A putative transmembrane domain, considered to be responsible for translocation of the toxin into eukaryotic cells, is contained within the N-terminal half of the molecule. CNF1 belongs to the family of Rho-activating toxins and

deamidates glutamine-63 (Gln^{63}) of RhoA and Gln^{61} of Rac1 and Cdc42. These deamidation reactions lead to the constitutive activation of the Rho GTPases and the subsequent upregulation of downstream cellular effectors of those molecules. The CNF1-mediated effects on eukaryotic cells result from specific binding to the target cell, translocation across the host membrane, trafficking within the cytoplasm, and enzymatic modification of the GTPase substrates. The regions within the toxin responsible for each step in intoxication of the host cell are only roughly delineated; in fact, only the C-terminus of CNF1 has been crystallized. In this study, I sought to more precisely define the area of CNF1 that is responsible for its enzymatic activities as well as the region of the toxin that binds to its receptor, laminin receptor precursor protein (LRP).

CNF1 has homology with several other toxins that include dermonecrotic toxin (DNT) of *Bordetella spp*. CNF1 and DNT share 27% identity and 13% similarity in the C-terminal enzymatic domains. First, I tested a set of CNF1/DNT hybrid toxins in several phenotypic assays to determine the regions of the toxins that control their phenotypes. I found that a 100 amino acid stretch of DNT (aa 1250-1314) with the highest homology to CNF1 is sufficient to cause a DNT-like phenotype (i.e., no multinucleation of HEp-2 cells, binucleation of Swiss 3T3 cells) when that segment was incorporated into a CNF1 backbone. Next, I narrowed this DNT-signature activity down to the amino acid level. I hypothesized that Lys^{1310} in the catalytic triad of DNT, but not CNF1, contributed to its specific phenotypes for HEp-2 and Swiss 3T3 cells, its enzymatic substrate preference (RhoA=Rac1>Cdc42) and its predilection to transglutaminate rather than deamidate Rho GTPases. Therefore, I made site-specific mutations in CNF (T884K) and DNT (K1310T) and found that that when lysine was

present instead of threonine at position 884 of CNF1, this mutant toxin generated a DNT-like phenotype, as defined above. Conversely, when a threonine residue was used in place of the lysine in DNT, the resultant toxin evoked a CNF1-like phenotype on cells, i.e., multinucleation of HEp-2 cells and binucleation and cytotoxicity of Swiss 3T3 cells. The lysine residue also appeared to be important for the enzymatic activity of DNT; the DNT site-directed mutant lost its capacity to deamidate Rho GTPases at wild-type levels. Similarly, while replacement of Lys^{1310} with a threonine led to less efficient transglutamination of RhoA by DNT K1310T, this toxin could still transglutaminate RhoA over time. This latter finding suggested that this Lys^{1310} residue in DNT does not determine the enzymatic preference of DNT for transglutamination.

The second facet of this project was to identify the region(s) of CNF1 that binds to its receptor, laminin receptor precursor protein. To accomplish my objective, I used a series of CNF1 truncated mutants and a newly-developed LRP binding assay. I concluded that CNF1 has two binding domains, one within aa 135 to 272 and a second beyond aa 546 based on several observations. First, binding of CNF1 and truncated mutants with these domains to HEp-2 cells was inhibited by the addition of exogenous LRP. Second, such adherence was also inhibited by two previously identified neutralizing anti-CNF monoclonal antibodies, BF8 and NG8. The epitopes of these antibodies were previously mapped to within aa 135-164 and 683-780, respectively. I also observed that addition of exogenous LRP prior to application of CNF1 and its truncated mutants did not result in absolute blockage of binding. This finding suggests that there is an additional receptor/co-receptor for CNF1.

Taken together, I have determined that the substitution of a 100 amino acid region of CNF1 with DNT leads to a change in phenotype on different eukaryotic cell lines. Second, substitution of lysine for threonine, or vice versa, in CNF1 or DNT results in switching of the phenotype of the parent toxin to that of the other. Finally, CNF1 contains two regions that bind LRP, amino acids 135-272 and a large region beyond amino acid 546.

Identification of the Regions of Cytotoxic Necrotizing Factor Type 1 Responsible for Receptor Binding and Enzymatic Activity

By

Beth Ann McNichol

Dissertation submitted to the Faculty of the Department of Microbiology and Immunology, Graduate Program in Emerging Infectious Diseases of the Uniformed Services University of the Health Sciences

F. Edward Hèbert School of Medicine

in partial fulfillment of the

requirements for the degree of

Doctor of Philosophy 2007

This work is dedicated to the two most important people in my life, my husband, Timothy McNichol, and my mother, Sandra Wrable. Their love, support and understanding through the years is what kept me going even when I thought things were impossible. I could not have done this without either of you.

Acknowledgments

I would like to thank the Department of Defense and the Emerging Infectious Diseases graduate program of the Uniformed Services University of the Health Sciences for accepting me into the program. This work would not have been possible without the support and guidance of the following people:

- Dr. Alison O'Brien, who allowed me to work in her laboratory and provided guidance and moral support both professionally and personally.
- The members of the O'Brien lab, past and present for their support and kindness. Most especially, I want to thank the following people:
    - Dr. Susan Rasmussen, who helped me troubleshoot, listened to me complain, let me cry on her shoulder and, most importantly, was a friend in every sense of the word.
    - Humberto Carvalho, who maintained tissue culture cells, assisted me in purifying copious amounts of toxins, and helped me with various experiments too numerous to mention! I appreciate all his help and his friendship.
    - Dr. James Sinclair, who allowed me the use of the FPLC equipment in his laboratory, drew hypothetical ribbon diagrams and provided me with biochemical advice when I needed it.
    - The CNF1 group—Susan, Kerian and Yarery—who listened, offered suggestions and gave support when things weren't going right.

  - Dr. Karen Meysick, who got me started on the project and was always willing to provide advice and insight.
- My thesis committee: Dr. Ann Jerse, Dr. Alison O'Brien, Dr. Teresa Dunn, Dr. Guangyong Ji and Dr. Drusilla Burns, who provided guidance, suggestions and support throughout the thesis process.
- My family, especially my mom, who would not let me give up when the going got tough. She has always believed in me even when I didn't believe in myself.
- My friends, especially Jennifer Wedgwood, who started the program with me, became my study partner, and then the sister I never had. Our endless conversations on the phone helped me get through the good and the bad times.
- Last, but most important, I want to thank my husband Timothy McNichol. I would not have been able to get through this without his love, support, patience and understanding. He provided the roof over our heads and the food that we ate. I could not have done this without him—he is my rock and my foundation.

Table of Contents

Table of Figures

Table of Tables

CHAPTER 1: INTRODUCTION

Preface

Uropathogenic *Escherichia coli* (UPEC) are the most common cause of uncomplicated urinary tract infections (UTI). Primary and recurrent infections in women and men can lead to infections of the bladder (cystitis) or kidneys (pyelonephritis), and the prostate (prostatitis), respectively. A majority of women will have at least 1 UTI in their lifetime, and 40% of these individuals are susceptible to recurrent infections. Most of the current microbiological research on how UPEC cause disease is directed toward the virulence factors that these bacteria use to establish infection and persistence. Examples of these microbial components include several classes of fimbriae, hemolysin, and Cytotoxic Necrotizing Factor type 1 (CNF1). Previous studies on CNF1 have concentrated on the role of this toxin in urinary tract infections, the method of secretion of the toxin from the bacteria, how the structure of CNF1 relates to its defined activities, and the interaction of the toxin with its eukaryotic cellular substrates. In this dissertation the enzymatic and cell-binding functions of CNF1 are the focus of evaluation. As a background to these experiments, an introduction is provided that is separated into several sections. In the first section, an overview of urinary tract infections is given in which the incidence of infection and the clinical implications associated with UTI are given. In the second part, the virulence factors associated with uropathogenic *E. coli* are described. In the third segment, characteristics of CNF1 and how the toxin may contribute to the pathogenesis of UPEC infection are discussed. This portion also includes overviews on the association of CNF1 with hemolysin, details of previous structure/function studies, as well as a synopsis of Rho GTPases, the cellular targets of CNF1. Additionally, the mode of action of CNF1 is described. In the fourth component,

the toxins that are related to CNF1 are presented with emphasis on the dermonecrotic toxin (DNT) of *Bordetella spp*. In this segment of the thesis, the mode of action of DNT is compared to that of CNF1. Finally, in the last section of the introduction, the specific aims and hypothesis of this dissertation are presented.

Urinary Tract Infections

Urinary tract infections (UTI) can be defined in at least three ways. First, UTIs can be classified by the site of infection [i.e. cystitis (bladder), pyelonephritis (kidney), prostatitis (prostate); (Nicolle, 2002)]. Second, UTIs can be categorized as uncomplicated, such as when the infected individual has a normal genitourinary tract, or complicated, such as when the infected individual has a genitourinary tract with structural abnormalities or an in-dwelling urinary catheter (Foxman, 2002). Third, UTIs can be grouped as asymptomatic or symptomatic with a range of possible manifestations from irritation when voiding to life-threatening sepsis and even death (Foxman, 2002). These clinical manifestations will be discussed in greater detail in a subsequent section.

Epidemiology

Urinary tract infections are considered to be the most common type of bacterial infection in the United States (Nicolle, 2001; Warren, 1996). In 1997 alone, UTIs were responsible for an estimated 7-8 million visits to physicians and approximately 1 million visits to hospital emergency rooms, resulting in roughly 100,000 hospitalizations. The precise incidence of UTIs is difficult to determine because these common infections are not reportable diseases (Foxman, 2002). More recent data show an upward trend both in number of visits to doctors as well as trips to the emergency room. From 1999-2000, the number of cases of UTI or cystitis treated by physicians in their offices increased from 7.9 million to 9.1 million. Similarly, hospital visits were on the rise with 1.78 million patients with UTIs treated in 2001, compared to 1.68 million cases in 2000 (U.S. Department of Health and Human Services, 2004). The economic burden placed on the

United States due to UTIs is considerable. Cases of uncomplicated cystitis result in $1 billion of direct health care costs annually as well as additional indirect costs, while treatment of patients with pyelonephritis costs $175 million per year (Russo and Johnson, 2003).

Acute, uncomplicated UTIs are more likely to occur in women than men, with otherwise healthy women experiencing 90% of such episodes (Warren, 1996); the variation in incidence of infection between women and men is largely due to their anatomical differences. The incidence is highest in young women in the 20-40 year age range who are sexually active and second highest in postmenopausal women (Nicolle, 2001). Current estimates state that 1 out of 3 women will have at least 1 diagnosed UTI before 24 years of age and that 40-50% of all women will have at least 1 UTI in their lifetime (Foxman, 2002).

Besides age and hormonal status, a number of genetic, biological, and behavioral risk factors contribute to the increased susceptibility of a subset of women in developed countries to UTIs. Examples of risk factors include family history of UTI, congenital abnormalities, spermicide use, frequent sexual intercourse, and use of antimicrobials for other bacterial infections (Foxman, 2002; Nicolle, 2001; U.S. Department of Health and Human Services, 2003; Zhang and Foxman, 2003). Furthermore, in addition to a greater susceptibility of women to UTI, women are more likely than men to suffer from recurrent urinary tract infections (RUTI). Roughly 30% of women will have RUTI within 6 months to 1 year after the initial episode (Warren, 1996). The underlying basis for these repeat occurrences could be relapse in which the same strain causes another infection after antibiotic treatment is completed or re-infection in which a different strain causes

the UTI (Foxman, 2002). About 80% of RUTIs are considered to be due to re-infection rather than relapse (Franco, 2005).

Clinical features of urinary tract infections

Urinary tract infections may present in a number of ways, and these diverse manifestations may pose difficulties in proper diagnosis and treatment. Because the urinary tract is a sterile environment, any number of pathogenic organisms detected constitutes a UTI (Nicolle, 2001; Zhang and Foxman, 2003). Bacteriuria, defined as 10^5 CFU/ml of urine, is a good indication of UTI, even though more than one-third of symptomatic women have bacterial counts as low as 100 CFU/ml (Orenstein and Wong, 1999). The majority of bacteria enter the urinary tract through the ascending route rather than the blood-borne route. Bacteria can ascend from the periurethral area and into the bladder by way of the urethra (Figure 1). From the bladder, the organisms can move through the ureters to the kidneys (Warren, 1996).

There are generally three clinical manifestations of UTI. These are asymptomatic bacteriuria, cystitis, and acute pyelonephritis (Warren, 1996; Zhang and Foxman, 2003). Asymptomatic bacteriuria is defined as such in an individual who has two consecutive urine cultures with greater than 10^5 CFU/ml but no overt symptoms (Warren, 1996). Cystitis and pyelonephritis both typically present with symptoms, but pyelonephritis is the more serious infection and can cause significant morbidity and even mortality (Zhang and Foxman, 2003). Symptoms of cystitis include dysuria, or painful urination, a

Figure 1: Diagram of the Normal Adult Urinary Tract

Uropathogenic *Escherichia coli* can enter the urinary tract through the urethra and can ascend to the bladder and cause cystitis. From there, bacteria can continue on to infect the kidneys via the ureters. Infection of the kidneys is designated pyelonephritis. Finally, UPEC can infect the bloodstream by exploiting the blood vasculature of the kidneys. In otherwise healthy men, bacteria can also infect the prostate (not shown) and cause acute prostatitis.

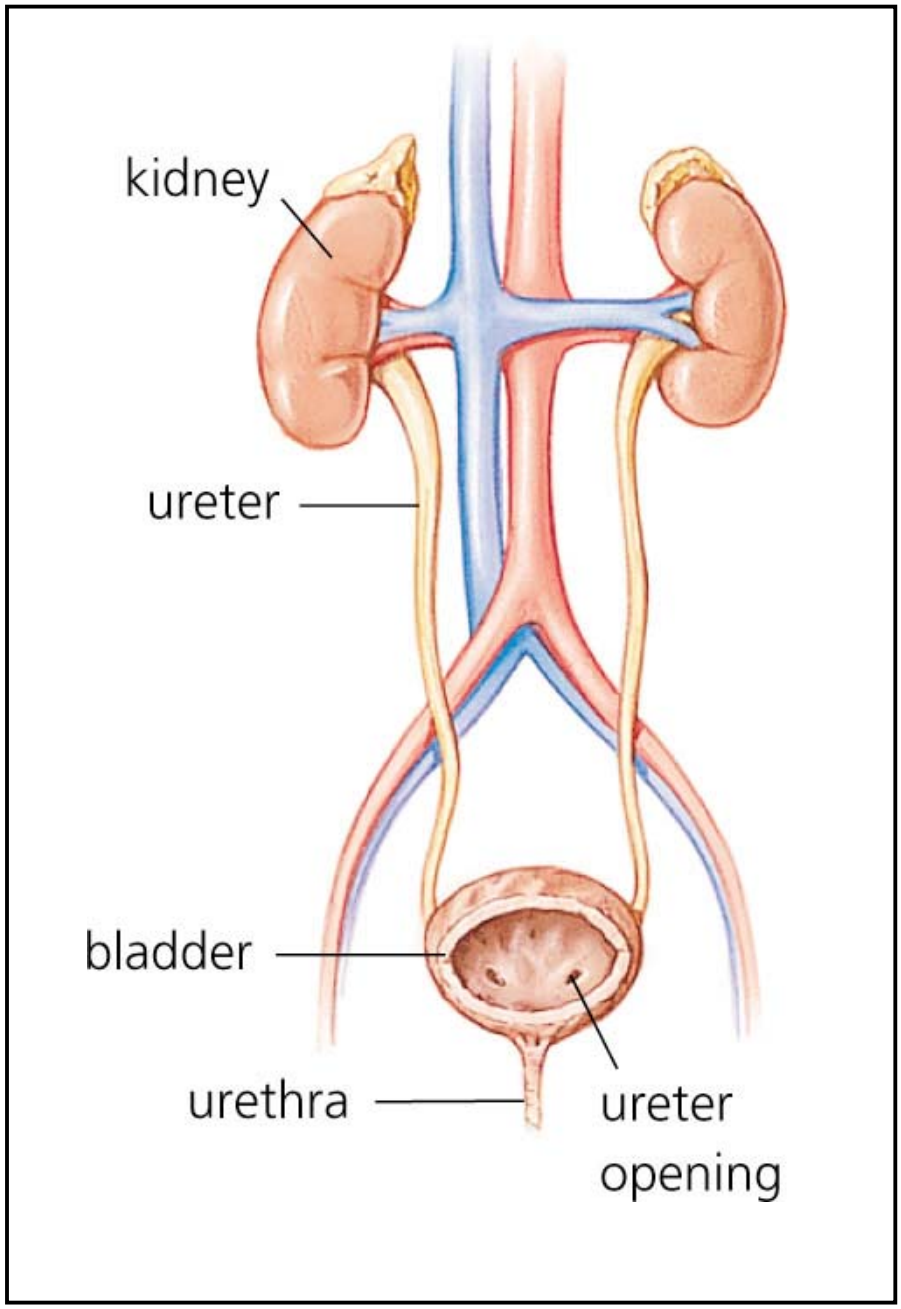

http://www.bartleby.com/images/A4images/A4urinar.jpg

frequent urge to urinate, pressure above the pubic bone, and cloudy or bloody urine (U.S. Department of Health and Human Services, 2003). Fever and flank pain, in addition to nausea, vomiting, sweats and general malaise are indications that the infection has moved to the kidneys (Warren, 1996). Bacteremia and sepsis occur about 30% of the time in patients with pyelonephritis (Bower *et al.*, 2005).

In the United States, uropathogenic *Escherichia coli* (UPEC) are responsible for 70-95% of all cases of community-acquired UTI, followed by *Staphylococcus saprophyticus* (10-15%), and, to a lesser degree, *Klebsiella, Enterobacter,* and *Proteus mirabilis* (D'Orazio and Collins, 1998; Kucheria *et al.*, 2005). UPEC are also more likely to cause recurrent infections. An epidemiological study by Foxman *et al.* found that the risk of succumbing to a second UTI from UPEC within six months of the first was 23.7% compared to 7.7% for infections caused by other agents (Foxman *et al.*, 2000). In addition, patients who suffer from recurrent infection are at an increased risk of developing bladder cancer (Bower *et al.*, 2005).

Uropathogenic *Escherichia coli*

Background

The majority of UPEC are found in the gut and are introduced into the bladder and kidneys through the urethra (Bower *et al.*, 2005). Nevertheless, these organisms differ significantly from commensal *E. coli* of the gastrointestinal tract. Indeed, UPEC comprise a diverse subset of *E. coli* that causes infections within the urinary tract. Through the expression of specific virulence factors (see Figure 2) that are often encoded on large segments of DNA called pathogenicity islands or PAIs, these bacteria

Figure 2: Diagrammatic representation of virulence factors of UPEC

UPEC employ a number of virulence factors to establish infection and maintain persistence within the urinary tract. Flagella propel the bacteria toward the desired site of infection. Fimbriae, including type 1, P, and Dr, aid in colonization of the uroepithelium. UPEC often produce two toxins, hemolysin and CNF1, as well as other virulence determinants such as lipopolysaccharide (LPS) and iron acquisition products (not shown).

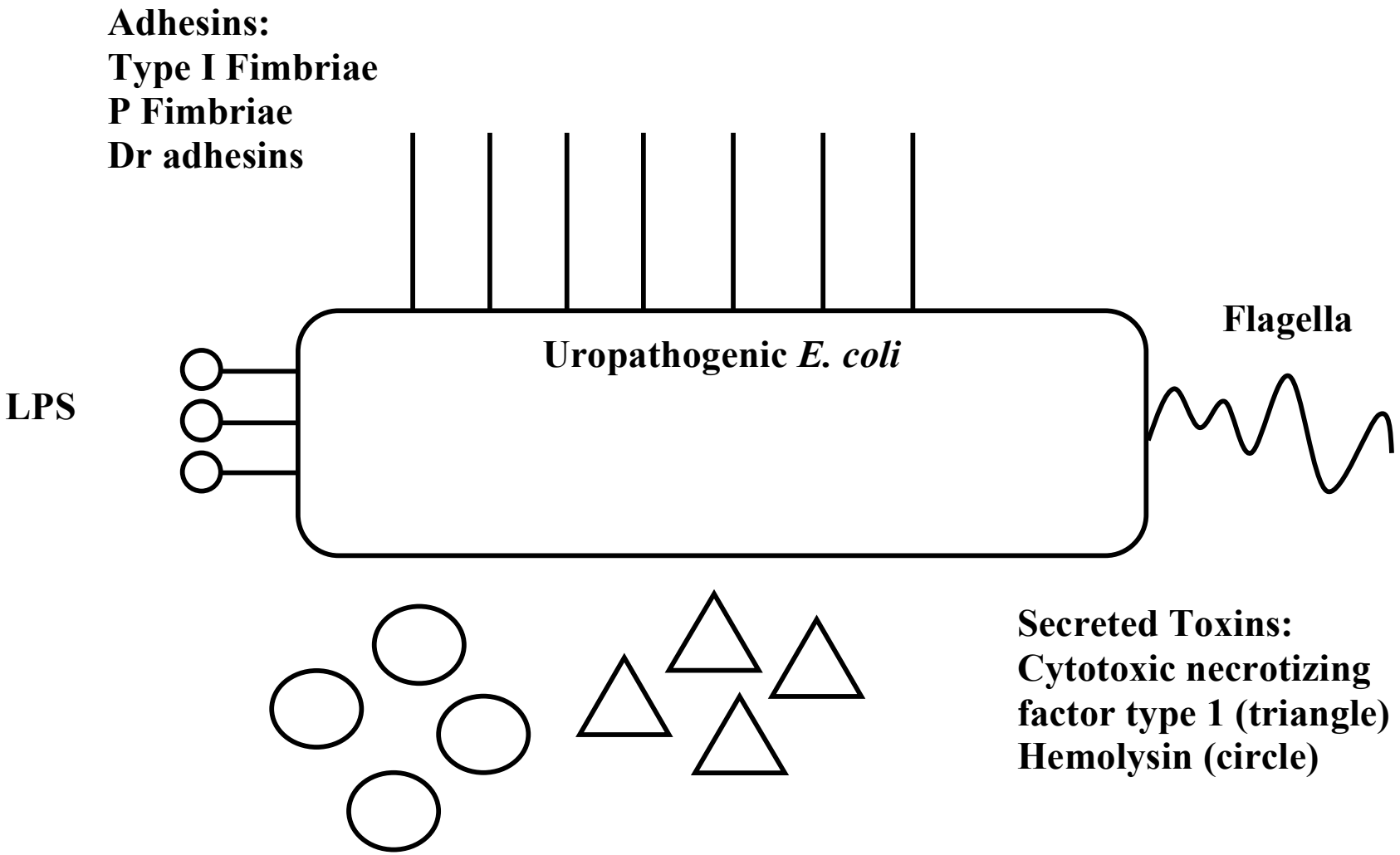
Adhesins:
Type I Fimbriae
P Fimbriae
Dr adhesins
Flagella
Uropathogenic *E. coli*
LPS
Secreted Toxins:
Cytotoxic necrotizing
factor type 1 (triangle)
Hemolysin (circle)

colonize and persist within the urinary tract (Mobley, 2000).

When the genome sequence of pyelonephritis isolate *E. coli* CFT073 was completed in 2002, comparisons were made between this and other pathogenic *E. coli* strains. Researchers found that the genomes of CFT073 and enterohemorrhagic *E. coli* (EHEC) isolate EDL933 differ considerably, and, in fact share only 39.2% of their genes (Welch *et al.*, 2002). Greater than 70% of genes unique to EDL933 are replaced with genes specific to CFT073 (Welch *et al.*, 2002). When the genome of CFT073 and other UPEC strains, such as J96 (human pyelonephritis strain) were evaluated for sequence homologies, investigators concluded that the UPEC strains present today, as well as other extraintestinal *E. coli* (ExPEC) strains, arose from multiple clonal lineages (Bower *et al.*, 2005; Welch *et al.*, 2002). Acquisition of PAIs appears to have allowed UPEC to infect and invade the urinary tract without compromising its ability to asymptomatically colonize the intestine (Welch *et al.*, 2002).

Virulence Factors

The urinary tract is normally a sterile environment in part because the body provides a number of defenses against invading bacteria such as the flow of urine and mucous secretions (D'Orazio and Collins, 1998). Therefore, UPEC and other uropathogens have evolved virulence factors to help establish infection and maintain persistence. These virulence factors are largely encoded on PAIs, acquired by UPEC through horizontal gene transfer (Emody *et al.*, 2003).

UPEC must stick to the uroepithelium to initiate infection. This adherence of UPEC is mediated by a number of types of fimbriae, i.e., type 1, P and Dr. Type 1 fimbriae are

produced by more than 80% of all strains of UPEC and, as such, are the most common virulence factor of UPEC (Kucheria *et al.*, 2005). Type 1 fimbriae facilitate the interaction of bacteria with bladder epithelial cells, as well as invasion and formation of biofilms (D'Orazio and Collins, 1998; Emody *et al.*, 2003; Schilling *et al.*, 2001). Expression of type 1 fimbriae is more important during the initial stage of infection in strains that cause cystitis as compared to those responsible for pyelonephritis (Oelschlaeger *et al.*, 2002). Invasion of the uroepithelium by type 1-piliated UPEC is mediated by FimH, the fimbrial adhesin. This binding of FimH activates signaling cascades in the host cells that promote rearrangement of the cytoskeleton and internalization of the bacteria (Schilling *et al.*, 2001).

Another type of fimbriae, P fimbriae, are present in 80% of all UPEC pyelonephritis isolates and play a role in the establishment of infection in the ascending urinary tract and kidneys rather than the bladder (Kucheria *et al.*, 2005). The *papG* gene encodes the fimbrial-tip adhesin. The products of the two classes of *papG* (Class II and Class III) not only aid UPEC in colonization but also, to the detriment of the infecting UPEC strain, induce the host immune response by triggering the Toll-like receptor 4 pathway (Marrs *et al.*, 2005). In addition to being important in adherence in the upper urinary tract, P fimbriae may also play a role in inducing the expression of other virulence genes that encode siderophores and their receptors (D'Orazio and Collins, 1998).

Finally, Dr adhesins are important for colonization of the upper urinary tract. Their receptor, decay accelerating factor, a component of the Dr blood group antigen, is ubiquitous in the urinary tract (Marrs *et al.*, 2005). UPEC strains that express this virulence factor are associated with pyelonephritis in pregnant women (30%) as well as

cystitis in children [(30-50%); (Kucheria *et al.*, 2005)]. In addition, UPEC strains that express Dr adhesins during primary infection are more likely to cause recurrent infections (Foxman *et al.*, 1995).

The adhesins that facilitate the attachment of UPEC to epithelial cells within the urinary tract are not the only virulence factors produced by these organisms. Many UPEC strains produce toxins that may cause some of the symptoms associated with UTI. These toxins include CNF1, which will be discussed in great detail in the next section, and hemolysin. Hemolysin acts on host cell membranes to promote the formation of aqueous pores that both facilitate the release of iron from and the influx of water into that cell. Lysis of the target cell can then occur (Kucheria *et al.*, 2005). Indeed, hemolysin was first characterized and subsequently named for its capacity to disrupt erythrocytes. However, the toxin can also lyse neutrophils and renal tubular cells (D'Orazio and Collins, 1998). Hemolysin has been considered an important virulence factor for UPEC for over 15 years. In 1991, O'Hanley and colleagues demonstrated in a mouse model of pyelonephritis that the capacity of the infecting UPEC strain to produce hemolysin was associated with septicemia and kidney damage (O'Hanley *et al.*, 1991). Other groups found that cystitis-causing strains of UPEC were more likely to have hemolytic activity than fecal *E. coli* isolates (Marrs *et al.*, 2005). Hemolysin production by UPEC can also lead to more serious sequelae, i.e. acute renal failure, in patients with septicemia (Oelschlaeger *et al.*, 2002).

The gene for the hemolysin protein, *hlyA*, is part of an operon (*hlyCABD)*. The *hlyBD* components code for a sec-independent secretion apparatus through which hemolysin is transported out of the bacterium; *hlyC* encodes the protein required for the

acetylation of hemolysin (D'Orazio and Collins, 1998). In addition to products of *hlyBD*, secretion of hemolysin from the bacterium requires the chaperone protein TolC (Wandersman and Delepelaire, 1990). The hemolysin operon is often found on the same pathogenicity island as the gene for CNF1 in strains of UPEC, and this association will be discussed in the next section.

Cytotoxic Necrotizing Factor Type 1

Epidemiology and animal models related to UTI

CNF1 was first identified in 1983 by Caprioli *et al.* in fecal isolates of children with severe diarrhea. Their initial characterization showed that CNF1 can cause multinucleation of HEp-2 and CHO cells, a phenomenon later discovered to be the result of endomitosis in the absence of concomitant cytokinesis (Donelli and Fiorentini, 1992; Fiorentini *et al.*, 1988). In the same study, Caprioli and colleagues observed that CNF can induce dermonecrotic lesions in rabbits after intradermal injection (Caprioli *et al.*, 1983). Subsequently, CNF1 was reported to be lethal for mice after intraperitoneal injection (De Rycke *et al.*, 1990). Further evaluation of CNF1 showed that it is a chromosomally-encoded 113 kDa single chain polypeptide protein toxin (Falbo *et al.*, 1993). As noted above, *cnf1* is located on a PAI and has a low GC content compared to the entire genome of uropathogenic *E. coli* (35% compared to 50% overall), an observation which suggested to Boquet and co-workers that the *cnf1* gene was recently acquired by UPEC (Boquet, 1998).

UPEC strains that express hemolysin also often contain the *cnf1* gene, a conclusion based on the results of a number of surveys that examined how frequently *cnf1* and *hly*

are encoded in the same isolate. Highlights of these studies are as follows. In 1987, Caprioli *et al.* found that 37% of UTI isolates studied (91 isolates total) produced CNF1 and hemolysin (Caprioli *et al.*, 1987). Several years later, Blanco *et al.* reported that 262 out of 356 Hly^+ strains were also positive for CNF1. More interestingly, the strains that expressed both toxins displayed greater lethality in mice and necrosis in rabbits than the negative control strains (73 and 96%, compared to 14 and 8%), a finding that suggested to Blanco *et. al*. that the presence of CNF1 increased the virulence of these *E. coli* strains (Blanco *et al.*, 1992). Indeed, Landraud *et al*. reported that of 175 UPEC strains isolated from hospitalized adults, about 31% of strains were positive for both the *cnf1* and *hly* genes (Landraud *et al.*, 2000). Another group of researchers reported that 93% of prostatitis strains (69 of 74) tested for the presence of *hly* also contained *cnf1*, compared to 69% (27 of 39) of pyelonephritis isolates (Mitsumori *et al.*, 1999). Finally, Yamamoto *et al*. found that 76% of hly^+ extraintestinal isolates were also $cnf1^+$, while 98% of $cnf1^+$ isolates also contained the hemolysin gene (Yamamoto *et al.*, 1995). These studies suggest that CNF1 and hemolysin may act together to contribute to the pathogenicity of UPEC.

The basis for the general observation that *cnf1* and *hly* are often co-expressed in a number of UPEC clinical isolates was suggested by the finding that in the prototypic UPEC strain J96, *cnf1* is encoded on pathogenicity island V (PAI V) between the hemolysin operon and adhesin genes (Boquet, 2001); other researchers use PAI II to describe the pathogenicity island on which *cnf1* and *hly* are encoded (Landraud *et al.*, 2003; Swenson *et al.*, 1996). Landraud and colleagues extended this observation of a physical link between these loci with the discovery of a 943 bp intergenic sequence

between the hemolysin operon and *cnf1* in 55 clinical isolates of UPEC (Landraud *et al.*, 2003). These investigators hypothesized that the expression of CNF1 was controlled through the promoter for the hemolysin operon in PAI V of strain J96. In the same study, Landraud and co-workers reported that RfaH, a transcriptional regulator for the *hlyB* and *hlyD* genes, also modulates the expression of CNF1 (Landraud *et al.*, 2003).

The mechanism of secretion of CNF1 is still unclear. The CNF1 protein does not contain a signal sequence nor are there genes found in UPEC that encode the components of the type III secretion system (Boquet, 2001). Currently, there are several hypotheses for how CNF1 is exported from the bacteria. The first idea is that CNF1 is not actively secreted but rather is released after lysis of the bacteria (Boquet, 2000). The second theory is that CNF1 becomes extracellular by transport through the hemolysin sec-independent type I secretion system (Boquet, 2001). The third and newest idea is that CNF1 is released from the bacterial cell through membrane blebs (Davis *et al.*, 2006; Kouokam *et al.*, 2006). These models are not mutually exclusive and in fact all three events may occur. Although the mechanism by which CNF1 is transported remains to be clarified, we do know that the toxin is produced *in vivo* because anti-CNF1 antibodies can be detected in the sera of patients infected with *E. coli* (Boquet, 2001).

Epidemiological data support the premise that CNF1 contributes to the virulence of UPEC. Specifically, the presence of *cnf1* has been linked to extraintestinal disease through analysis of clinical isolates. For example, Yamamoto *et al*. found the CNF1 gene in 38% of isolates that cause bacteremia in addition to 61% of UTI isolates, as opposed to only 10% of commensal fecal isolates (Yamamoto *et al.*, 1995). Additional analysis performed by this group demonstrated the presence of *cnf1* in 64% of prostatitis isolates

and 36% of pyelonephritis isolates (Mitsumori *et al.*, 1999). Andreu *et al.* also studied clinical isolates and reported that they found that *cnf1* in 63%, of prostate isolates, 48% of pyelonephritis isolates, and 44% of cystitis isolates (Andreu *et al.*, 1997).

The precise role for CNF1 in the virulence of UPEC has been the subject of debate for a number of years. One possible function for CNF1 is that of a facilitator of bacterial invasion of epithelial cells. Invasion requires reorganization of the cytoskeleton (Falkow *et al.*, 1992), an activity that has been attributed to CNF1 by a number of researchers. Indeed, Fiorentini *et al.* demonstrated that CNF1 induced multinucleation in tissue culture cells as well as actin filament reorganization (Fiorentini *et al.*, 1988). Moreover, Falzano *et al.* found that the presence of CNF1 induced phagocytosis of latex beads as well as *Listeria innocua*, a non-invasive bacterial strain, in HEp-2 cells (Falzano *et al.*, 1993). Similarly, Hofman *et al*. discovered that CNF1 treatment of polarized T84 colonic cells caused effacement of microvilli at the apical surface and evoked the formation of stress fibers on the basolateral face (Hofman *et al.*, 1998). In addition to the rearrangement of the cytoskeleton, these investigators reported that the presence of CNF1 led to transepithelial migration of polymorphonuclear leukocytes (PMNs) in both directions (luminal to basolateral and basolateral to luminal); they concluded that this induced PMN migration was due to the interaction of CNF1 with the epithelial cells and not with any effect of CNF1 on the PMNs themselves (Hofman *et al.*, 1998).

The impact of CNF1 on tissue culture cells discussed to this point is from cell lines that are not physiologically relevant to urinary tract infections. Mills *et al*. sought to determine a role for CNF1 in a model that would more closely reflect the *in vivo* situation. Therefore, these researchers chose 5637 cells, a primary cell line derived from

human bladder carcinoma, for further investigation of the toxin:cell interaction (Mills *et al.*, 2000). These cells have a number of attributes that mimic the characteristics of uroepithelial cells in the human host. For example, 5637 cells secrete interleukin (IL)-1α/β, IL-6 and IL-8, TNF-α/β (tumor necrosis factor) and colony-stimulating factors (i.e. G-CSF), and these cytokines have been found in the urine and/or serum of UTI patients (Agace *et al.*, 1996; Kaashoek *et al.*, 1991; Mills *et al.*, 2000).

Mills and colleagues discovered that CNF1 caused frank cytotoxicity in the 5637 bladder cell line in a dose-dependent manner and showed that this toxicity could be neutralized by antisera raised against the toxin (Mills *et al.*, 2000). Furthermore, they demonstrated that the toxin-treated cells died by an apoptotic mechanism (Mills *et al.*, 2000). This observation was of particular note because in a mouse model of ascending UTI done in the same laboratory, $CNF1^{+}$ strains caused shedding of bladder epithelial cells into the urine (Rippere-Lampe *et al.*, 2001b). The model proposed by Rippere-Lampe and co-workers was that release of CNF1 by the bacteria resulted in the shedding of the uroepithelium, an event that allowed UPEC to penetrate further into the bladder (Mills *et al.*, 2000).

Another role CNF1 may play in virulence would be to help the bacteria evade the effects of the immune system. Indeed, Davis *et al.* proposed that CNF1 is important for protection of UPEC from the innate immune system, specifically from PMNs (Davis *et al.*, 2005). They observed that PMNs incubated with CNF1-expressing bacteria exhibited a diminished capacity to phagocytose bacteria and to remodel their cytoplasmic membranes and cluster the CD11b receptor (complement receptor 3) on their surfaces. Davis and colleagues also demonstrated that the *cnf1* isogenic mutant was more

susceptible to the microbicidal action of the respiratory burst produced by the PMNs than was the wild-type strain. Finally, Davis and coworkers reported that there was an up-regulation of Rac2, the GTPase important for functional NADPH oxidase in PMNs, in neutrophils incubated with CNF1-producing bacteria (Davis *et al.*, 2005). Taken together, these data demonstrate that the expression of CNF1 by UPEC strains is sufficient to reduce phagocytosis and reactive oxygen species, thereby protecting the bacteria from elimination by the innate immune system and allowing the organisms to persist within the urinary tract (Davis *et al.*, 2005).

Rippere-Lampe *et al.* used a mouse model of ascending urinary tract infection to assess the role of CNF1 in the virulence of UPEC *in vivo*. In that study, they tested several UPEC clinical isolates and their respective *cnf1*$^{-}$ isogenic mutants in CH3/HeOuJ mice to determine whether CNF1 was required for infection and/or invasion of the bladder and kidney. They showed that, in general, the CNF1^{+} strains attained greater colony counts and induced a greater inflammatory response than did their respective isogenic mutant in the bladders of infected mice (Rippere-Lampe *et al.*, 2001b).

In addition to the mouse model of ascending urinary tract infection, Rippere-Lampe *et al.* also tested the role of CNF1 in a rat model of acute prostatitis (Rippere-Lampe *et al.*, 2001a). This animal model is a good indicator of human disease for two reasons. First, the prostate of the rat and human are similar both histologically, as well as morphologically. Second, the rats are infected intraurethrally, a route by which men are proposed to acquire the bacteria responsible for prostatitis (Rippere-Lampe *et al.*, 2001a). The results of this study by Rippere-Lampe *et al.* were that rats infected with CP9, a CNF1^{+} clinical isolate, showed more severe damage to the prostate in addition to a

greater degree of inflammation and influx of neutrophils compared to rats infected with the *cnf1*$^-$ isogenic mutants (Rippere-Lampe *et al.*, 2001a).

CNF1 is characteristically found in a number of uropathogenic *E. coli* strains (Landraud *et al.*, 2000), but the gene has also been located in other types of *E. coli* isolates. Pathogenicity island V of J96 (UPEC pyelonephritis strain), which contains the *cnf1, hly* and P-fimbriae genes, has been identified in *E. coli* K1 strain C5 that causes neonatal meningitis. The elements of this PAI have been proposed to contribute to the virulence of strain C5 by inducing high levels of bacteremia in a neonatal rat model (Houdouin *et al.*, 2002). In addition, Khan *et al.* reported that the presence of CNF1 in K1 strain E44, a neonatal meningitis isolate, resulted in the invasion of brain microvascular endothelial cells as well as traversion of the blood-brain barrier in a rat meningitis model (Khan *et al.*, 2002). More recently, a CNF gene was discovered in *Yersinia pseudotuberculosis* (Lockman *et al.*, 2002). The gene, denoted *cnf*$_Y$, is 65.1% identical to *cnf1* at the genetic level, and the expressed CNF_Y protein has 60.8% identity and 68.5% similarity to the CNF1 of *E. coli* (Lockman *et al.*, 2002). Despite this high homology, neither goat polyclonal antisera nor mouse monoclonal antibodies raised against CNF1 of UPEC could cross-neutralize CNF_Y (Lockman *et al.*, 2002). Whether CNF_Y of *Yersinia* contributes to virulence has yet to be determined.

Molecular characteristics

Overview: CNF1 is a member of the family of A-B toxins, with a putative N-terminal binding domain and C-terminal enzymatic domain. Two hydrophobic regions that lie between the binding and enzymatic domains appear to be membrane-spanning

regions and are thought to be responsible for toxin translocation. Only the C-terminus of CNF1 has been crystallized (Buetow *et al.*, 2001).

Structure–function studies: Lemichez *et al.* first described the activities of the two domains of CNF1 in 1997 (Lemichez *et al.*, 1997). By testing Glutathione S-transferase (GST)-tagged fragments of CNF1 (N-terminal and C-terminal) in competitive binding experiments as well as phenotypic assays, these investigators determined that the enzymatic activity of the toxin lay in the C-terminus of the protein, while the N-terminus (the first 320 amino acids) contained the region important for binding to eukaryotic cells (Lemichez *et al.*, 1997). Subsequently, Fabbri and colleagues narrowed the critical binding region of CNF1 to the first 190 amino acids and proposed that amino acids 53-75 were critical for the binding of the toxin to a eukaryotic receptor (Fabbri *et al.*, 1999). However, when a synthetic peptide that mimicked amino acids 53-75 was used in a competitive binding assay with wild-type CNF1, toxin activity was not inhibited. This finding suggests that: 1.) there was a technical problem with the competition experiment; 2.) amino acids 53-75 are in fact not part of the binding domain; or, 3.) that these amino acids represent only part of the eukaryotic receptor-binding region (Fabbri *et al.*, 1999). Thus, the precise amino acids within the N-terminus of CNF1 that are responsible for binding to eukaryotic cells remain to be defined.

Toxin receptor: One factor that made identifying the CNF1 binding domain difficult was that the eukaryotic receptor for CNF1 was unknown until recently. However, in 2002, Khan *et al.* used a yeast two-hybrid screen to identify the 37 kDa laminin receptor

precursor protein (LRP) as a candidate for the CNF1 ligand (Khan *et al.*, 2002). More recent data suggest that CNF1 can also bind the 67 kDa mature laminin receptor [(LR); (Kim *et al.*, 2005)]. These studies were done with *E. coli* K1 as the model CNF1-expressing organism. That CNF1 released during UPEC infection also uses LRP as the receptor is likely, but no studies to confirm this presumption have been published.

The LRP gene was cloned and found to encode a 295 amino acid protein with a molecular mass of approximately 37 kDa (Rao *et al.*, 1989). The modification process by which the precursor develops into the mature receptor is not clear. While there are sites in the sequence for putative O-linked glycosylation, Landowski *et al.* only found three fatty acids, palmitate, stearate and oleate, that were covalently associated with the 67 kDa LR (Landowski *et al.*, 1995). This latter observation suggests that acylation is the preferred method of post-translational modification of the 37 kDa precursor (Landowski *et al.*, 1995). Along with acylation, homo- or heterodimers are formed that produce the mature 67 kDa laminin receptor (Menard *et al.*, 1998). However, the mechanism of this conversion from LRP monomer to LR multimer is still not well understood (Jaseja *et al.*, 2005).

The function of LRP is to bind the extracellular glycoprotein laminin, a substance that plays a role in cell movement, attachment, growth and differentiation in addition to being a structural component of chromosomes, membranes, and ribosomes (Mecham, 1991; Sorokin *et al.*, 2000). However, the cDNA that encodes the 37 kDa LRP is identical to that of p40, a ribosomal protein, an observation that suggests that LRP can also interact with the 40S ribosomal subunit (Jaseja *et al.*, 2005). Because laminin is important to cells, LRP is ubiquitous; the 67 kDa form can be found on muscle cells,

neutrophils, macrophages, endothelial and epithelial cells, hepatocytes, and neurons, in addition to tumor cells (Mecham, 1991). LRP is well conserved among many organisms, including yeast, worms, insects and mammals with a homology of roughly 95% among different mammalian species (Sorokin *et al.*, 2000). The LRP gene can be found in multiple copies in mice (6) as well as humans (26) (Rieger *et al.*, 1999).

There is some precedent for both the precursor and mature laminin receptor serving as receptors for other microorganisms. LRP can interact with the cellular prion protein (PrP^{c}/PrP^{sc}), and higher levels of LRP are detected in the organs of scrapie-infected mice and hamsters as compared to uninfected controls (Rieger *et al.*, 1999). Whether LRP is the sole receptor for PrP^{c}/PrP^{sc} or whether it acts as a co-receptor (Rieger *et al.*, 1999) remains to be determined. LRP can also function as a receptor for binding and entry of Venezuelan Equine Encephalitis virus (Ludwig *et al.*, 1996). Moreover, LR is one, but not the only, receptor for Sindbis virus (Wang *et al.*, 1992). CNF1 is the first bacterial protein described to date that uses LRP/LR as receptors for binding and internalization.

Toxin entry and transport in target cells: Many bacterial toxins are enzymes with intracellular targets (Sandvig *et al.*, 2004). These toxins must first bind to specific receptors on the outside of the cell, and they are then internalized by receptor-mediated endocytosis (Falnes and Sandvig, 2000). There are two general mechanisms by which the toxins are transported through target cells. The internalization pathway of CNF1 resembles that of diphtheria toxin. Upon binding to its eukaryotic receptor, CNF1 is endocytosed by both clathrin-dependent and independent pathways (Contamin *et al.*, 2000). The toxin is transferred from the early to late endosome through a microtubule-

dependent mechanism. Treatment of HEp-2 cells with brefeldin A, a substance that disrupts the Golgi apparatus, has no effect on the capacity of CNF1 to multinucleate cells, an observation that suggests that toxin translocation does not involve the trans-Golgi network. After acidification of the late endosome, CNF1 is injected into the cytosol by a mechanism that depends upon low pH (Contamin *et al.*, 2000). Once inside the cytosol, CNF1 does not need to undergo cleavage to be catalytically active (Boquet, 2001).

A proposed membrane-spanning region has been identified between the binding and enzymatic domains of CNF1; this segment is thought to facilitate translocation of CNF1 into eukaryotic cells (Falbo *et al.*, 1993; Lemichez *et al.*, 1997). This hydrophobic portion of the molecule spans residues 331-414 but is bifurcated by a brief stretch of hydrophilic amino acids (aa 372-391), a structural pattern common to other translocated toxins, such as diphtheria toxin (Pei *et al.*, 2001). The acidic amino acid residues that reside in the hydrophilic domain of CNF1, a potential helix-loop-helix motif, are important for insertion of the toxin into eukaryotic cell membranes following internalization into the endocytic compartment (Pei *et al.*, 2001). After internalization of CNF1 into eukaryotic cells, the acidic residues in the hydrophilic region are protonated, a reaction that allows the hydrophobic domains to insert deeply into the lipid bilayer (Pei *et al.*, 2001). Mutation of aspartic acid residues 373 and 379 to positively-charged lysines results in a significant loss in the capacity of CNF1 to induce multinucleation, even though binding and *in vitro* enzymatic activities of the mutant toxin are not affected (Pei *et al.*, 2001). In sum, after CNF1 is internalized into endosomes, the low pH in those compartments promotes unfolding of the toxin and protonation of the acidic amino acid

residues in the proposed transmembrane domain; these changes facilitate insertion of the toxin into eukaryotic cell membranes (Pei *et al.*, 2001).

Crystal structure of the C-terminal enzymatic domain of CNF1: The enzymatic segment of CNF1 has been crystallized (Buetow *et al.*, 2001). The X-ray crystal structure of amino acids 720-1014 folds in a fashion that is characteristic of the superfamily of catalytic triad enzymes (Buetow *et al.*, 2001). Moreover, Cys^{866} and His^{881} in CNF1 are required for enzymatic activity of CNF1 (Schmidt *et al.*, 1998), and the positions of these amino acids in the folded toxin are consistent with locations of the same amino acids in catalytic triad superfamily members (Buetow *et al.*, 2001). These findings provide additional evidence that this region of CNF1 contains the active site of this deamidase (Buetow *et al.*, 2001).

Mode of action

CNF1 acts on cellular targets through the deamidation of the Rho GTPases, including RhoA, Rac1 and Cdc42. These Rho GTPases belong to the Ras superfamily [(Rho stands for Ras-homologous); (Ridley, 2001a)] and play a number of roles in signal transduction and regulation of the actin cytoskeleton of eukaryotic cells (Aktories and Barbieri, 2005). The interaction of CNF1 with the Rho GTPases will be discussed in more detail following an overview of the role of small GTPases in eukaryotic cell function.

Rho GTPases: The mammalian family of Rho GTPases consists of 14 members, including RhoA-E, G and H, Rac1-3, Cdc42, Rnd1 and 2, and TC10 that share 50%

similarity among each other and roughly 30% identity to the Ras superfamily; the best characterized members of this family are RhoA, Rac1 and Cdc42 (Aktories, 1997; Aspenstrom, 1999). In general, Rho GTPases not only play an important role in the regulation and organization of the actin cytoskeleton, but they are also crucial to many other functions of eukaryotic cells including signal transduction, endocytosis, transcription, and apoptosis (Aktories, 1997). Each GTPase controls a unique cytoskeletal arrangement. While RhoA activation evokes stress fiber formation as well as focal adhesions, Rac1 activation is important for membrane ruffling (lamellipodia); Cdc42 activation causes filopodia, or microspike, formation (Vojtek and Cooper, 1995).

Mediators of activated GTPases: The process by which activation of RhoA induces stress fiber formation and focal adhesions involves a number of downstream effector proteins (Figure 3). These proteins include members of the family of Rho kinases, specifically ROCK-I and ROCK-II [(Rho-kinases I and II); (Aspenstrom, 1999)]. Activation of ROCK by RhoA results in phosphorylation of the myosin light chain (MLC), an event that stimulates the interaction of myosin and actin filaments and contraction of the cell (Ridley, 2001a, b). ROCK also plays a role in the accumulation of F-actin, an additional factor important for cell migration. Upon activation of ROCK by RhoA, LIMK (LIM kinase) is stimulated and inhibits cofilin; this inhibition prevents actin depolymerization and thus induces the accumulation of actin at the leading edge of cells (Ridley, 2001b). Conversely, activation of the phosphatidylinositol 4-phosphate 5-kinase (PIP5K pathway) results in actin polymerization (Ridley, 2001b). Another

Figure 3: **Important effector proteins of RhoA**

Activation of RhoA triggers the interaction of the GTPase with a number of downstream effectors. Activated ROCK (Rho-kinase) can phosphorylate the myosin light chain (MLC), a modification that results in contraction of the cell. Activated ROCK can also stimulate LIM kinase (LIMK), which, in turn prevents actin depolymerization. Upregulation of the phosphatidylinositol 4-phosphate 5-kinase (PIP5K) pathway causes the polymerization of actin. RhoA can also interact with citron kinase and thus promote cell division.

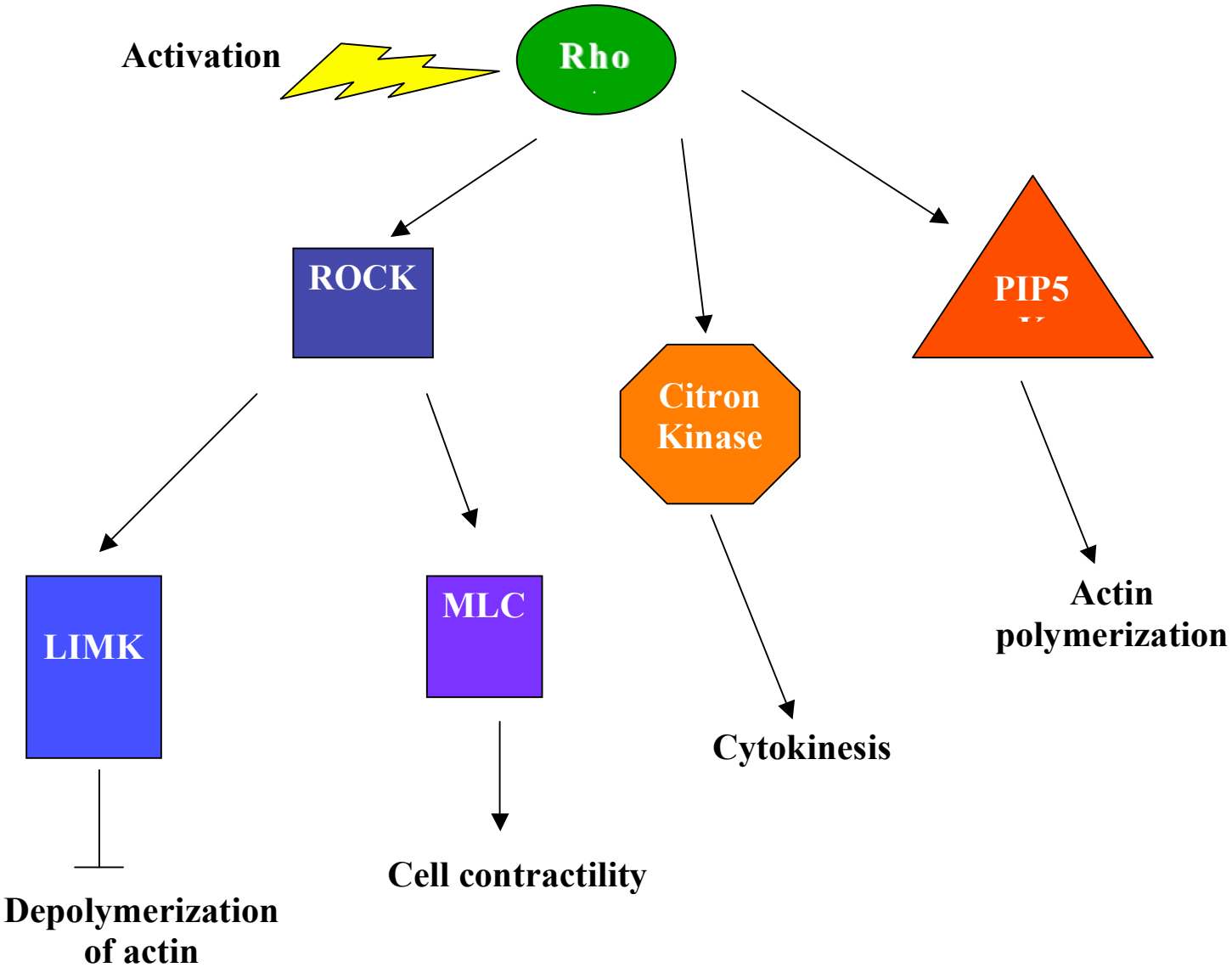
Activation
Rho
ROCK
PIP5
Citron
Kinase
LIMK
MLC
Actin
polymerization
Cytokinesis
Cell contractility
Depolymerization
of actin

effector of RhoA is citron kinase, an enzyme critical for cytokinesis (Madaule *et al.*, 1998).

Prior to RhoA-mediated cell contraction and motility, lamellipodia extension and focal adhesion formation occurs (Ridley, 2001b). Rac1 coordinates extension of lamellipodia by stimulating actin polymerization, while Cdc42 controls the formation of filopodia and focal contacts through interaction with the Arp2/3 complex [(actin-related protein 2/3 complex); (Figure 4); (Ridley, 2001b)]. The Arp2/3 complex consists of seven proteins that nucleate G-actin into F-actin after activation (Boquet and Lemichez, 2003). This complex plays an essential role in phagocytosis, cell migration, and polarity (Aktories and Barbieri, 2005). Arp2/3 binds ATP and becomes activated upon interaction with several proteins that promote nucleation; these proteins include members of the Wiskott-Aldrich syndrome protein (WASP) family and the SCAR/WAVE (WASP-related) family, in addition to other factors (Aktories and Barbieri, 2005; Ridley, 2001a). Both Rac1 and Cdc42 can activate the Arp2/3 complex and cause actin polymerization through their interactions with WASP and SCAR/WAVE. Similar to RhoA, Rac1 and Cdc42 can also activate MLC and LIMK; however, this activation occurs after the interaction of Rac1 and Cdc42 with p21-activated kinase [(PAK); (Bishop and Hall, 2000; Ridley, 2001a)].

Figure 4: **Interaction of Rac1 and Cdc42 with the Arp2/3 complex.**

Activated Rac1 and Cdc42 interact with WAVE and N-WASP, respectively, which in turn associate with the Arp2/3 complex. Activation of this complex results in actin polymerization and nucleation. Through an interaction with PAK (p21-activated kinase), Rac1 and Cdc42 can activate MLC (myosin light chain) and LIMK (LIM kinase), resulting in cell contraction and actin depolymerization.

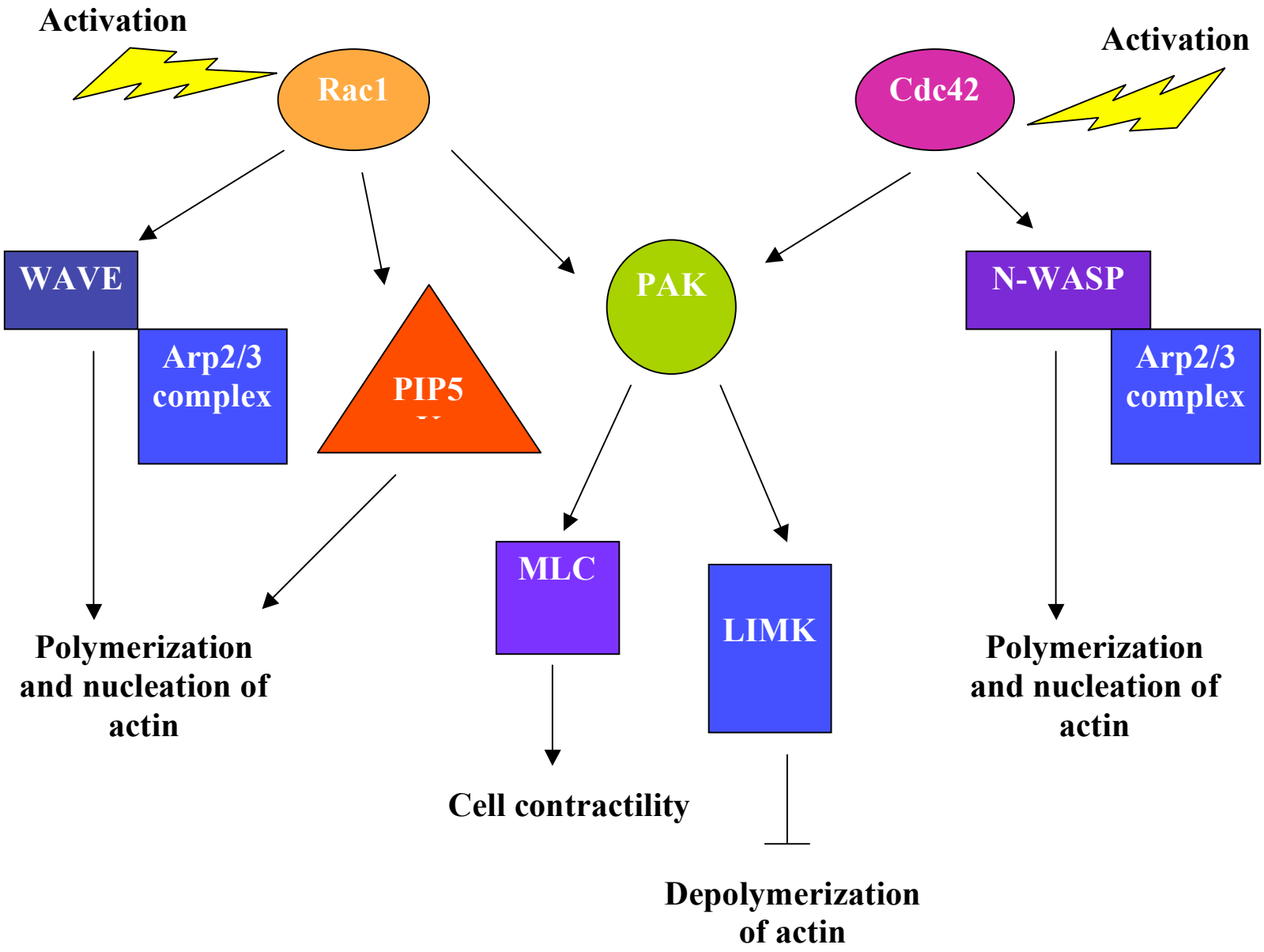
Activation
Rac1
Activation
Cdc42
WAVE
Arp2/3 complex
PIP5
PAK
N-WASP
Arp2/3 complex
MLC
LIMK
Polymerization and nucleation of actin
Cell contractility
Depolymerization of actin
Polymerization and nucleation of actin

Rho GTPase cycle: In normal mammalian cells, Rho GTPases cycle between GDP-bound and GTP-bound forms (Figure 5). When bound to GDP, the GTPases are inactive and remain so until GDP dissociates. An upstream signal triggers the activation of guanine nucleotide releasing factor (GEP/GEF), a reaction that causes the dissociation of GDP from the GTPase. The GDP/GEP complex is released and GTP is allowed to bind to and activate the Rho GTPase. The Rho GDP dissociation inhibitor (Rho GDI) can negatively regulate the cycle and prevent the release of GDP; this regulation keeps the GTPases in their inactive states. Upon activation of the small G proteins, a conformation change occurs in the effector-binding region of RhoA/Rac1/Cdc42. This change facilitates the interaction of downstream effectors with the GTPases. Intrinsic hydrolytic activity converts the GTP-bound form back to its inactive GDP-bound state. This intrinsic activity is relatively slow and can be stimulated by GTPase activating proteins [(GAPs); (Takai *et al.*, 2001)].

Deamidation: While the effects of CNF1 on various eukaryotic cells were clear as early as 1983 (Caprioli *et al.*, 1983), it was not until 1997 that researchers were able to determine that the mode of action of CNF1 was deamidation. Schmidt *et al.* found that incubation of RhoA with CNF1 resulted in an upward electrophoretic mobility shift on SDS-PAGE (Schmidt *et al.*, 1997). Analysis of CNF1-modified RhoA by mass spectrometry revealed an increased mass shift of about 1 dalton compared to unmodified RhoA. Tandem MS showed that the affected amino acid residue of RhoA was Gln^{63}, which was changed to glutamic acid (E) due to the removal of the amine group of glutamine (Schmidt *et al.*, 1997). The process of deamidation involves the removal of an

Figure 5: Rho GTPase cycle.

Under normal conditions, Rho GTPases, including RhoA, Rac1 and Cdc42, cycle between inactive, GDP-bound and active, GTP-bound states. This process is controlled by positive and negative regulators. Activation of the Rho GTPases results in interaction with a number of downstream effectors. CNF1 and DNT interfere with GTP hydrolysis by modifying Gln^{63} of RhoA and Gln^{61} of Rac1 and Cdc42 and cause constitutive activation of these GTPases.

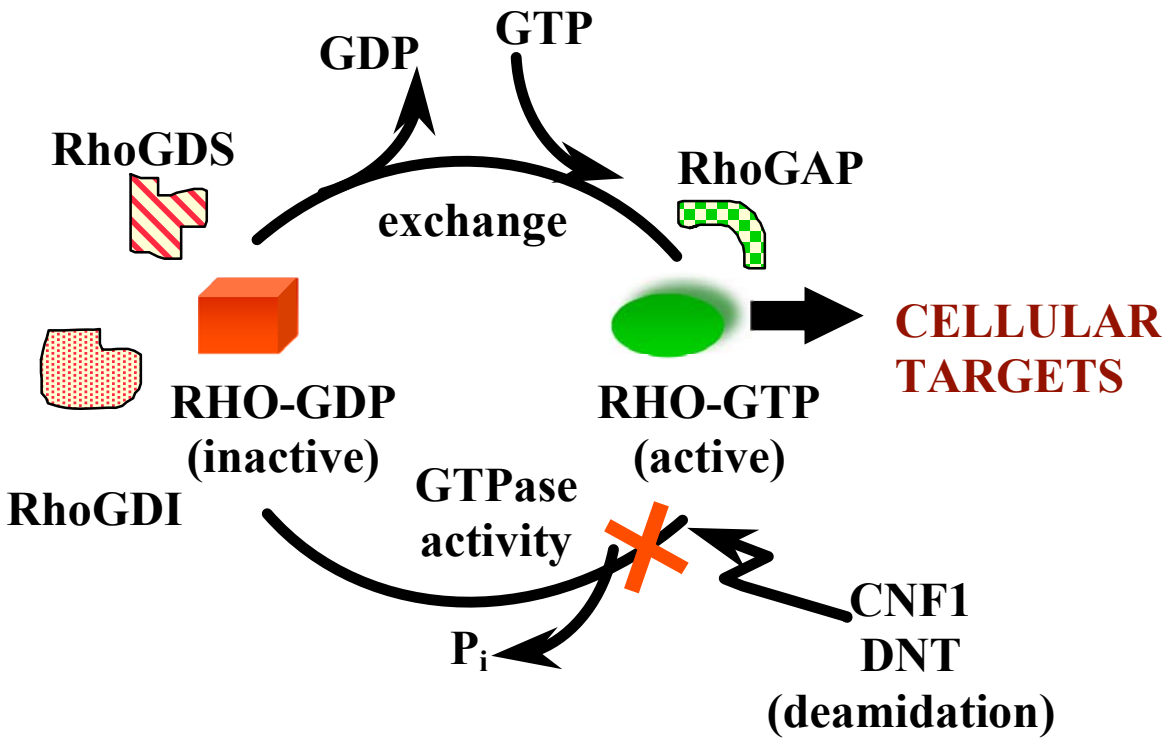

Adapted from Dr. Karen Meysick (used with permission)

amine group from the glutamine-63 (Gln^{63}) residue of RhoA as shown in the following reaction:

$$Rho + H_2O \rightarrow RhoQ63E + NH_3$$

(Barbieri *et al.*, 2002). Gln^{63} is critical for hydrolysis of GTP into GDP and modification of the amino acid results in constitutive activation of the GTPases (Barbieri *et al.*, 2002).

In addition to modification of RhoA, CNF1 was also shown to deamidate Rac1 and Cdc42 at Gln^{61}, the equivalent of Gln^{63} in RhoA. A number of experiments led to this conclusion. Incubation of HeLa cells in the presence of CNF1 resulted in both microspike and membrane ruffle formation, phenotypes specific for Cdc42 and Rac1, respectively (Lerm *et al.*, 1999b). *In vitro* deamidation assays demonstrated that both Rac1 and Cdc42 were modified by CNF1, as shown by a 1 dalton shift on mass spectrometry. Site-directed mutations of Gln^{61} confirmed these findings, leading to the conclusion that both Rac1 and Cdc42, in addition to RhoA, can be targeted and subsequently deamidated in the presence of CNF1 (Lerm *et al.*, 1999b). CNF1 prefers RhoA and Cdc42 as substrates for deamidation over Rac1 (Horiguchi, 2001).

When Rho GTPases cycle from their GDP-bound to their GTP-bound states, conformational changes occur in two domains of these GTPases. Switch I (aa 34-42 in RhoA) activates downstream cellular effectors, while the switch II region (aa 61-79 in RhoA) plays a role in hydrolysis of GTP (Flatau *et al.*, 2000). Using RhoA/Ras1 switch mutants in which Ras1, a small G protein not normally affected by CNF1, was modified to contain the switch II domain of RhoA (Ala^{61}-Asp^{78}), Lerm *et al.* found that CNF1 could now deamidate the altered Ras1 (Lerm *et al.*, 1999a). In addition, an Asp^{59}-Asp^{78} peptide was an adequate substrate for CNF1 modification. However, while this region of

RhoA is sufficient for deamidation by CNF1, the activity is less than that shown with the full-length RhoA; this observation suggests that other amino acid residues enhance the binding of the toxin to this substrate even though these GTPase amino acids are not required for activity (Lerm *et al.*, 1999a). Because all Rho GTPases are nearly identical to RhoA in the switch II region (amino acids 61-78), it can be assumed that this domain is also sufficient for deamidation of Rac1 and Cdc42 (Lerm *et al.*, 1999a). Further research demonstrated that the smallest region of RhoA that can be modified by CNF1 is comprised of amino acid residues 59-69, a segment of the protein that lies at the beginning of the switch II domain (Flatau *et al.*, 2000).

Related toxins (CNF2, DNT and PMT)

Overview

CNF1 shares homology to several toxins, including Cytotoxic Necrotizing Factor Type 2 (CNF2), dermonecrotic toxin of *Bordetella spp.* (DNT) and *Pasteurella multocida* toxin (PMT). The region of homology and percent identity vary depending on the toxin. CNF1 and CNF2 have almost 90% homology and 85% identity over their 1014 amino acids (Horiguchi, 2001; Sugai *et al.*, 1999). In the N-terminal binding region, CNF1 has 24% homology to the N-terminal 500 residues of PMT (Wilson *et al.*, 1999). However, this homology is highest in a region thought to be responsible for toxin translocation [(aa 250-530 of PMT and aa 200-465 of CNF1); (Pullinger *et al.*, 2001)]. In the C-terminal enzymatic domain, CNF1 shares 27% amino acid similarity and 13% identity with the enzymatic domain of DNT (McNichol *et al.*, 2006). However, when the regions of CNF1

(amino acids 824-888) and DNT (amino acids 1250-1314) that encompass the active sites are compared, the identity increases to 45% (McNichol *et al.*, 2006).

CNF2

CNF2 was first discovered in 1974 in a strain of *E. coli* that caused septicemia in a lamb (Smith, 1974). The toxin was encoded on the Vir plasmid, and was originally called the Vir toxin. CNF2 was finally given its name in 1990 when Oswald *et al.* were able to identify a 110 kDa protein from Vir^+ cell lysates (Oswald and De Rycke, 1990). Like CNF1, CNF2 is also 1014 amino acids, has a similar GC content (roughly 50%) and lacks a signal peptide, a finding that led to the conclusion that the toxin is not secreted (De Rycke *et al.*, 1999).

A few years after the first description of CNF2, researchers found that this toxin, although similar to CNF1 in its capacity to multinucleate HeLa cells, was only partially cross-neutralizable by anti-CNF1 sera, an observation that suggested that it was a distinct toxin (De Rycke *et al.*, 1987). Further evidence that CNF1 and CNF2 are different came from mouse footpad assay and rabbit skin test data. While both toxins induced strong inflammatory responses in the mouse footpad assay, only CNF2 caused necrosis (De Rycke *et al.*, 1989). Similarly, CNF2 evoked an intense necrosis in the rabbit skin test, but the necrosis caused by CNF1 was only moderate (De Rycke *et al.*, 1990). When injected intraperitoneally into mice, all CNF2 isolates tested were 100% lethal, whereas the CNF1-positive strains were only partially lethal (De Rycke *et al.*, 1990). Using these criteria, CNF1 and CNF2 appear to have some distinct biological activities despite their high amino acid similarity.

Enzymatically, CNF1 and CNF2 have the same mode of action, but different substrate preferences. Oswald *et al.* discovered that RhoA and CNF2 could interact and produce a shift on SDS-PAGE, the result of an unknown biochemical process (Oswald *et al.*, 1994). In 1999, Sugai *et al.* determined that the modification of RhoA was the result of deamidation of the Gln^{63} residue of RhoA, the same method by which CNF1 activation of RhoA occurs (Sugai *et al.*, 1999). However, while they found that CNF2 deamidated RhoA and Rac1 equivalently, this toxin had little or no enzymatic activity on Cdc42 (Sugai *et al.*, 1999). Sugai and colleagues concluded that the substrate preference of CNF2 (RhoA=Rac1>Cdc42) differs from CNF1 (RhoA=Cdc42>Rac1) but is the same as DNT (Horiguchi, 2001; Sugai *et al.*, 1999).

PMT

Another toxin with homology to CNF1 is *Pasteurella multocida* toxin (PMT). PMT is a 146 kDa toxin that is considered to be a major virulence factor of *P. multocida* and its expression is linked with atrophic rhinitis in pigs, respiratory disease in cattle, and dermonecrosis and bacteremia in infected animals (Wilson *et al.*, 1999). We now know that, like CNF1 and DNT, the binding and translocation region of PMT lies in the N-terminus of the molecule, while the C-terminus contains the enzymatic domain (Pullinger *et al.*, 2001).

PMT is described as a potent mitogen that can stimulate DNA synthesis and cell division (Ward *et al.*, 1998). While the exact mechanism of action of this toxin is still unknown, current research suggests that PMT interacts with the Gq protein, a member of the family of heterotrimeric G proteins (Baldwin *et al.*, 2004). This association between

PMT and the Gq protein causes a cascade in several signal transduction pathways that result in increased inositol phosphate levels, Ca^{2+} mobilization, protein kinase C stimulation, and actin rearrangement (Baldwin *et al.*, 2004; Busch *et al.*, 2001). In addition, the mitogenic effect of the toxin may be caused by an upregulation of the mitogen-activated protein kinase pathway, again as a consequence of interaction with the Gq protein.

Rozengurt *et al.* demonstrated in a series of experiments that PMT appears to act intracellularly, a finding that suggests a function for the PMT translocation domain (Rozengurt *et al.*, 1990). Hydrophobic amino acid residues 340-470 of PMT lie within a possible membrane-spanning region that shares 30% amino acid homology with the putative transmembrane domain of CNF1 (Lax *et al.*, 1990; Pei *et al.*, 2001; Wilson *et al.*, 1999). The transmembrane domain of PMT is composed of two hydrophobic helices (aa 402-423 and 437-457) that are connected by a short loop (Baldwin *et al.*, 2004). Mutational analysis of the loop region in PMT revealed that Asp^{425}, Asp^{431} and Glu^{434} are critical for activity and are therefore important for translocation of the toxin into eukaryotic cells (Baldwin *et al.*, 2004).

Despite the homology between CNF1 and PMT within their putative N-terminal binding domains, the two toxins have different binding affinities on Swiss 3T3 cells (Pullinger *et al.*, 2001). In addition, the two toxins use different receptors for internalization into eukaryotic cells. In 2002 Shime *et al*. demonstrated that PMT interacts with vimentin, a component of type III intermediate filaments, structures that appear to contribute to the motility, shape and cytokinesis of eukaryotic cells (Shime *et*

al., 2002). Precisely how the interaction of PMT with vimentin leads to activation of the Gq protein remains to be determined (Shime *et al.*, 2002).

Dermonecrotic Toxin of *Bordetella spp.*

Background

Dermonecrotic toxin (DNT) was described by Bordet and Gengou in 1909 as one of the first virulence factors for *Bordetella pertussis* (Walker and Weiss, 1994). A member of the family of A-B toxins, DNT is a heat-labile, single-chain polypeptide with a mass of about 145 kDa (Horiguchi *et al.*, 1989). DNT causes skin lesions when injected intradermally into rabbits, mice and guinea pigs, and is also lethal in mice after intraperitoneal or intravenous injection (Horiguchi, 2001). Like CNF1, DNT is a cytoplasmic protein that does not appear to be secreted due to its lack of a signal sequence (Walker and Weiss, 1994). DNT is produced by all species of *Bordetella* and the gene is nearly identical (Horiguchi, 2001; Pullinger *et al.*, 1996; Walker and Weiss, 1994).

DNT and disease

DNT has not been linked to virulence in *B. pertussis*. A DNT transposon mutant, termed BPM1809, was found to be just as virulent as wild-type *B. pertussis* in an infant mouse lethal infection model (Weiss and Goodwin, 1989). These researchers proposed that DNT may not play a role in disease because its inefficient secretion would prevent lung endothelial cells from coming into contact with the toxin (Weiss and Goodwin, 1989). Other investigators have suggested that the lack of a good animal model (i.e. one

that displays the cough associated with pertussis) has prevented accurate evaluation of the role of DNT in *B. pertussis* (Fukui and Horiguchi, 2004). Regardless, this toxin plays an important role in *B. bronchiseptica* disease in pigs (Oswald *et al.*, 2005).

Atrophic rhinitis is a disease in swine associated with *B. bronchiseptica* as well as *P. multocida*. Symptoms and sequelae include bone loss in the nasal turbinates, inflammation of nasal mucosa and epithelial necrosis in the upper respiratory tract (Horiguchi *et al.*, 1995a). Electron microscopic analysis of infected tissue showed degeneration in osteoblasts, the cells involved in bone formation; however, no changes were detected in osteoclasts, the cells responsible for bone resorption (Horiguchi *et al.*, 1991). This finding suggested to the authors that DNT interferes with osteogenesis (bone generation) by damaging osteoblasts in such a way that new bone cannot be generated, which, in turn, leads to atrophy in the nasal skeletal structure (Horiguchi *et al.*, 1991).

In vitro, MC3T3-E1 cells, an osteoblastic cell line, were intoxicated with DNT and observed for their capacity to differentiate. When cells were intoxicated with DNT, there was a reduced accumulation of collagen and decreased levels of alkaline phosphatase, indicating that the toxin prevented osteoblastic differentiation (Horiguchi *et al.*, 1991). Data from two animal models demonstrated that DNT was the major factor associated with turbinate atrophy. In an *in vivo* rat model, DNT caused necrosis in the nasal cavity and degeneration of osteoblasts two days after toxin injection, with severe nasal bone damage appearing by day 9 (Horiguchi *et al.*, 1995a). These data were subsequently confirmed by infecting pigs with wild-type, DNT^+ *B. bronchiseptica* as well as isogenic *dnt* mutants. Pigs challenged with the *dnt* mutant strains did not succumb to pneumonia or turbinate atrophy as did the animals challenged with the wild-type strains. Taken

together, DNT production is required for the establishment of disease in pigs infected with *B. bronchiseptica* (Brockmeier *et al.*, 2002).

Molecular characteristics

Because DNT contributed to atrophic rhinitis in pigs, researchers speculated that the mode of action of the toxin was similar to PMT, another toxin that as noted earlier also causes atrophic rhinitis. However, instead of acting as a mitogen in the manner of PMT, DNT stimulates DNA synthesis and causes multinucleation in MC3T3-E1 cells (Horiguchi *et al.*, 1993). Horiguchi and co-workers demonstrated that cells incubated with DNT for 24 hours displayed thick actin fibers and focal adhesions compared to untreated cells, and these investigators also showed that DNT could modify RhoA *in vitro* (Horiguchi *et al.*, 1995b). Taken together, these data suggested that DNT activates RhoA, although the mode of action was undefined.

Studies of the effects of DNT on eukaryotic cells preceded investigations of the functional domains of the molecules. In 1999, Kashimoto *et al*. identified the N-terminal 531 amino acids as responsible for the binding of DNT to cells by showing that this fragment of the toxin blocked the attachment of the wild-type DNT to target cells (Kashimoto *et al.*, 1999). In a more direct binding assay, other researchers determined that the smallest region still able to bind to MC3T3 cells spanned amino acids 1-54 (Matsuzawa *et al.*, 2002). While the receptor is still unknown, current thought is that it is an uncommon molecule since DNT only intoxicates a few cell types.

By expressing RhoA and various DNT truncated mutants in a co-expression system, Kashimoto *et al.* found that the catalytic domain lies in the C-terminus, specifically

amino acids 1162-1464 (Kashimoto *et al.*, 1999). This region also contains the cysteine residue then thought to be responsible for enzymatic activity (Kashimoto *et al.*, 1999). Further research identified the amino acids of DNT required for its enzymatic activity. Cysteine 1292 and histidine 1307 are homologous to the residues required for activity by CNF1; an additional amino acid, lysine 1310, is also necessary for DNT activity (Schmidt *et al.*, 1999). The mode of action of DNT will be discussed in more detail in the subsequent section.

Mode of action

Overview: Like CNF1, DNT also constitutively activates RhoA, Rac1 and Cdc42. The capacity of DNT to deamidate GTPases was described in 1997 for RhoA and in 2002 for Rac1 and Cdc42 (Horiguchi *et al.*, 1997; Masuda *et al.*, 2002). However, while DNT can effectively deamidate Rho GTPases, the preferred mode of action is transglutamination (Schmidt *et al.*, 1999).

Transglutamination: Transglutaminases are a group of enzymes that catalyze the formation of cross-links between the γ-carboxyamine group of peptide-bound glutamine residues and the amino groups of primary amines, including putrescine, spermidine, and cadaverine in a calcium-dependent manner (Kleman *et al.*, 1995; Wilhelm *et al.*, 1996). This transglutamination reaction is quite common in eukaryotic cells and plays a role in a number of physiological processes in mammals (Kleman *et al.*, 1995). Examples of transglutaminases and their biological functions are as the follows: Factor XIII (plasma transglutaminase), helps to stabilize fibrin-clot formation during hemostasis; epidermal

transglutaminase, contributes to skin development; and tissue transglutaminase, involved in programmed cell death and stabilizing the extracellular matrix (Kleman *et al.*, 1995).

Like the eukaryotic transglutaminases, DNT also works to cross-link primary amines to Gln^{63} of RhoA (Gln^{61} of Rac1 and Cdc42) as shown in the following reaction:

$$Rho + NH_2\text{-}R \rightarrow RhoQ63\text{-}R + NH_3$$

(Barbieri *et al.*, 2002). However, in contrast to the transglutaminases in mammalian cells, DNT does not cross-link RhoA molecules to each other (Schmidt *et al.*, 1999). Transglutamination of Rho GTPases results in their constitutive activation and subsequent cytoskeletal rearrangement. Measurement of ammonia release in the presence and absence of ethylenediamine, a co-substrate for transglutamination, revealed that DNT-induced ammonia release was greater when ethylenediamine was present in the reaction. This latter finding indicated to Schmidt *et al.* that this toxin acts preferentially as a transglutaminase (Schmidt *et al.*, 1999). In addition, cell lysates incubated with DNT displayed a downward mobility shift on SDS-PAGE. This observation suggested that transglutamination of the substrate had occurred since an increased mass was detected by MALDI-TOF analysis, a difference that corresponded to DNT cross-linked with the co-substrate (Masuda *et al.*, 2000; Schmidt *et al.*, 1999). While CNF1 can act as a transglutaminase *in vitro*, there are no data to suggest that this biochemical reaction is physiologically relevant (Schmidt *et al.*, 1999).

Because primary amines serve as co-substrates for transglutamination, researchers sought to determine which compounds were aiding the toxin in its Rho-modifying capacity. Casein and fibronectin, mammalian substrates for transglutamination, were not modified by DNT (Schmidt *et al.*, 1999). Subsequently, putrescine, spermidine and free

lysine were identified as effective substrates for DNT (Schmidt *et al.*, 2001). In addition, Schmidt *et al*. found that in a competition assay with radiolabeled ethylenediamine, L-lysine was more effective in preventing incorporation of ethylenediamine than either spermidine or putrescine, a finding that suggested that lysine is the preferred co-substrate for transglutamination (Schmidt *et al.*, 2001). The capacity of lysine to act as a co-substrate for transglutamination is also relevant physiologically because it has been demonstrated that free lysine is present in millimolar concentrations compared to the free concentrations of spermidine and putrescine [(5-10-fold less); (Schmidt *et al.*, 2001)].

Hypothesis and Specific Aims

The main goal of this project is to accurately pinpoint the regions of CNF1 required for its enzymatic and binding activities through the use of CNF1/DNT chimeric toxins or CNF1 truncated mutants. Our hypothesis is two-fold. First, we propose that when the region of DNT with the highest homology to CNF1 is inserted into the CNF1 backbone, the hybrid toxin will simulate a phenotype and/or enzymatic activity specific to DNT. Second, we speculate that truncation of the N-terminus of CNF1 will lead to a precise determination of the region of CNF1 that binds to LRP.

The specific aims for this project are as follows:

1. Construct CNF1/DNT chimeric toxins to identify the regions of the toxins that control their phenotypic and enzymatic activities.
2. Derive site-specific mutants in CNF1 and DNT, to determine whether Lys^{1310} of DNT is responsible for the enzymatic preference of DNT for transglutamination, as well as its inability to produce a phenotypic response in HEp-2 cells.
3. Locate the region of CNF1 that is responsible for binding its receptor, laminin receptor precursor protein (LRP), through the use of CNF1 truncated mutants and a newly-generated LRP binding assay.

CHAPTER 2: A SINGLE AMINO ACID SUBSTITUTION IN THE ENZYMATIC DOMAIN OF CYTOTOXIC NECROTIZING FACTOR TYPE 1 OF *ESCHERICHIA COLI* ALTERS THE TISSUE CULTURE PHENOTYPE TO THAT OF THE DERMONECROTIC TOXIN OF *BORDETELLA SPP.*

Published as: Beth A. McNichol, Susan B. Rasmussen, Karen C. Meysick, and Alison D. O'Brien. 2006. A single amino acid substitution in the enzymatic domain of cytotoxic necrotizing factor type 1 of *Escherichia coli* alters the tissue culture phenotype to that of the dermonecrotic toxin of *Bordetella spp.* Mol. Micro. 60(4): 939-950.

Note: All of the figures and tables shown reflect the work of Beth McNichol with the exception of the CNF1/DNT hybrid constructs that were created by Dr. Karen Meysick. Drs. Rasmussen, Meysick, and O'Brien contributed to the experimental design and interpretation of the data as well as preparation of the manuscript.

Abstract

Cytotoxic necrotizing factor type 1 (CNF1) and dermonecrotic toxin (DNT) share homology within their catalytic domains and possess deamidase and transglutaminase activities. Although each toxin has a preferred enzymatic activity (*i.e.*, deamidation for CNF1 and transglutamination for DNT) as well as target substrates, both modify a specific glutamine residue in RhoA, Rac1, and Cdc42, which renders these GTPases constitutively active. Here we show that despite their similar mechanisms of action CNF1 and DNT induced unique phenotypes on HEp-2 and Swiss 3T3 cells. CNF1 induced multinucleation of HEp-2 cells and was cytotoxic for Swiss 3T3 cells (with binucleation of the few surviving cells) while DNT showed no morphological effects on HEp-2 cells but did induce binucleation of Swiss 3T3 cells. To determine if the enzymatic domain of each toxin dictated the induced phenotype, we constructed enzymatically active chimeric toxins and mutant toxins that contained single amino acid substitutions within the catalytic site and tested these molecules in tissue culture and enzymatic assays. Moreover, both site-directed mutant toxins showed reduced time to maximum transglutamination of RhoA compared to the parent toxins. Nevertheless, the substitution of threonine for Lys^{1310} in the DNT-based mutant, while affecting transglutamination efficiency of the toxin, did not abrogate that enzymatic activity.

Introduction

Cytotoxic necrotizing factor type 1 (CNF1) is produced by many strains of uropathogenic *Escherichia coli* (UPEC) (Donnenberg and Welch, 1996a). This toxin has been linked with the virulence of UPEC both epidemiologically (Andreu *et al.*, 1997; Mitsumori *et al.*, 1999) and in animal models of ascending urinary tract infection (Rippere-Lampe *et al.*, 2001b) and acute prostatitis (Rippere-Lampe *et al.*, 2001a). CNF1 is a 115 kDa cytoplasmic polypeptide toxin that is a member of the family of A:B toxins (Barbieri *et al.*, 2002) with a putative N-terminal binding domain and a C-terminal enzymatic domain (Buetow *et al.*, 2001; Fabbri *et al.*, 1999; Lemichez *et al.*, 1997). CNF1 deamidates glutamine 63 (Gln^{63}) of RhoA (Flatau *et al.*, 1997; Schmidt *et al.*, 1997) or glutamine 61 (Gln^{61}) of Rac1 and Cdc42 (Lerm *et al.*, 1999b). These specific glutamine residues are essential for GTP hydrolysis, and such modifications prevent the targeted members of the Rho family of small GTPases from cycling back to their inactive, GDP-bound states (Aktories and Barbieri, 2005). The constitutive activation of RhoA, Rac1, and Cdc42 results in the formation of actin stress fibers, lamellipodia, and filopodia, respectively (Fiorentini *et al.*, 1997; Hall, 1998; Lerm *et al.*, 2002).

The enzymatic domain of CNF1 shares 27% amino acid similarity (Kashimoto *et al.*, 1999) and 13% identity with the C-terminal portion of the dermonecrotic toxin (DNT) of *Bordetella spp*. (Schmidt *et al.*, 1999). However, the extent of this homology increases to 45% identity when smaller regions of CNF1 (amino acids 824-888) and DNT (amino acids 1250-1314) are compared. These sequences encompass the active sites of both toxins (Meysick *et al.*, 2001).

DNT of *Bordetella spp.* is a cytoplasmic toxin of approximately 140 kDa (Walker and Weiss, 1994) that is required for *B. bronchiseptica* to cause turbinate atrophy and bronchopneumonia in swine (Brockmeier *et al.*, 2002). DNT shares the same cellular targets as CNF1, i.e. members of the Rho family of small GTPases. However, the primary enzymatic activity associated with DNT is different from that of CNF1. Although DNT can deamidate target substrates, it preferentially acts as a transglutaminase, whereby it modifies Gln^{63} of RhoA and Gln^{61} of Rac1 and Cdc42 by cross-linking these specific residues to primary amines, such as ethylenediamine, spermidine, and putresceine (Aktories, 2003; Lerm *et al.*, 1999a; Schmidt *et al.*, 2001). In addition, CNF1 and DNT have different substrate preferences; CNF1 modifies the GTPases most efficiently in the order RhoA = Cdc42 > Rac1, whereas DNT favors RhoA = Rac1 > Cdc42 (Horiguchi, 2001).

The enzymatic active sites of CNF1 and DNT consist of two or three amino acids, respectively. Amino acid substitutions at Cys^{866} and His^{881} in CNF1 render the toxin unable to deamidate RhoA (Schmidt *et al.*, 1998). DNT also requires these same residues (Cys^{1292} and His^{1307}), in addition to a third, Lys^{1310} (Schmidt *et al.*, 1999). Mutation of any of these residues abolishes DNT activity; however, the precise mechanism whereby this inactivation occurs remains unclear (Lerm *et al.*, 1999a; Pullinger *et al.*, 1996; Schmidt *et al.*, 1999).

Although CNF1 and DNT share similar modes of action and target substrates, various reports indicate that these toxins elicit different morphological changes to eukaryotic cells. In this study, we examined whether the enzymatic domain of each toxin mediated these phenotypic differences. For this purpose, CNF1/DNT chimeric toxins

were constructed and evaluated along with wild-type CNF1 and DNT for their capacity to induce morphological and cytopathic effects in HEp-2 and Swiss 3T3 cells after intoxication. In addition, site-specific mutants of CNF1, DNT, and hybrid CNF1/DNT toxins were generated and examined in tissue culture assays to determine the amino acid residues necessary for the phenotypic differences observed between CNF1 and DNT. Lastly, comparative deamidation and transglutamination assays were undertaken with CNF1, DNT, and two site-specific mutant toxins to establish whether the phenotypic differences observed in tissue culture cell assays could correlate with changes in enzymatic activity attributed to single amino acid substitutions within the catalytic domain of each toxin.

Materials and Methods

Bacterial strains, plasmids and growth conditions

The bacterial strains and plasmids used in this study are listed in Table 1. The plasmid pQEDNTwt (DNT) was a gift from Dr. Yasuhiko Horiguchi (Osaka University, Osaka, Japan) (Matsuzawa *et al.*, 2002)], and pDNT103 was a gift from Dr. Alison Weiss (University of Cincinnati, Cincinnati, OH) (Walker and Weiss, 1994). pCNF24 (CNF1), pHisCDHyb1, pHisCDHyb2, and pQEDNTwt (DNT) were transformed into *E. coli* M15(pREP4) and grown in Luria-Bertani (LB) broth supplemented with 100 μg/ml ampicillin and 25 μg/ml kanamycin. After induction of the cultures with a final concentration of 0.1 mM isopropyl-β-D-thiogalactopyranoside (IPTG), CNF1 and CNF1/DNT chimeric proteins were grown at 22-25°C. Expression of DNT and the histidine-tagged control protein dihydrofolate reductase (DHFR) was carried out at 37°C.

Table 1: Bacterial Strains and Plasmids, part 1

Strain or plasmid	Relevant characteristics	Source or reference
E. coli		
XL1-Blue	*recA1 endA1 gyrA96 thi-1 hsdR17supE44 relA1 lac*[F' *proAB*$^{+}$ *lacI*^{q}*Z* ΔM15::Tn *10*(Tet^{r})]	Stratagene
M15(pREP4)	NaI^{s} Str^{s} Rif^{s} Δ*lac-ara-gal-mtl* F^{-} *recA uvr* (pREP4 *lacI* Kan^{r})	Qiagen
DH5α	F- Φ80 d*LacZ*ΔM15 Δ(*lacZYA-argF*)*U169 endA1 recA1 hsdR17* ($r_k^-m_k^+$) *deoR thi-1 phoA supE44λ*$^{-}$*gyrA96 relA*	Invitrogen
Cloning vectors		
pBluescript II SK^{-}	*E. coli* phagemid cloning vector (Amp^{r})	Stratagene
pQE30	*E. coli* expression vector with 6x-His tag 5' to the polylinker (Amp^{r})	Qiagen
pQE40	*E. coli* expression vector with 6x-His tag upstream of the *dhfr* gene and polylinker (Amp^{r})	Qiagen
pGEX-2T	*E. coli* expression vector with GST tag 5' to the polylinker (Amp^{r})	Qiagen
Plasmids		
pQEDNTwt[a]	wt *dnt* gene cloned into BamHI/HindIII sites of pQE40	(Matsuzawa *et al.*, 2002)
pHLK102	wt *cnf1* gene (nt -31-3069) from UPEC strain J96 cloned into SmaI site of pBluescript II SK^{-}	(Meysick *et al.*, 2001)
pDNT103	3.1 kb Not-ApaI fragment of the *dnt* gene cloned into pBluescript II KS^{+}	(Walker and Weiss, 1994)
pCNF24	wt *cnf1* gene (nt 1-3045) amplified from pHLK102 and cloned into BamHI/KpnI sites of pQE30	(Meysick *et al.*, 2001)
pHisCDHyb1	Chimeric toxin gene that encodes the first 823 amino acids of CNF1 followed by the last 202 amino acids of DNT cloned into the BamHI/ KpnI sites of pQE30	This study

Table 1 (cont.)

pHisCDHyb2	Chimeric toxin gene that encodes the first 823 amino acids of CNF1, 102 amino acids of DNT, and the last 89 amino acids of CNF1 cloned into the BamHI/KpnI sites of pQE30	This study
pHisCNF1 T884K	pCNF24 with a site-specific mutation that results in a threonine to lysine substitution at amino acid position 884	This study
pHisDNT K1310T	pQEDNTwt with a site-specific mutation that results in a lysine to threonine substitution at amino acid position 1310	This study
pHisCDHyb2 K1310T	pHisCDHyb2 with a site-specific mutation that results in a lysine to threonine substitution within the DNT portion of the hybrid toxin	This study
pGEX-2T-wtRhoA	*rhoA* gene cloned into pGEX-2T	(Hall, 1994)
pGEX-2T-wtRac1	*rac1* gene cloned into pGEX-2T	(Hall, 1994)
pGEX-2T-G25K	*cdc42* gene cloned into pGEX-2T	(Hall, 1994)

[a] The GenBank accession number for the *dnt* gene is AB020025.

Proteins were purified over HisTrap™ Ni^{2+}-affinity columns with the fast phase liquid chromatography (FPLC) ÄKTA system as per the manufacturer's protocol (GE Healthcare). Plasmids pGEX-2T-wtRhoA, pGEX-2T-wtRac1, and pGEX-2T-G25K (Cdc42) were gifts from Dr. Alan Hall (University College London, London, UK) (Self and Hall, 1995) and were maintained in *E. coli* DH5α grown on LB agar or in LB broth supplemented with 100 μg/ml ampicillin. RhoA, Rac1 and Cdc42 were purified over GSTrap HP™ affinity columns with the FPLC ÄKTA system as per the manufacturer's protocol (GE Healthcare).

Generation of CNF1/DNT hybrids and mutants

Splicing by overlap extension polymerase chain reaction (SOEing PCR) (Horton, 1993) was used to construct hybrid toxin genes with the primers listed in Table 2. To generate pHisCDHyb1, a 456 bp fragment of the *cnf1* gene from pHLK102 was amplified with primers CSO1 and CNDN5 while a 608 bp fragment of *dnt* was amplified from pDNT103 with primers DSO1 and DSO2. These two fragments were then spliced together by amplification with primers CSO1 and DSO2. The final 1064 bp product was cloned into the NcoI and KpnI sites of pHLK102 and then the fragment subcloned into the BamHI and KpnI sites of the histidine-tagged expression vector pQE30 (Qiagen) to yield pHisCDHyb1. Plasmid pHisCDHyb2 was constructed in a similar manner. Briefly, a 453 bp segment of *dnt*, which encodes the 100 amino acid stretch with the greatest homology to CNF1, was amplified from pHisCDHyb1 with primers 3195F and CNDN3, and a 273 bp fragment that encodes the last 89 amino acids of CNF1 was amplified from

Table 2: Primers used for splicing by overlap extension PCR

Primer	Sequence[a]
CSO1	5'-TTCATATGTTAATCATTGGG
CNDN5	5' GATCCGCACATTGTCGGTCAGATTATACTTCTTCCAATAAGT TGAGCC
DSO1	5'-CTGACCGACAATGTGCGGATC
DSO2	5'-ACGGGTACCTCAGACCGGCGCCGGAAAC
3195F	5'-AAAGATCGCTTTGATAACCATGGC
CNDN3	5'-TTCCGACAGATAATCGACCAAGTCGTCATTGCGC
CN3630	5'-GTCGATTATCTGTCGGAA
3900	5'-ACGGGTACCTCAAAATTTTTTTGAAAATACC
T884KT	5'-CCAGCCAAAGATTTTGTT**T**TACCAGTATGTACC
T884KB	5'-GGTACATACTGGTA**A**AACAAAATCTTTGGCTGG
1310TT	5'-GAGTTCGGTCGAC**G**TGCCAGTGTGGTAGAA
1310TB	5'-TTCTACCACACTGGCA**C**GTCGACCGAACTC

[a]Overlapping *dnt* or *cnf1* sequences are underscored, bold and underlined nucleotides indicate those residues that have been mutagenized.

pHLK102 with primers CN3630 and 3900. These two fragments were then spliced together by amplification with primers 3195F and 3900 and, after a series of subcloning steps, the final fragment was inserted into the BamHI and KpnI sites of pQE30 to yield pHisCDHyb2. Site-directed mutants of CNF1, DNT, and the chimeric CDHyb2 toxin were generated with either the QuikChange or QuikChange XL site-directed mutagenesis kits from Stratagene. To construct the CNF1 mutant plasmid pCNF1 T884K, pCNF24 was amplified with primers designed to generate a Thr to Lys substitution at position 884 (primers T884KT and T884KB, Table 2). The DNT and chimeric CDHyb2 mutant plasmids, pQEDNTwt K1310T and pHisCDHyb2 K1310T, were generated by amplification of either pQEDNTwt or pHisCDHyb2 with primers specifically engineered to convert Lys^{1310} to a threonine residue (primers 1310TT and 1310TB, Table 2). The mutated *dnt* gene from pQEDNTwt K1310T was then subcloned into pQE30 to yield pDNT K1310T.

Cell lines and media

HEp-2 cells, a human laryngeal cell line (ATCC CCL-23), were grown at 37°C with 5% CO_2 in Eagle's minimal essential medium with Earle's balanced salt solution (BioWhittaker) supplemented with 10% fetal bovine serum (Biosource), 2 mM L-glutamine (Invitrogen), 10 µg/ml gentamicin, 10 U/ml penicillin, and 10 µg/ml streptomycin. Mouse fibroblast Swiss 3T3 cells (ATCC CCL-92) were grown at 37°C with 5% CO_2 in Dulbecco's modified Eagle's medium that contained 4.5 g/l glucose and 1.5 g/l sodium bicarbonate (Invitrogen) and was supplemented with 4 mM L-glutamine

(Invitrogen) and 10% bovine calf serum (Gemini Bio-Products).

Determination of the conformational integrity of the CNF1/DNT hybrids

Native and denatured dot blot analyses were used to assess the conformational structure of each chimeric toxin. Briefly, 100 µg/ml stocks of purified CNF1 and CNF1/DNT hybrids were diluted in either phosphate-buffered saline (PBS; native) or 6X sodium dodecyl sulfate (SDS)/dithiothreitol (DTT) buffer (denatured) to a final concentration of 6.67 µg/ml and transferred to nitrocellulose membranes with a Minifold Micro-Sample Filtration Manifold (Schleicher & Schuell). Toxins diluted in denaturation buffer were boiled at 95°C for 5 minutes prior to transfer. Membranes were dried and then blocked overnight at 4°C in BLOTTO (Tris-buffered saline, 5% skim milk, 0.05% Tween-20). Blots were probed with a panel of CNF1-specific monoclonal antibodies (Meysick *et al.*, 2001), followed by incubation with horseradish peroxidase (HRP)-conjugated goat anti-mouse IgG (Roche). Reactive proteins were visualized with diaminobenzamidine (DAB; Sigma).

Tissue culture assays

HEp-2 cell multinucleation assay: HEp-2 multinucleation assays were performed as previously described (Mills *et al.*, 2000) with several modifications. Cells (4×10^3 cells/well) were seeded into 96-well microtiter plates (Costar) and incubated for 4 hours at 37°C with 5% CO_2. Purified CNF1, DNT, CNF1/DNT hybrids and mutant toxins were added at concentrations that ranged from 100 ng to 0.2 ng per well and plates were incubated for 72 hours at 37°C in 5% CO_2. The cells were then fixed and stained with

Hema-3 (Fisher Scientific) and subsequently scored for the degree of multinucleation by light microscopy.

Swiss 3T3 binucleation: Swiss 3T3 binucleation assays were done according to a previously described method (Horiguchi *et al.*, 1993) with several modifications. Briefly, Swiss 3T3 cells (2 x 10^3 cells/ml) were seeded into 24-well plates (Costar) and incubated for 48 hours at 37°C with 5% CO_2. Purified CNF1, DNT, CNF1/DNT hybrids and mutant toxins were added to the cells at concentrations that ranged from 25 ng to 20 μg per well and the plates then incubated for 6 days at 37°C in 5% CO_2. Intoxicated cells were fixed and stained with Hema-3 (Fisher Scientific), and scored for the degree of binucleation by light microscopy.

Swiss 3T3 cell cytotoxicity assay

Cytotoxicity assays were done as previously described (Teel *et al.*, 2002) with the following modifications. Twenty-four well plates (Costar) were seeded with 2 x 10^3 cells/ml and intoxicated with purified wild-type, hybrid, and mutant toxins as described above. After incubation, cells were fixed, stained with Hema-3 and the absorbance of wells measured at 540 nm with an automated SpectraMax M2 multimode microtiter plate reader (Molecular Devices). Statistical significance was determined by analysis of variance (ANOVA) with SPSS version 11.0 software.

Modification of small Rho GTPases

Deamidation assay: Deamidation assays were done according to previously described procedures (Schmidt *et al.*, 1997) with the following modifications. Briefly, a 20:1 molar

ratio of GTPase (RhoA, Rac1 or Cdc42) to toxin was incubated in deamidation buffer (50 mM NaCl, 50 mM Tris-HCl pH 7.4, 5 mM $MgCl_2$, 1 mM dithiothreitol, 1 mM phenylmethanesulfonyl fluoride) for either 30 minutes or 2 ½ hours at 37°C. Untreated RhoA served as a negative control. After toxin treatment, samples were concentrated by the addition of 10% trichloroacetic acid and stored overnight at 4°C. Precipitated proteins were pelleted, washed with acetone, air-dried and resuspended in 20 mM Tris-HCl pH 7.4. Samples were subjected to sodium dodecyl sulfate-polyacrylamide gel electrophoresis (SDS-PAGE) (12% acrylamide) and then proteins were transferred to 0.45 μm pre-cut nitrocellulose membranes (Bio-Rad) with a Trans-Blot semi-dry electrophoretic transfer cell (Bio-Rad). Membranes were blocked overnight at 4°C in BLOTTO and then incubated with either an anti-RhoA (1:1500, Santa Cruz Biotechnology), anti-Rac1 (1:5000, Upstate Biotechnology), or anti-Cdc42 (1:1000, Santa Cruz Biotechnology) monoclonal antibody or rabbit polyclonal antisera (1:2000) that had been raised against a peptide antigen specifically designed to detect modified/deamidated RhoA/Rac1/Cdc42 (Sugai *et al.*, 1999). Reactive proteins were detected with either a HRP-conjugated goat-anti mouse IgG (Roche) or donkey anti-rabbit IgG (1:3000, GE Healthcare) followed by visualization with DAB (Sigma). The pixel density of total and modified GTPases was analyzed with NIH ImageJ 1.34S software (http://rsb.info.nih.gov/ij/). Percent modification was calculated using the values derived from ImageJ and the following formula: (modified GTPase value/total GTPase value) x 100%.

Transglutamination assay: Transglutamination assays were done as previously described (Schmidt *et al.*, 1999) with several modifications. Briefly, a 2:1 molar ratio of RhoA to

toxin was incubated in transglutamination buffer (50mM Tris-HCl pH 7.4, 8mM $CaCl_2$, 5mM $MgCl_2$, 1mM dithiothreitol, 1mM EDTA) in the presence of ethylenediamine (50mM, pH 9) for 10 minutes or 1 hour at 37°C. As a negative control, RhoA was incubated with ethylenediamine but without toxin. Samples (0.25 μg RhoA/well) were subjected to SDS-PAGE and then processed for Western blot analyses as described above. Immunoblots were probed with a mouse anti-RhoA monoclonal antibody (1:1500, Santa Cruz Biotechnology) and reactive proteins visualized with ECL (GE Healthcare) after incubation with a HRP-conjugated goat anti-mouse IgG secondary antibody.

Results

Comparison of the morphological responses of HEp-2 and Swiss 3T3 cells to intoxication with wild-type CNF1 and DNT

Whereas many tissue culture cell lines appear to be sensitive to CNF1 intoxication (Chung *et al.*, 2003; Horiguchi, 2001), only a few cell lines are known to be susceptible to DNT (Horiguchi, 2001). HEp-2 cells, a human laryngeal cell line, demonstrate extreme sensitivity to CNF1 intoxication and exhibit prominent multinucleation as a result of endomitosis in the absence of cytokinesis (Fiorentini *et al.*, 1988); however, the effects of DNT on this cell line have not been reported. Therefore, we tested wild-type CNF1 and DNT toxins in a standard HEp-2 multinucleation assay (Mills *et al.*, 2000). HEp-2 cells were intoxicated with 100 ng/well of each wild-type toxin, or serial dilutions thereof, and wells were scored from 0-5 for the degree of multinucleation, with 5 representative of greater than 90% multinucleation of the cells and 0 indicative of

background levels. At the highest concentration of toxin used (100 ng), HEp-2 cells incubated with CNF1 exhibited greater than 90% multinucleation (Figure 6A), while cells incubated with DNT showed only background levels of multinucleation (Figure 6B). Even when a 1000-fold higher concentration of DNT (100 µg/well) was used to intoxicate HEp-2 cells, multinucleation remained at background levels (data not shown). This finding suggests that HEp-2 cells may not express the receptor for DNT. As HEp-2 cells were resistant to DNT intoxication, we next exposed Swiss 3T3 cells, a DNT-sensitive fibroblast cell line (Fukui and Horiguchi, 2004), to both toxins. Swiss 3T3 cells were intoxicated with increasing concentrations of either CNF1 or DNT, and wells were scored for binucleation as described above. In the presence of wild-type DNT, Swiss 3T3 cells showed significant binucleation as well as a lesser degree of multinucleation (Figure 6E). CNF1-intoxicated Swiss 3T3 cells also showed binucleation (Figure 6D); however, CNF1 appeared to be cytotoxic to Swiss 3T3 cells and induced cytoplasmic projections from cells that were intoxicated with 10 µg or more of purified toxin. This apparent cytotoxicity is unique to CNF1, in that, the same concentration of DNT caused binucleation without any disruption of the monolayer. The finding that CNF1 is cytotoxic to Swiss 3T3 cells has not been previously reported.

CNF1/DNT hybrid toxins are conformationally similar to CNF1 but phenotypically resemble DNT

CNF1 and DNT share homology in their C-termini, which contain the enzymatic domains of each toxin. The highest degree of similarity (45%) between these two toxins lies within a 100 amino acid (aa) stretch (CNF1 aa 824-888, DNT aa 1250-1314) that

Figure 6: Morphological Responses of HEp-2 and Swiss 3T3 Cells After Intoxication with CNF1 or DNT

HEp-2 cells incubated for 72 hours with 100 ng of each toxin are shown in panels A-C and Swiss 3T3 cells incubated for 6 days with 10 μg of each toxin are shown in panels D-F. Panels A and D, cells intoxicated with CNF1; panels B and E, cells intoxicated with DNT; and panels C and F, cells incubated with DHFR (negative control). 10x objective. The final images of Swiss 3T3 cells were prepared with Adobe Photoshop version 6.0.1.

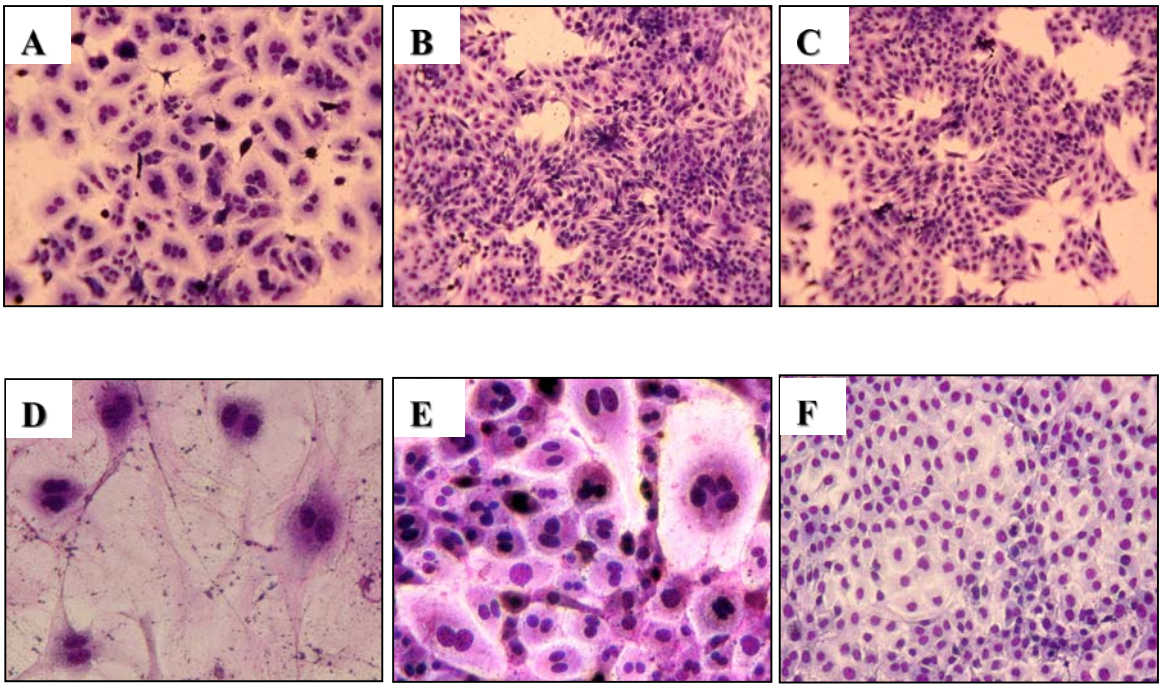
A
B
C
D
E
F

includes amino acids previously shown to be essential for enzymatic activity (Meysick *et al.*, 2001). Two CNF1/DNT hybrid toxins were generated to determine whether the phenotypic differences observed between HEp-2 and Swiss 3T3 cells intoxicated with CNF1 or DNT were directly related to the C-terminus of the toxin. As shown in Figure 7, hybrid toxins were designed to contain either CNF1 with the entire C-terminus of DNT (CDHyb1) or CNF1 with only a small portion of DNT (CDHyb2), namely the 100 amino acid region with highest homology between CNF1 and DNT, which includes the three amino acids essential for the enzymatic activity of DNT (Cys^{1292}, His^{1307} and Lys^{1310}). To ensure that the CNF1/DNT hybrid toxins were folded correctly and structurally similar to wild-type CNF1, each toxin was evaluated in native and denatured dot blot analyses against a panel of CNF1 monoclonal antibodies that recognized various regions of the toxin molecule (Fig. 8A) (Meysick *et al.*, 2001). As shown in Figure 8B, the CNF1 monoclonal antibodies used were able to recognize both wild-type CNF1 (lane 1) as well as the CNF1 portions of the two CNF1/DNT hybrid molecules (lanes 3 and 4) under native conditions but not under denaturing conditions. These findings strongly suggest that while each hybrid toxin contains various portions of DNT both toxins remain conformationally similar to CNF1.

To determine whether the CNF1/DNT chimeric toxins induced phenotypic changes more indicative of CNF1 or DNT, the hybrid molecules were used to intoxicate HEp-2 and Swiss 3T3 cells. In HEp-2 cell multinucleation assays, greater than 50% of the cells could be induced to multinucleate by the addition of as little as 0.2 ng of wild-type CNF1; however, even when higher concentrations were used (10 to 100 μg, data not shown), neither of the hybrid toxins demonstrated the capacity to elicit multinucleation

Figure 7: Diagrammatic Representation of Wild-type CNF1, DNT, Hybrid and Mutant Toxins

For all toxin molecules, the amino acid residues required for enzymatic activity or those that were mutated are shown.

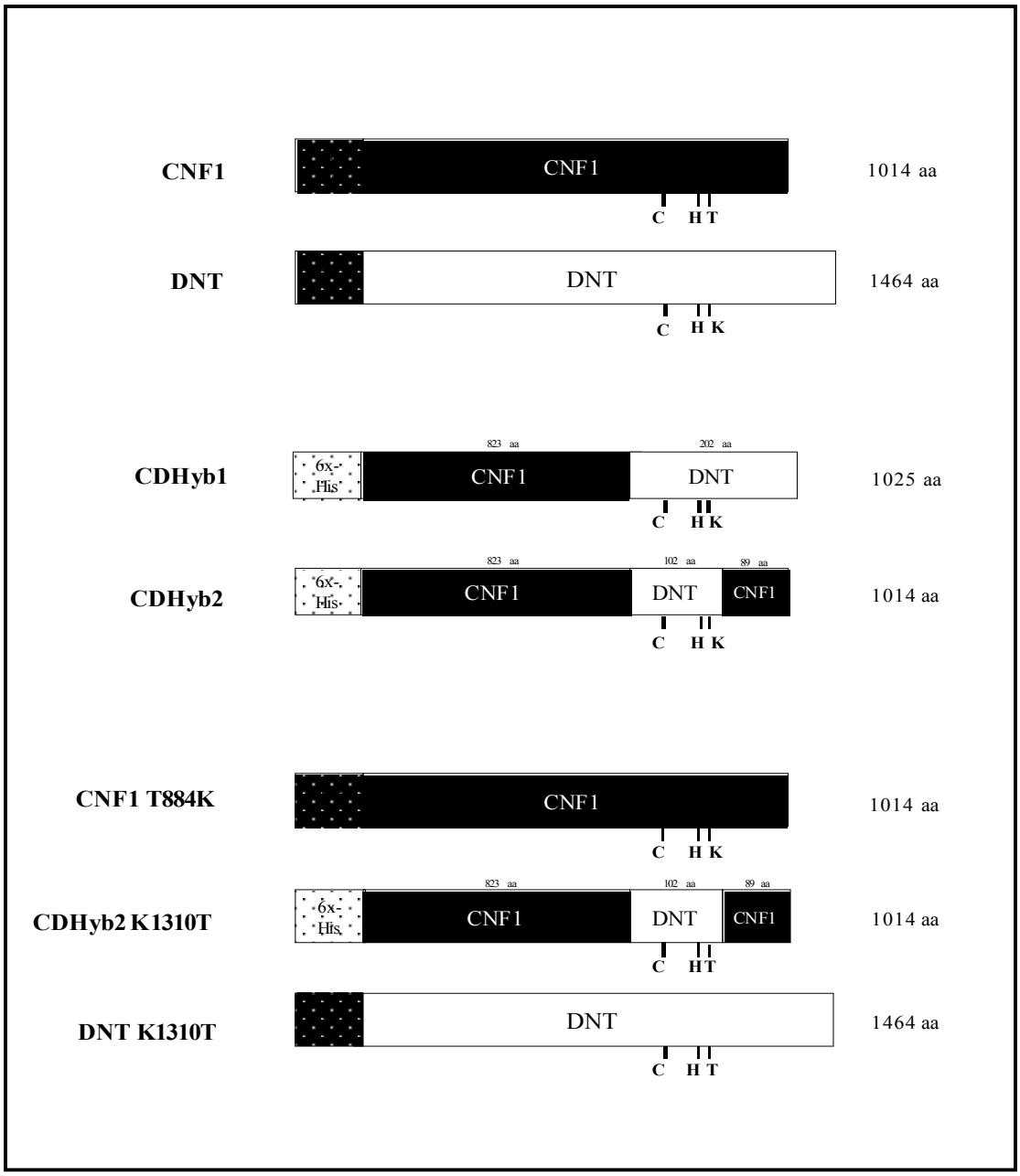
CNF1
CNF1
1014 aa
C H T
DNT
DNT
1464 aa
C H K
CDHyb1
6x-His
823 aa
CNF1
202 aa
DNT
1025 aa
C H K
CDHyb2
6x-His
823 aa
CNF1
102 aa
DNT
89 aa
CNF1
1014 aa
C H K
CNF1 T884K
CNF1
1014 aa
C H K
CDHyb2 K1310T
6x-His
823 aa
CNF1
102 aa
DNT
89 aa
CNF1
1014 aa
C H T
DNT K1310T
DNT
1464 aa
C H T

Figure 8: Dot Blot Analysis of the CNF1/DNT Hybrids and Site-Directed Mutants

Panel A: Schematic diagram of CNF1 with the epitopes recognized by the select CNF1 monoclonal antibodies indicated. Patterned areas signify the DNT regions in the hybrid toxins. Panel B: Purified toxins (667 ng) were either applied directly to nitrocellulose strips (left-hand panels) or were denatured (SDS/DTT/boiling) prior to their use (right-hand panels). Blots were probed with the indicated anti-CNF1 monoclonal antibodies and reactive proteins visualized with an appropriate HRP-conjugated secondary antibody and diaminobenzamidine (DAB) substrate. Lane 1, CNF1; lane 2, CNF1 T884K; lane 3, CDHyb1; lane 4, CDHyb2; lane 5, CDHyb2 K1310T.

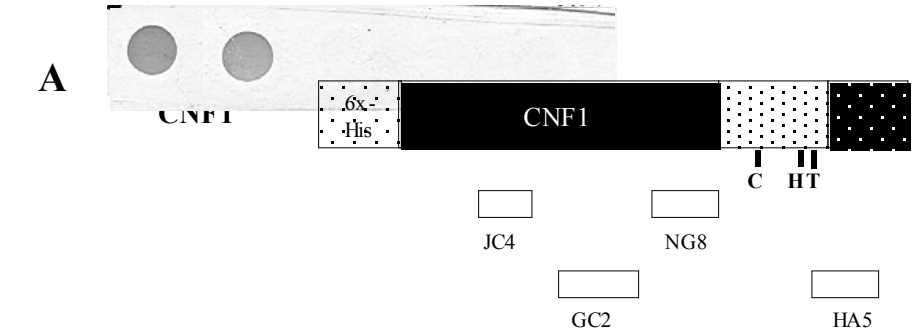
A
6x-His
CNF1
C
HT
JC4
NG8
GC2
HA5

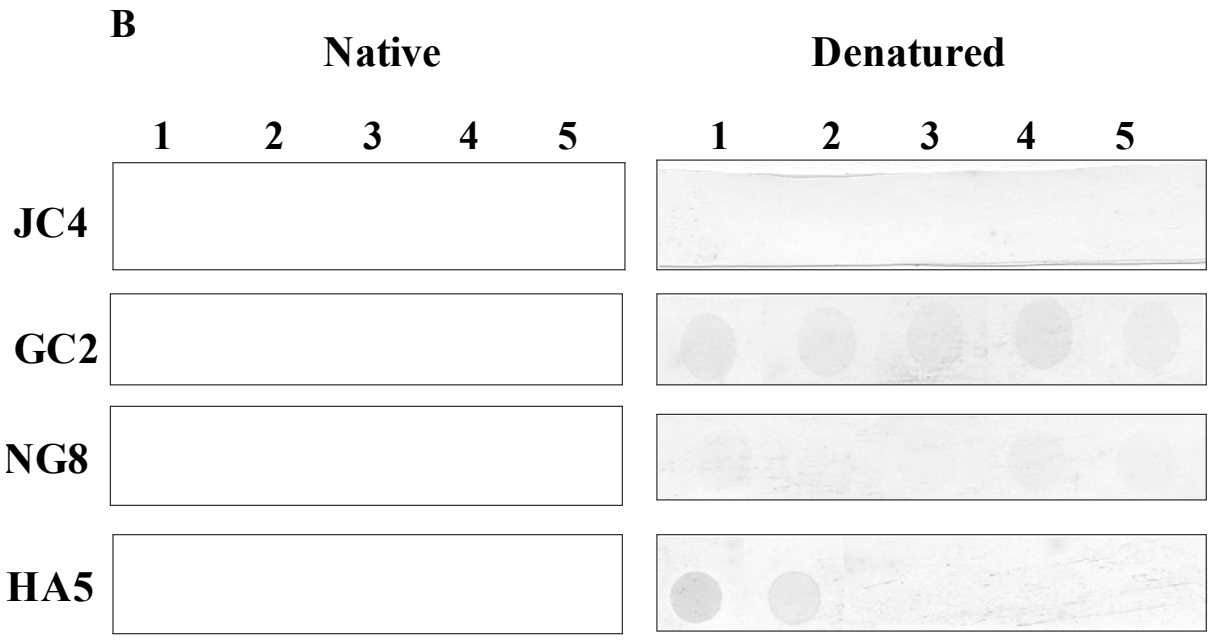
B
Native
Denatured
1 2 3 4 5
1 2 3 4 5
JC4
GC2
NG8
HA5

above background levels. The inability of the hybrid toxins to induce a notable phenotype on HEp-2 cells resembled our earlier observations made when wild-type DNT was incubated with this cell line (Fig. 6B). Although the CNF1/DNT hybrids appeared to behave more like DNT than CNF1 when assayed on HEp-2 cells, the possibility did exist that although the chimeric toxins maintained the same conformational properties as CNF1, they were enzymatically inactive. To assess whether the hybrids were enzymatically active, RhoA deamidation assays were performed. RhoA was incubated in the presence of each purified toxin and then samples were examined in Western blots probed with specific modified RhoA peptide anti-sera that would only recognize deamidated RhoA. We found that RhoA was deamidated by wild-type CNF1 and DNT as well as both of the hybrid toxins (data not shown), observations that demonstrated the enzymatic activity of these hybrids.

Since the hybrid toxins did not mediate a phenotype similar to that of CNF1 in HEp-2 cells, we next investigated the effects produced by these chimeric toxins on Swiss 3T3 cells, a DNT-sensitive cell line. In binucleation and cytotoxicity assays, the morphological responses induced by the CNF1/DNT hybrids were found to be closer to the effects seen after DNT intoxication. Although CNF1, DNT and the chimeric toxins could mediate binucleation of Swiss 3T3 cells (Fig. 9, panels B, F, J and data not shown), only CNF1 appeared cytotoxic to this cell line [Fig. 10; CNF1 versus DNT, $p=0.024$ (10µg); CNF1 versus CDHyb2, p values of 0.077 (10µg) and 0.022 (20 µg)]. Taken together, these findings indicate that the C-terminal portion of DNT and, more specifically, a small 100 amino acid stretch of this region was sufficient to impart a DNT-like phenotype to CNF1.

Figure 9: The Effects of CNF1, DNT and Site-Directed Mutant Toxins on HEp-2 and Swiss 3T3 Cells

Left-hand panels: HEp-2 cells intoxicated for 72 hours with 100 ng of each toxin. Right-hand panels: Swiss 3T3 cells intoxicated for 6 days with 10 μg of each toxin. Because of its high level of cytotoxicity, only 300 ng of DNT K1310T was used to show the morphological changes induced in Swiss 3T3 cells (panel H). 10x objective. Final images of Swiss 3T3 cells were prepared with Adobe Photoshop version 6.0.1.

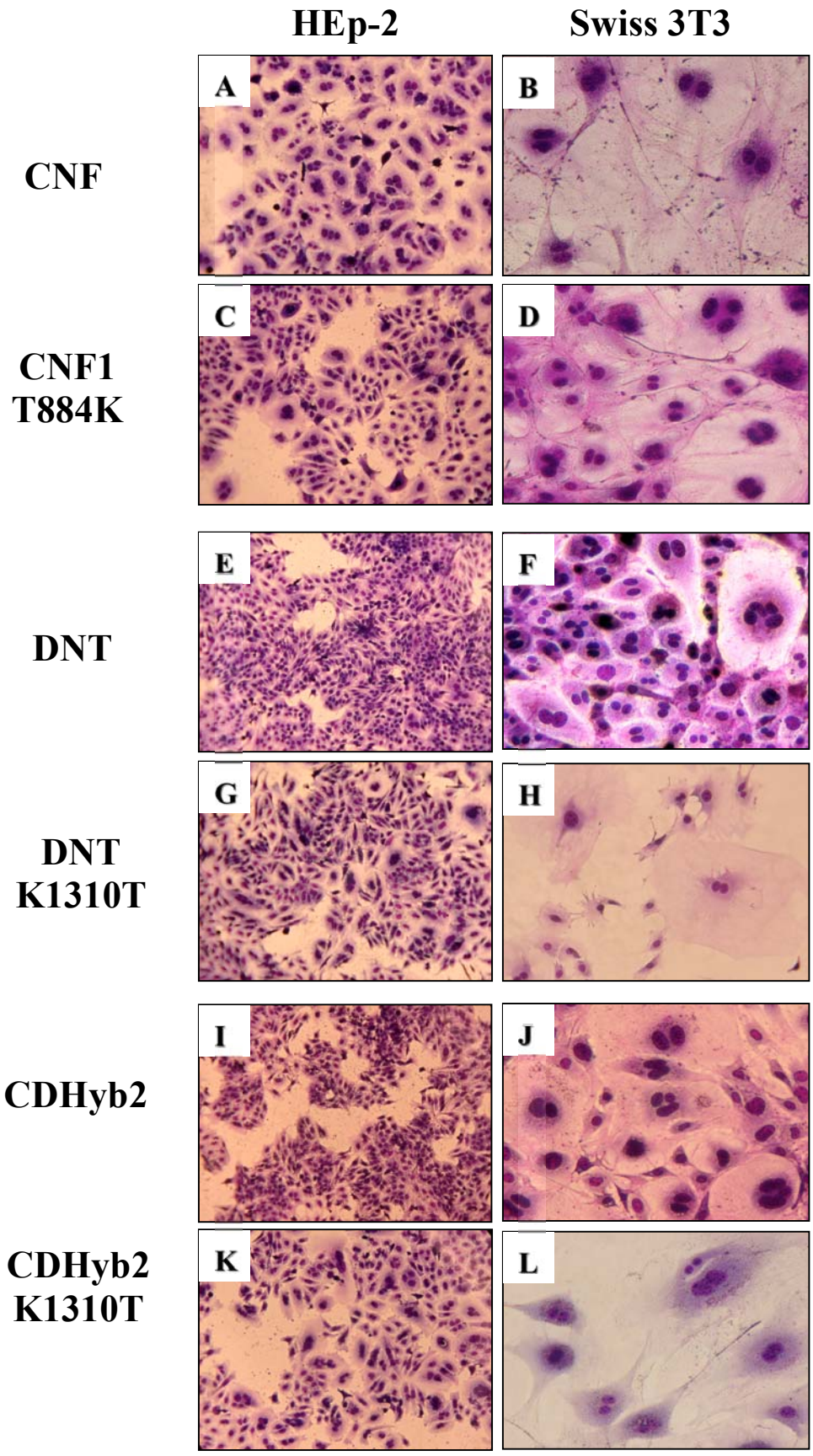
HEp-2
Swiss 3T3
CNF
CNF1 T884K
DNT
DNT K1310T
CDHyb2
CDHyb2 K1310T
A
B
C
D
E
F
G
H
I
J
K
L

Figure 10: Swiss 3T3 Cytotoxicity Assays

Toxin-treated Swiss 3T3 cells were fixed, stained and assessed for cytotoxicity at A_{540nm} with a microtiter plate reader. Data were analyzed by ANOVA, and statistical differences between wild-type and mutant toxins are indicated with an asterisk or cross. Results shown are the averages from 3 separate experiments. Standard error bars based on ANOVA analysis (not shown) extend 0.08 units above and below the mean.

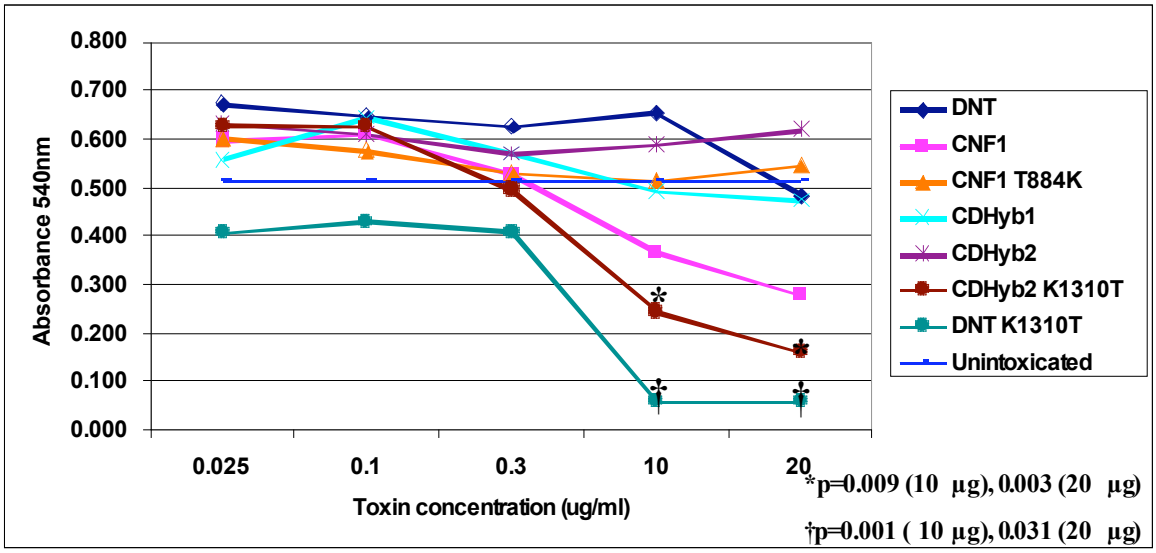
0.800
0.700
0.600
0.500
0.400
0.300
0.200
0.100
0.000
Absorbance 540nm
0.025
0.1
0.3
10
20
Toxin concentration (ug/ml)
DNT
CNF1
CNF1 T884K
CDHyb1
CDHyb2
CDHyb2 K1310T
DNT K1310T
Unintoxicated
*p=0.009 (10 µg), 0.003 (20 µg)
†p=0.001 (10 µg), 0.031 (20 µg)

Single amino acid substitutions in the catalytic region of wild-type CNF1 and DNT can mediate phenotypic changes to intoxicated cells and alter enzymatic activity

Since the replacement of a small portion of the C-terminal region of CNF1 (aa 824-888) with the homologous region of DNT (aa 1250-1314) conferred a DNT-like phenotype to hybrid toxin CDHyb2, we next examined whether specific amino acids within this region were responsible for the alteration in phenotype. In DNT, three amino acids (Cys^{1292}, His^{1307} and Lys^{1310}) are known to be essential for enzymatic activity and are believed to compose a catalytic triad within the toxin (Schmidt *et al.*, 1999). CNF1 also requires specific cysteine (Cys^{866}) and histidine (His^{881}) residues for enzymatic activity (Boquet, 2001); however, unlike the catalytic triad identified in DNT, CNF1 contains a threonine (Thr^{884}) residue at the third position of the triad rather than a lysine (Boquet, 2001; Schmidt *et al.*, 1998). Since the last residue within the catalytic triad is unique to each toxin, we reasoned that this amino acid could be important in conferring the different phenotypes attributed to each toxin. To test this possibility, a series of mutant toxins were constructed in which the specific threonine residue was changed to a lysine (CNF1 T884K) or the reciprocal change was made (DNT K1310T and CDHyb2 K1310T; Fig. 7). Native and denatured dot blot analyses with the same CNF1 monoclonal antibodies previously used to confirm the conformational integrity of the CNF1/DNT hybrid toxins indicated that the amino acid substitutions in the CNF1 T884K or CDHyb2 K1310T toxins did not significantly alter the structure of either of these toxins from that of wild-type CNF1 (Fig. 8B, lanes 2 and 5).

Next, the effects of these mutant toxins were assessed on HEp-2 and Swiss 3T3 cell lines to determine the specific phenotype mediated by each. In HEp-2 multinucleation

assays at equivalent concentrations, mutant toxin CNF1 T884K showed a dramatic reduction in its capacity to induce multinucleation compared to wild-type CNF1 (Fig. 9C and A, respectively). Whereas 0.2 ng of wild-type CNF1 was sufficient to multinucleate 50% of HEp-2 cells, 100 ng of CNF1 T884K was required to produce an equivalent degree of multinucleation (data not shown). Cells intoxicated with either CDHyb2 K1310T (Fig. 9K) or DNT K1310T (Fig. 9G) exhibited a moderate increase in the degree of multinucleation induced compared to their respective toxin controls (CDHyb2 and DNT, Fig. 9I and E, respectively). These results suggest that within the catalytic triad the nature of the third amino acid can strongly influence the extent of the multinucleation phenotype in HEp-2 cells, with the presence of a threonine found to enhance multinucleation and that of a lysine shown to significantly diminish this effect.

Similar changes in morphological responses were also seen when the mutant toxins were incubated with Swiss 3T3 cells. Compared to wild-type CNF1, the CNF1 T884K mutant toxin still appeared to possess the capacity to binucleate cells (Fig. 9D); however, its cytotoxicity against this cell line was reduced (Fig. 10) and more closely resembled the phenotype induced by DNT (Fig. 9F). Likewise, the substitution of a threonine for a lysine in the DNT K1310T and CDHyb2 K1310T mutants caused these toxins to become significantly more cytotoxic than the toxins from which they were derived [Fig. 10, DNT K1310T p values of 0.001 (10μg) and 0.031 (20 μg) compared to DNT; CDHyb2 K1310T p values of 0.009 (10 μg) and 0.003 (20 μg) compared to CDHyb2], findings that were comparable to the effects observed after intoxication with CNF1. In addition, those cells that survived treatment with DNT K1310T or CDHyb2 K1310T were more similar in morphology to CNF1-intoxicated Swiss 3T3 cells with binucleation and

numerous cytoplasmic extensions projected from affected cells (Fig. 9H and L, respectively). Taken together, these results indicate that the identity of the third amino acid within the catalytic triad of CNF1 (threonine) or DNT (lysine) can specifically control the cellular phenotype mediated by either one of these toxins.

To determine whether the phenotypic differences mediated by CNF1, DNT, and their respective site-directed mutants correlated with the previously established substrate specificities and preferences of the two prototype toxins, we tested wild-type and mutant toxins for their capacity to deamidate RhoA, Rac1 and Cdc42 at 30 minutes and 2 ½ hours. To examine the enzymatic efficiency of each toxin, duplicate blots were prepared from deamidation reactions, probed with either a GTPase-specific monoclonal antibody or a peptide antibody, which only recognizes the deamidated form of each GTPase, and the percent deamidation calculated after densitometric analysis. As shown in Figure 11, CNF1, DNT and CNF1 T884K demonstrated similar reaction kinetics and levels of modified RhoA; however, each toxin differed in its capacity to deamidate Rac1. While prolonged incubation with CNF1 resulted in equivalent levels of deamidated RhoA and Rac1, data obtained after 30-minute exposure to the toxin indicated a higher percentage of modified RhoA compared to Rac1 (Figure 11, 44% versus 31%). Although several factors may contribute to this difference in substrate susceptibility (*i.e.*, different enzyme kinetics or efficiency of deamidation), the data are consistent with the substrate preferences previously described for CNF1 [RhoA = Cdc42 > Rac1; (Horiguchi, 2001; Sugai *et al.*, 1999)]. Similarly, the capacity of DNT to modify Rac1 to levels comparable to RhoA at both early and late time points (Figure 11, 56% modified RhoA and Rac1 at

Figure 11: Deamidation of RhoA and Rac1 by Wild-type and Site-directed Mutant Toxins

RhoA and Rac1 were incubated in the presence CNF1 (lane 2), DNT (lane 3), CNF1 T884K (lane 4), or DNT K1310T (lane 5) for the indicated times at 37°C. RhoA or Rac1 alone served as negative controls (lane 1). Left-hand panels were probed with monoclonal antibodies against RhoA (top) or Rac1 (bottom). Right-hand panels were probed with rabbit polyclonal antisera raised against a modified peptide antigen. The pixel density of total and modified GTPases from two independent experiments was used to calculate the average percent modification and is indicated below representative blots.

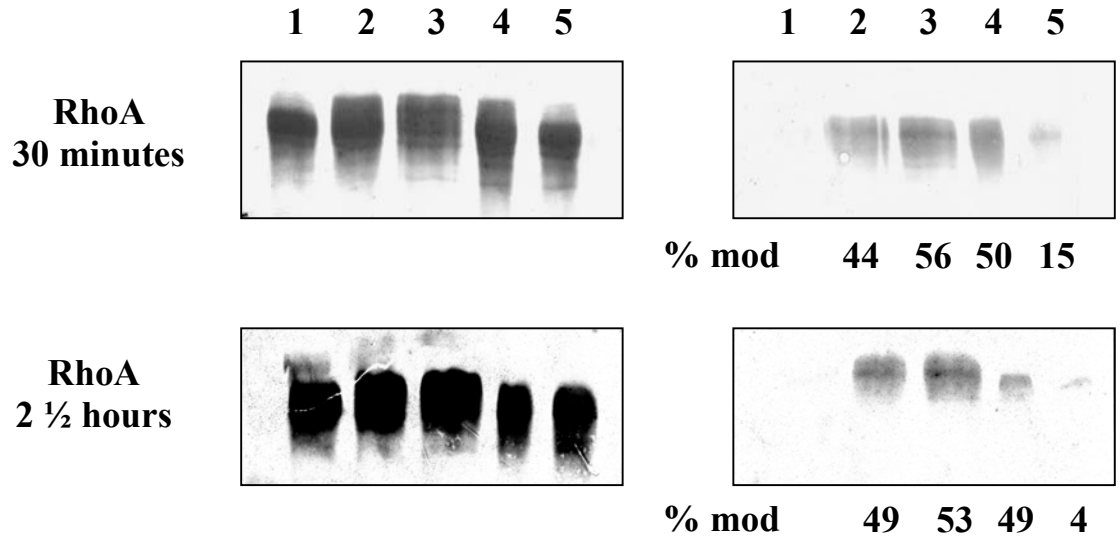
1 2 3 4 5
1 2 3 4 5
RhoA
30 minutes
% mod 44 56 50 15
RhoA
2 ½ hours
% mod 49 53 49 4

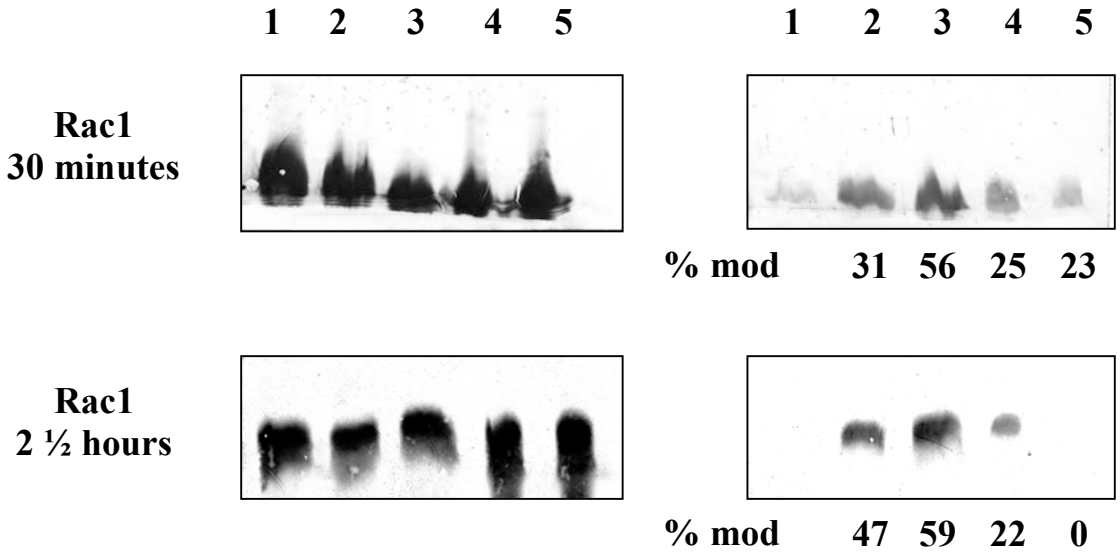
1 2 3 4 5
1 2 3 4 5
Rac1
30 minutes
% mod 31 56 25 23
Rac1
2 ½ hours
% mod 47 59 22 0

30 min and 53-59% modified RhoA and Rac1 at 2 ½ h) was in keeping with the established substrate preferences of DNT [RhoA = Rac1 >Cdc42; (Horiguchi, 2001)]. The findings also indicate that mutant toxin CNF1 T884K possesses an "intermediate" enzymatic phenotype compared to CNF1 and DNT. Although CNF1 T884K was clearly as effective as both wild-type toxins in its capacity to modify RhoA, it exhibited a consistent but much lower level of Rac1 deamidation at both time points examined (Figure 11). From this result, it appears that CNF1 T884K retains the same general substrate specificity as CNF1 but, in terms of enzyme kinetics, appears more like DNT in that maximal deamidation is achieved relatively early and then maintained. Finally, analysis of the DNT K1310T mutant showed this toxin to be severely defective in its capacity to deamidate either RhoA or Rac1, with maximal activity achieved within 30 minutes followed by a rapid decline in modification. This observation indicates that Lys^{1310} of DNT is essential for deamidation activity and is in accordance with the results of an earlier DNT mutagenesis study (Schmidt *et al.*, 1999). With the exception of DNT K1310T, all toxins were also found to deamidate Cdc42 (data not shown); however, results from kinetic studies with this target substrate proved inconsistent and were therefore not included in the analysis.

Although both CNF1 and DNT possess deamidase and transglutaminase activities, DNT has been shown to preferentially act as a transglutaminase. To determine whether the amino acid changes made to CNF1 and DNT adversely affected transglutaminase activity, wild-type and mutant toxins were incubated with RhoA in the presence of ethylenediamine and samples analyzed by Western blot. As shown in Figure 12, RhoA treated for one hour with the wild-type or site-directed mutant toxins demonstrated a

Figure 12: Transglutamination of RhoA by Wild-type and Mutant Toxins

RhoA was incubated with CNF1, DNT, CNF1 T884K, or DNT K1310T in the presence of ethylenediamine for 10 minutes (top) or one hour (bottom) at 37°C. Western blots were probed with an anti-RhoA monoclonal antibody and reactive proteins visualized with an appropriate HRP-conjugated secondary antibody and ECL. Vertical lines are drawn on the blots to emphasize the downward shift of transglutaminated RhoA compared to the unmodified GTPase.

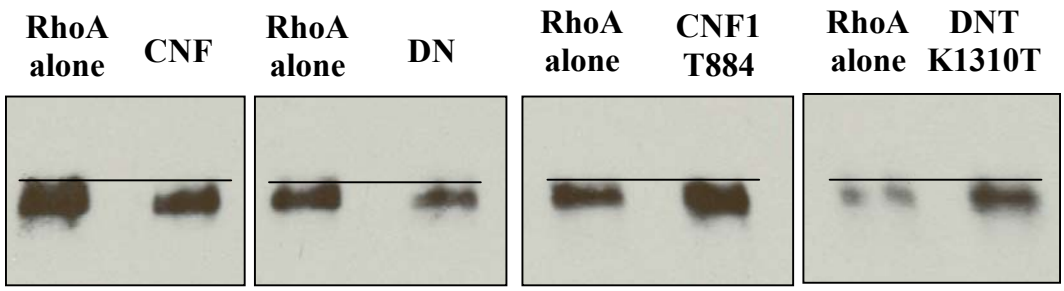
RhoA alone
CNF
RhoA alone
DN
RhoA alone
CNF1 T884
RhoA alone
DNT K1310T

1 hour

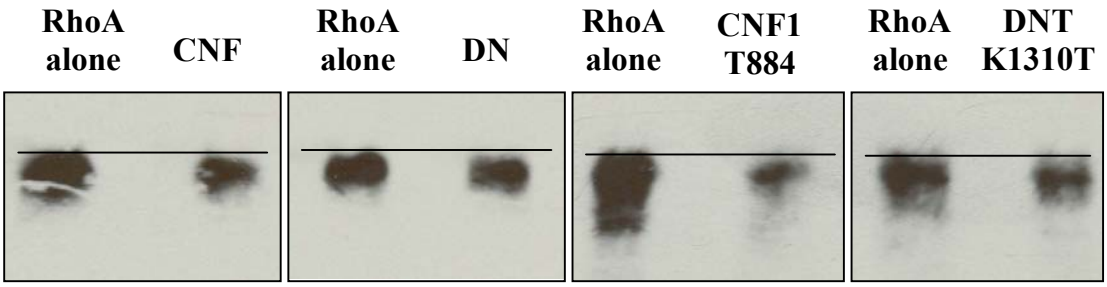
RhoA alone
CNF
RhoA alone
DN
RhoA alone
CNF1 T884
RhoA alone
DNT K1310T

small downward shift in mobility compared to untreated substrate, indicative of RhoA transglutamination (Masuda *et al.*, 2000; Schmidt *et al.*, 1999). A similar shift was apparent when RhoA was incubated in the presence of CNF1 and DNT for 10 minutes (Figure 12); however, the site-directed mutant toxins, CNF1 T884K and DNT K1310T, did not appear to transglutaminate RhoA within this short incubation period (Figure 12). This latter observation suggests that the site-directed mutant toxins are less efficient than the parent toxins in their capacity to transglutaminate RhoA. Taken together with the results from deamidation assays, these data suggest that Lys^{1310} of DNT is critical for deamidation of all three GTPase substrates but may not be essential for transglutamination of RhoA.

The fact that DNT K1310T retained the capacity to transglutaminate was unexpected given that previous published reports indicate that a $Lys^{1310}\rightarrow$Ala substitution in DNT produces an enzymatically inactive, non-cytotoxic molecule (Pullinger *et al.*, 1996; Schmidt *et al.*, 1999). Interestingly, DNT engineered with an alternative substitution at this site ($Lys^{1310}\rightarrow$Arg) retained cytoxicity against embryonic bovine lung cells (Pullinger *et al.*, 1996). These data, along with the results obtained in this study, suggest that structural changes within the vicinity of the catalytic His^{1307} of DNT (*i.e.*, amino acid substitutions at Lys^{1310}) could indirectly influence the enzymatic activity of the toxin and hence the phenotypic effects observed in cell culture.

Conclusions

The A:B toxins CNF1 and DNT contribute to the virulence of uropathogenic *E. coli* and *B. bronchiseptica*, respectively. These toxins also display similar but distinguishable

modes of action and share up to 45% identity in small stretches of their C-terminal catalytic domains. Despite their similarities, numerous independent reports indicate that CNF1 and DNT induce dramatically different morphological changes in eukaryotic cells; however, none of these studies have directly compared the phenotypic effects induced by each toxin on the same cell line. Therefore, we chose to examine the effects of CNF1 and DNT on two cell lines: HEp-2 cells, which have been previously identified as being CNF1 sensitive (Donelli and Fiorentini, 1992; Fiorentini *et al.*, 1988; Mills *et al.*, 2000), and Swiss 3T3 cells, a DNT-sensitive fibroblast cell line (Fukui and Horiguchi, 2004). As expected, HEp-2 cells intoxicated with CNF1 became enlarged and showed significant multinucleation; however, this cell line did not appear to be sensitive to DNT. In contrast, Swiss 3T3 cells were not only found to be sensitive to DNT, as previously reported (Fukui and Horiguchi, 2004), but were also highly sensitive to CNF1. Both DNT and CNF1 could mediate the binucleation of Swiss 3T3 cells at low toxin concentrations (25 ng), but only high doses of CNF1 (≥ 10 μg) caused frank cytotoxicity with binucleation and prominent cytoplasmic extensions apparent in the few Swiss 3T3 cells that survived. Although the mechanism of cytotoxicity and its physiological relevance remains unclear, Swiss 3T3 cells appear to be one of only a few cell lines in which CNF1-mediated cytotoxicity has been reported (Mills *et al.*, 2000).

The distinct morphological differences displayed by HEp-2 and Swiss 3T3 cells after intoxication with either CNF1 or DNT provided a means by which to more closely examine the relationship between the enzymatic regions of each toxin and the effects that specific amino acids within these regions have on the observed cellular phenotypes. A series of enzymatically active, structurally intact chimeric toxins were constructed and

evaluated for specific CNF1- or DNT-mediated morphological changes to both HEp-2 and Swiss 3T3 cells in a simple cell assay system. Results obtained from these studies indicated that replacement of as little as 100 amino acids of CNF1 with the corresponding homologous region of DNT could alter the induced cellular phenotype. Hybrid toxin CDHyb2, which was comprised primarily of CNF1 sequence (~90%) and contained only a small enzymatic portion of DNT, completely lost the capacity to multinucleate HEp-2 cells. This loss of activity occurred despite the fact that the hybrid toxin was enzymatically active *in vitro*, possessed the putative N-terminal CNF1 cell binding domain, and remained conformationally similar in structure to wild-type CNF1. Conversely, CDHyb2 was still found to mediate the binucleation of Swiss 3T3 cells but was no longer cytotoxic to this cell line. These data indicate that even within the context of CNF1, DNT amino acids 1250-1314 are sufficient to confer a DNT-like phenotype to intoxicated HEp-2 and Swiss 3T3 cells. This region of DNT contains the catalytic triad (Cys^{1292}, His^{1307} and Lys^{1310}) required for both the deamidation and transglutamination activities of DNT against the small Rho GTPases (Schmidt *et al.*, 1999). CNF1 also preferentially deamidates RhoA, Rac1 and Cdc42; however, it shares only two of the three amino acid members that compose the catalytic triad of DNT (Cys^{866} and His^{881}) (Boquet, 1998; Schmidt *et al.*, 1998). The findings obtained from site-specific mutant derivatives of CNF1, DNT, and the toxin hybrid CDHyb2 strongly suggest that it is the amino acid located at the third position of the catalytic triad that is largely responsible for the phenotypic differences observed between toxin-treated HEp-2 and Swiss 3T3 cells. CNF1 that harbored a threonine to lysine conversion at position 884 showed markedly reduced multinucleation levels on HEp-2 cells and was non-toxic for Swiss 3T3 cells,

whereas the reciprocal conversion (Lys^{1310} to Thr^{1310}) in DNT produced a molecule that was highly toxic to Swiss 3T3 cells and could mediate a low degree of multinucleation in HEp-2 cells. Given that both the wild-type and the site-directed DNT mutant toxins possess the putative N-terminal DNT receptor binding domain (Kashimoto *et al.*, 1999), this latter result suggests that the lack of an apparent phenotype after DNT intoxication of HEp-2 cells may be attributed to the presence of the lysine residue at position 1310 rather than the absence of a DNT receptor on this cell line.

Several possible scenarios exist that may explain how a single amino acid residue substitution within the enzymatic domain of CNF1 or DNT can result in the phenotypic changes observed in intoxicated cells. One possibility is that the changes to the catalytic triad could subsequently alter the way in which each toxin interacts with its cellular substrates. The recently solved crystal structure of the C-terminal enzymatic domain of CNF1 revealed that the active site of CNF1 resides within a deep and narrow pocket that contains His^{881} as well as the catalytic Cys^{886} residue positioned at the base of the pocket (Buetow *et al.*, 2001; Buetow and Ghosh, 2003). From the crystal structure, Thr^{884} appears to reside at the base of one of the nine loop structures that form the entrance to the pocket. Because of the small size of the active CNF1 pocket relative to its target substrates, it is believed that one or both of these proteins may undergo a conformational change to permit binding and catalysis (Buetow *et al.*, 2001). The Thr^{884} residue in wild-type CNF1 with its relatively short side chain may therefore allow target substrates greater accessibility to the enzymatic pocket compared to a longer side chain that would be encountered when a lysine residue is substituted in that position. Additionally, these substitutions, which occur on the outer edge of a loop surrounding the catalytic pocket,

could also modify the binding capacity of each toxin to its cellular target and thus alter substrate specificity. The replacement of a threonine with a lysine (or the converse) is also expected to result in a change in the electrostatic nature of this catalytic pocket. While the catalytic pocket of wild-type CNF1 is considered to be relatively neutral, molecular modeling predicts that the enzymatic pocket of DNT is highly negatively charged (Buetow *et al.*, 2001). This possibility has led investigators to theorize that the catalytic pocket of DNT may attract positively charged primary amines and that such charge-charge interactions may explain why DNT preferentially transglutaminates small GTPases (Buetow *et al.*, 2001). While this study does not directly address what factors influence the enzymatic preference of DNT (*i.e.*, deamidation versus transglutamination), the results obtained with the DNT K1310T mutant toxin indicate that conversion of a charged lysine residue at position 1310 to an uncharged threonine affected deamidase activity but did not alter the capacity of DNT to transglutaminate RhoA. This result, together with earlier work which showed that a Lys^{1310} to Ala substitution in DNT could negate transglutaminase activity (Schmidt *et al.*, 1999), suggests that specific structural changes within the vicinity of the catalytic His^{1307} residue can significantly impact enzymatic activity. In addition to the enzymatic changes mediated by amino acid substitutions within the catalytic domain of each toxin, other factors such as the state of the substrate (GDP- or GTP-bound) encountered by the toxin or the capacity of the intoxicated cell type to specifically degrade modified GTPases may also influence the morphological effects induced by these toxins.

CHAPTER 3: TWO DOMAINS OF CYTOTOXIC NECROTIZING FACTOR TYPE 1 BIND THE CELLULAR RECEPTOR, LAMININ RECEPTOR PRECURSOR PROTEIN

Submitted for publication as: Beth A. McNichol, Susan B. Rasmussen, Humberto M. Carvalho, Karen C. Meysick and Alison D. O'Brien. Two Domains of Cytotoxic Necrotizing Factor Type 1 Bind the Cellular Receptor, Laminin Receptor Precursor Protein. Infect Immun.

Note: All of the figures and tables shown reflect the work of Beth McNichol with the exception of the CNF1 truncated mutant toxin constructed that were created by Dr. Karen Meysick. Mr. Carvalho assisted with several experiments. Drs. Rasmussen, Meysick, and O'Brien contributed to experimental design and interpretation of the data as well as preparation of the manuscript.

Abstract

Cytotoxic necrotizing factor types 1 (CNF1) and 2 (CNF2) are highly homologous toxins that are produced by certain pathogenic strains of *Escherichia coli.* These 1014 amino acid toxins catalyze the deamidation of specific glutamine residues in RhoA, Rac1, and Cdc42 and consist of a putative N-terminal binding region, a transmembrane segment, and a C-terminal catalytic domain. To define the regions of CNF1 that are responsible for binding of the toxin to its cellular receptor, the laminin receptor precursor protein (LRP), a series of CNF1-truncated toxins were characterized and assessed for toxin binding. Although the truncated toxins were inactive on HEp-2 cells, these mutant proteins were immunologically reactive against a panel of anti-CNF1 monoclonal antibodies (MAbs) and retained *in vitro* enzymatic activity. Based on a comparison of these truncated toxins with wild-type CNF1 and CNF2 in LRP and HEp-2 cell binding assays, MAb- and LRP binding-inhibition assays, and by confocal microscopy, we concluded that CNF1 contains two major LRP binding regions: one located between amino acids 135-272 and the second beyond amino acid 546. These data further indicate that CNF1 can bind to an additional receptor(s) on HEp-2 cells and that LRP can also serve as a cellular receptor for CNF2.

Introduction

Cytotoxic necrotizing factor type 1 (CNF1) is produced by many strains of uropathogenic *Escherichia coli* (UPEC), agents that are responsible for the majority of uncomplicated urinary tract infections (Donnenberg and Welch, 1996b). CNF1 is a 115 kDa cytoplasmic protein that is a member of a family of toxins that target small GTPases. Specifically, CNF1 deamidates glutamine-63 (Gln^{63}) of RhoA and Gln^{61} of Rac1 and Cdc42, modifications that result in the constitutive activation of these small GTPases (Aktories, 1997). This activation leads to the formation of stress fibers and focal adhesions (RhoA), lamellipodia (Rac1) and filopodia (Cdc42) in the CNF1-intoxicated cells and ultimately results in rearrangement of the cytoskeleton (Flatau *et al.*, 1997; Lerm *et al.*, 1999b; Schmidt *et al.*, 1997). Phenotypically, CNF1 causes multinucleation of various tissue culture cells (Donelli and Fiorentini, 1992; Fiorentini *et al.*, 1988) but can also be cytotoxic to certain cell lines [(*i.e.* Swiss 3T3 and 5637 bladder cells); (McNichol *et al.*, 2006; Mills *et al.*, 2000)]. *In vivo*, CNF1 evokes necrosis when injected intradermally in rabbit skin (Caprioli *et al.*, 1983). Moreover, members of our laboratory, in collaboration with colleagues, demonstrated in two animal systems that CNF1 expression contributes to the virulence of UPEC strains. In a rat model of acute prostatitis, we found that intraurethral infection with a CNF1-positive strain leads to a significantly enhanced inflammatory response compared to that elicited by an isogenic, CNF1-negative mutant, even when bacterial counts are equivalent (Rippere-Lampe *et al.*, 2001a). Similarly, in a mouse model of urinary tract infection, the production of CNF1 by UPEC strains results in higher bacterial counts and increased inflammation compared

to *cnf1* isogenic mutants, in part due to the capacity of the toxin to alter the phagocytic and killing activities of murine PMNs (Davis *et al.*, 2005; Rippere-Lampe *et al.*, 2001b).

CNF1 is composed of an N-terminal binding domain that also contains a region postulated to be responsible for toxin translocation and a C-terminal enzymatic domain (Boquet, 2001). Earlier work by Fabbri and colleagues localized the binding domain of CNF1 to the first 190 amino acids of the toxin (Fabbri *et al.*, 1999). In that seminal study, the investigators concluded that hydrophilic amino acids that span residues 53-75 play a role in the association of CNF1 with its then unidentified cellular receptor. However, a synthetic peptide of this region failed to inhibit holotoxin binding. Therefore, the authors considered the possibility that the conformational structure of a larger portion of the CNF1 N-terminus was required for receptor binding (Fabbri *et al.*, 1999).

Recently, the receptor for CNF1 produced by an *E. coli* K1 meningitis strain was identified as the 37 kDa laminin receptor precursor protein (LRP) present in human brain microvascular endothelial cells (HBMEC) (Chung *et al.*, 2003). The natural ligand of LRP is laminin, a ubiquitous substance present in all eukaryotic cells. The wide cellular distribution of LRP may in part explain the high degree of LRP sequence conservation noted among many organisms (Mecham, 1991; Sorokin *et al.*, 2000). Through a process that is not well understood, LRP can dimerize to form the mature 67 kDa laminin receptor protein (Jaseja *et al.*, 2005). Moreover, recently, Kim *et al.* demonstrated that an *E. coli* K1 strain that expresses CNF1 can be internalized by HBMEC cells after the toxin binds to the mature laminin receptor (Kim *et al.*, 2005). Both precursor and mature forms of the laminin receptor are expressed on the surface of eukaryotic cells and are therefore accessible to CNF1 released from bacteria; however, it is unclear whether CNF1 binds

preferentially to one of the two receptor forms. After CNF1 attaches to susceptible target cells, the toxin is internalized via clathrin-dependent and -independent mechanisms and subsequently moves to late endosomes where it is released into the cytosol after vacuole acidification (Contamin *et al.*, 2000).

The N-terminal binding domain of CNF1 shares homology with two other bacterial toxins: Cytotoxic Necrotizing Factor type 2 (CNF2) and *Pasteurella multocida* toxin (PMT); (Oswald *et al.*, 1994). CNF1 and CNF2 share 85% amino acid identity and 90% similarity over the entire length of the toxins (Horiguchi, 2001; Sugai *et al.*, 1999). Although the receptor for CNF2 has not been identified, the high degree of sequence similarity between CNF1 and CNF2 suggests that they may share the same or a related receptor. CNF1 and PMT share only 24% homology within their respective N-termini with the greatest level of amino acid conservation found between the regions considered to be responsible for toxin translocation [(amino acids 250-530 of PMT and amino acids 200-465 of CNF1); (Pullinger *et al.*, 2001)]. Moreover, it has recently been suggested that vimentin, a component of type III intermediate filaments, serves as the receptor for PMT (Shime *et al.*, 2002).

In this investigation, we analyzed a series of CNF1 truncated toxins to determine the precise regions of CNF1 that directly bind to HEp-2 cells and to LRP. From this work, we identified two domains of CNF1 that are important for binding to LRP: amino acids 135-272 and a large region beyond amino acid 546. Additionally, we observed binding of CNF1 to HEp-2 cells in the presence of saturating amounts of LRP, a finding that suggests the presence of a second receptor for CNF1 on these cells. Lastly, we

addressed whether LRP can serve as a cellular receptor for CNF2 and showed that LRP can indeed function in that capacity.

Materials and Methods

Bacterial strains, plasmids, growth conditions, and protein purification

The bacterial strains and plasmids used in this study are listed in Table 3. The plasmid pGEX-2T-LRP (Chung *et al.*, 2003) was a gift from Dr. Kwang Sik Kim (Johns Hopkins University School of Medicine, Baltimore, MD). Plasmids pCNF24 (CNF1), p2CNF (CNF2), pΔN63, pΔN75, pΔN134, pΔN272, pΔN545, pΔC469, and pΔ442 were transformed into *E. coli* M15(pREP4) and grown in Luria-Burtani broth supplemented with 100 μg/ml ampicillin and 25 μg/ml kanamycin. Expression of CNF1, CNF2, CNF1 truncated proteins, and LRP was induced from cultures grown at 22-25°C by addition of isopropyl-β-D-thiogalactopyranoside (IPTG) to a final concentration of 0.1 mM. N-terminal histidine (His)-tagged proteins were purified over HisTrap™ Ni^{2+}-affinity columns with the fast phase liquid chromatography (FPLC) ÄKTA system as per the manufacturer's protocol (GE Healthcare, Piscataway, NJ). Buffer exchange of affinity column-eluted proteins from 250 mM imidazole to 20 mM Tris-HCl, pH 7.8 was done by FPLC with HiTrap HP desalting columns (GE Healthcare) or by dialysis.

Construction of Histidine-tagged LRP and CNF2 expression plasmids

To subclone the *lrp* gene into the His-tag expression vector pQE30 (Qiagen, Valencia, CA), plasmids pGEX-2T-LRP and pQE30 were digested with XmaI and BamHI and the respective 899 bp and 3 kb fragments purified from a 1% sodium borate agarose gel

Table 3: Bacterial Strains and Plasmids, part 2

Strain or plasmid	Relevant characteristics	Source or reference
E. coli		
XL1-Blue	*recA1 endA1 gyrA96 thi-1 hsdR17supE44 relA1 lac*[F' *proAB*$^+$ *lacI*^{q}*Z* ΔM15::Tn *10*(Tet^r)]	Stratagene
M15(pREP4)	Nal^s Str^s Rif^s Δ*lac-ara-gal-mtl* F$^-$ *recA uvr* (pREP4 *lacI* Kan^r)	Qiagen
Cloning vectors		
pBluescript II SK$^-$	*E. coli* phagemid cloning vector (Amp^r)	Stratagene
pQE30	*E. coli* expression vector with 6x-His tag 5' to the polylinker (Amp^r)	Qiagen
pGEX-2T	*E. coli* expression vector with GST tag 5' to the polylinker (Amp^r)	Qiagen
Plasmids		
pCNF24	wt *cnf1* gene (nt 1-3045) amplified from pHLK102 and cloned into BamHI/KpnI sites of pQE30	(Meysick *et al.*, 2001)
p2CNF	coding region of *cnf2* cloned into SacI/KpnI sites of pQE30	This study
pEOSW30	3.3 kb BanI/HaeII fragment containing the *cnf2* gene cloned into the SmaI site of pK184	(Oswald *et al.*, 1994)
pΔN63	pCNF24 with a deletion of 187 nt from the 5' end of the *cnf1* gene	(Meysick *et al.*, 2001)
pΔN75	2.8 kb BamHI/KpnI *cnf1* fragment (nt 226 to 3045) cloned into pQE30	(Meysick *et al.*, 2001)
pΔN134	2.6 kb BamHI/KpnI *cnf1* fragment (nt 403 to 3045) cloned into pQE30	(Meysick *et al.*, 2001)
pΔN272	2.2 kb BamHI/KpnI *cnf1* fragment (nt 817 to 3045) cloned into pQE30	(Meysick *et al.*, 2001)
pΔN545	1.4 kb Pst *cnf1* fragment (nt 1637 to 3045) cloned into pQE30	(Meysick *et al.*, 2001)
pΔC469	BamHI/PstI *cnf1* fragment (nt 1 to 1637) cloned into pQE30	(Meysick *et al.*, 2001)
pΔ442	pCNF24 with an internal in-frame BclI deletion (nt 1115 to 2348)	(Meysick *et al.*, 2001)
pGEX-2T-LRP	full-length *lrp* gene cloned into BamHI/EcoRI sites of pGEX-2T	(Chung *et al.*, 2003)

Table 3 (cont.)

pHisLRP	full-length *lrp* gene subcloned into BamHI/XmaI sites of pQE30	This study

(Faster Better Media LLC, Hunt Valley, MD) with the QIAEX® II Gel Extraction kit (Qiagen) according to the manufacturer's instructions. Purified DNA fragments were ligated and transformed into supercompetent XL1-Blue cells (Stratagene, Cedar Creek, TX) prior to transformation into *E. coli* M15(pREP4) for protein expression of the 37 kDa LRP.

To subclone the *cnf2* gene into pQE30, the full-length gene was amplified from pEOSW30 (Oswald *et al.*, 1994) with primers CNF2F1 (5' ATGAGCTCATGAACGTT CAATGGCAAC) and CNF2R3045 (5' ATGGTACCTCAAAAATCTTTTGAAAAAAC ATGC) that were designed to incorporate SacI and KpnI restriction sites at the respective 5' ends in order to facilitate directional cloning into pQE30. The *cnf2* gene amplicon and pQE30 were each digested with SacI/KpnI, ligated, and the resultant plasmid, p2CNF, was transformed into chemically-competent *E. coli* XL1-Blue cells. For protein purification and examination of toxin activity on HEp-2 cells, p2CNF was subsequently transformed into *E. coli* M15(pREP4) and lysates examined as previously described (McNichol *et al.*, 2006).

Cell lines and media

HEp-2 cells, a human laryngeal cell line (ATCC CCL-23), were grown at 37°C with 5% CO_2 in Eagle's minimal essential medium with Earle's balanced salt solution (Cambrex, East Rutherford, NJ) supplemented with 10% fetal bovine serum (Invitrogen-Biosource, Carlsbad, CA), 2 mM L-glutamine (Invitrogen), 10 μg/ml gentamicin, 10 U/ml penicillin, and 10 μg/ml streptomycin.

Dot blot analysis of truncated CNF1 toxins

Dot blots of native and denatured toxin samples were done as previously described with the following modifications (McNichol *et al.*, 2006). Briefly, purified CNF1, CNF2, and truncated CNF1 toxins, were diluted in either phosphate-buffered saline (PBS; native) or 6X sodium dodecyl sulfate (SDS)/dithiothreitol (DTT) buffer (denatured) to a final concentration of 10 μg/ml and 100 μl of each sample were then transferred to nitrocellulose membranes with a Minifold Micro-Sample Filtration Manifold (Schleicher & Schuell, Keene, NH). Toxins diluted in denaturation buffer were boiled at 95°C for 5 minutes prior to transfer. Membranes were washed with 1X PBS, dried and then blocked overnight at 4°C in BLOTTO (Tris-buffered saline, 5% skim milk, 0.05% Tween-20). Blots were probed with a panel of CNF1-specific monoclonal antibodies (MAbs) (Meysick *et al.*, 2001) as well as polyclonal anti-CNF1 sera (Mills *et al.*, 2000) and a MAb directed against the His-tag (Qiagen), followed by incubation with horseradish peroxidase (HRP)-conjugated goat anti-mouse IgG (Roche, Indianapolis, IN). Reactive proteins were visualized with diaminobenzamidine (DAB; Sigma, St. Louis, MO).

LRP receptor binding ELISA

Vinyl alphanumeric 96-well U-bottom ELISA plates (Thermo Fisher Scientific) were coated with purified native LRP in 1X PBS at a concentration of 200 μg/ml (20 μg/well), and plates incubated overnight at 4°C. Wells were washed with 1X PBS/0.1% Tween-20 (PBS-T) and then blocked with PBS that contained 3% bovine serum albumin (BSA) for 2 hours at 37°C. Once blocked, wells were again washed with PBS-T, and purified toxins added at a concentration of 50 μg/ml (5 μg/well). Plates were incubated for 2

hours at 37°C, washed with PBS-T and then sequentially incubated with goat anti-CNF1 polyclonal sera (1:5000) for 1 hour at 37°C, followed by an anti-goat IgG-HRP-conjugated antibody (1:7500; Roche) for 1 hour at room temperature. Color development was achieved with TMB substrate (Bio-Rad, Hercules, CA) as per the manufacturer's instructions and plates were read in an EL_x800 plate reader (BioTek Instruments, Winooski, VT) at 405 nm. To ensure equal binding of the antisera to each toxin, a concurrent ELISA was done as described above in the absence of LRP.

HEp-2 receptor binding ELISA

Approximately 5 x 10^4 HEp-2 cells/well were seeded in 96-well plates and incubated overnight at 37°C with 5% CO_2. The following day, cells were fixed with 2% formalin for 20 minutes at room temperature and then wells washed with PBS-T prior to blocking for 1 hour at 37°C with 1X PBS- 3% BSA. Once blocked, wells were washed with PBS-T and purified toxins added at a concentration of 50 μg/ml (5 μg/well). Controls without toxin were included to determine the degree of non-specific antibody binding to cells. Plates were incubated for 1 hour at 37°C, washed, and then the wells were sequentially incubated with goat anti-CNF1 polyclonal sera (1:5000) for 1 hour at 37°C followed by anti-goat HRP-conjugated IgG (1:7500; Roche) for 1 hour at room temperature. Color development was achieved with TMB substrate (Bio-Rad) as per the manufacturer's instructions and the reaction stopped by addition of 1N H_2SO_4. To prevent interference from HEp-2 cell monolayers, samples (100 μl) were transferred to a 96-well plate subsequent to being read in an EL_x800 plate reader (BioTek Instruments) plate reader at 405 nm.

Binding inhibition assays

Preliminary binding experiments were initially done to determine the concentrations of CNF1, CNF2, ΔN134, and ΔN545 that yielded approximately the same absorbance value in the HEp-2 receptor binding ELISA. Based on this information, CNF1 (2.5 μg/well), CNF2 (5 μg/well), ΔN134 (5 μg/well) and ΔN545 (2.5 μg/well) were incubated with 5 μg of either CNF neutralizing MAbs BF8 (CNF1, CNF2 and ΔN134) or NG8 (CNF1, ΔN134 and ΔN545) or a mixture of both MAbs (CNF1 and ΔN134) for 2 hours at 37°C. As internal controls, the toxins were also incubated with non-neutralizing CNF1 monoclonal antibodies GC2 and CA6, as well as an irrelevant anti-Stx1 monoclonal antibody 13C4 (purified, Hycult, Netherlands) as described above. The toxin/MAb samples were added to fixed and blocked HEp-2 cells, and the assay continued as per the receptor binding ELISA protocol described above. For competitive inhibition of binding with exogenous LRP, the same concentrations of CNF1, ΔN134, and ΔN545 as noted above were pre-incubated with 200 μg/ml (20 μg/well) of purified LRP for 2 hours at 37°C and the samples then used in the HEp-2 receptor binding ELISA. Paired, two-tailed t-tests were used to determine whether statistically significant differences existed between untreated toxin samples and toxin that had been pre-incubated with CNF1 MAbs or exogenous LRP.

In vitro deamidation of Rho GTPases

Deamidation of RhoA, Rac1 and Cdc42 was done as described previously (McNichol *et al.*, 2006). Briefly, a 20:1 molar ratio of GTPase to toxin was incubated in deamidation buffer (50 mM NaCl, 50 mM Tris-HCl pH 7.4, 5 mM $MgCl_2$, 1 mM dithiothreitol, 1 mM

phenylmethanesulphonyl fluoride) for 2.5 hours at 37°C. Untreated GTPases served as negative controls. After toxin treatment, samples were concentrated by addition of 10% trichloroacetic acid and stored overnight at 4°C. Precipitated proteins were pelleted, washed with acetone, air-dried and resuspended in 20 mM Tris-HCl, pH 7.4. Samples were subjected to SDS-PAGE with 12% acrylamide, and proteins were transferred to 0.45µm nitrocellulose membranes. Membranes were blocked overnight at 4°C in BLOTTO and then probed with either MAbs against RhoA (1:1500, Santa Cruz Biotechnology, Santa Cruz, CA), Rac1 (1:5000, Upstate Biotechnology), or Cdc42 (1:1000, Santa Cruz Biotechnology) or a rabbit polyclonal antisera raised against the deamidated RhoA peptide [(1:2000); (McNichol *et al.*, 2006; Sugai *et al.*, 1999)]. Reactive proteins were visualized after incubation with HRP-conjugated goat anti-mouse IgG (1:2000, 1:7500 and 1:3000, respectively for RhoA, Rac1 and Cdc42 samples, Roche) or donkey anti-rabbit IgG (1:3000, GE Healthcare) followed by detection with ECL Plus (GE Healthcare). The pixel density of total and modified RhoA was analyzed with NIH ImageJ 1.34S software (http://rsb.info.nih.gov/ij/). Percent modification was calculated as described previously (McNichol *et al.*, 2006) using the values derived from ImageJ and the following formula: [(modified RhoA value/total RhoA value) x 100%] - [(RhoA control modified RhoA value/RhoA control total RhoA value) x 100%].

Co-localization of CNF1 and LRP by immunofluorescence

Immunofluorescence experiments were done as follows. HEp-2 cells were seeded in 8-well glass or Permanox chamber slides at a concentration of approximately 5 x 10^6 cells/well and incubated for 24 hours at 37°C with 5% CO_2. Slides were then chilled to

4°C, and washed with cold Hank's balanced salt solution (Invitrogen/Gibco) prior to the addition of purified CNF1, CNF2, ΔN134, or ΔN545 which had been diluted to a final concentration of 12 μg/well in cold binding buffer without maltose (Frankel *et al.*, 1994; Mills *et al.*, 2000). Control wells received binding buffer in the absence of toxin. Cells were incubated with toxin for 1 hour at 4°C, washed with PBS and then fixed with 2% formalin for 20 minutes at room temperature. After fixation, wells were washed and blocked with 1% BSA in PBS overnight at 4°C. The following day, wells were sequentially incubated for 1 hour at 4°C with goat anti-CNF1 polyclonal antiserum (1:500) followed by AlexaFluor 488 conjugated chicken anti-goat IgG (1:300; Invitrogen-Molecular Probes), rabbit anti-LRP polyclonal antiserum (1:500; Abcam, Cambridge, MA) and AlexaFluor 555 conjugated donkey anti-rabbit IgG (1:300; Invitrogen-Molecular Probes). Prior to examination, slides were treated with Fluoromount G (Southern Biotech, Birmingham, AL) and coverslips applied. Cells were visualized at 100x magnification and confocal images taken with a Zeiss LSM Pascal Confocal microscope and processed with LSM Image 5 Browser software.

Results

Evaluation of CNF1 truncated toxins

Prior to the evaluation of a series of truncated CNF1 toxins (Figure 13) in binding domain studies, the proteins were assessed for activity and conformational integrity. Mutant toxins were initially examined for the capacity to multinucleate HEp-2 cells, a hallmark phenotype of CNF1 intoxication; however, none of the truncated toxins evoked

Figure 13: Schematic diagram of CNF1 truncated mutants

Schematic diagram of CNF1 truncated toxins with the regions/epitopes recognized by several CNF monoclonal antibodies (MAbs) indicated above. MAbs JC4 and NG8 can neutralize CNF1, while MAb BF8 can neutralize both CNF1 and CNF2.

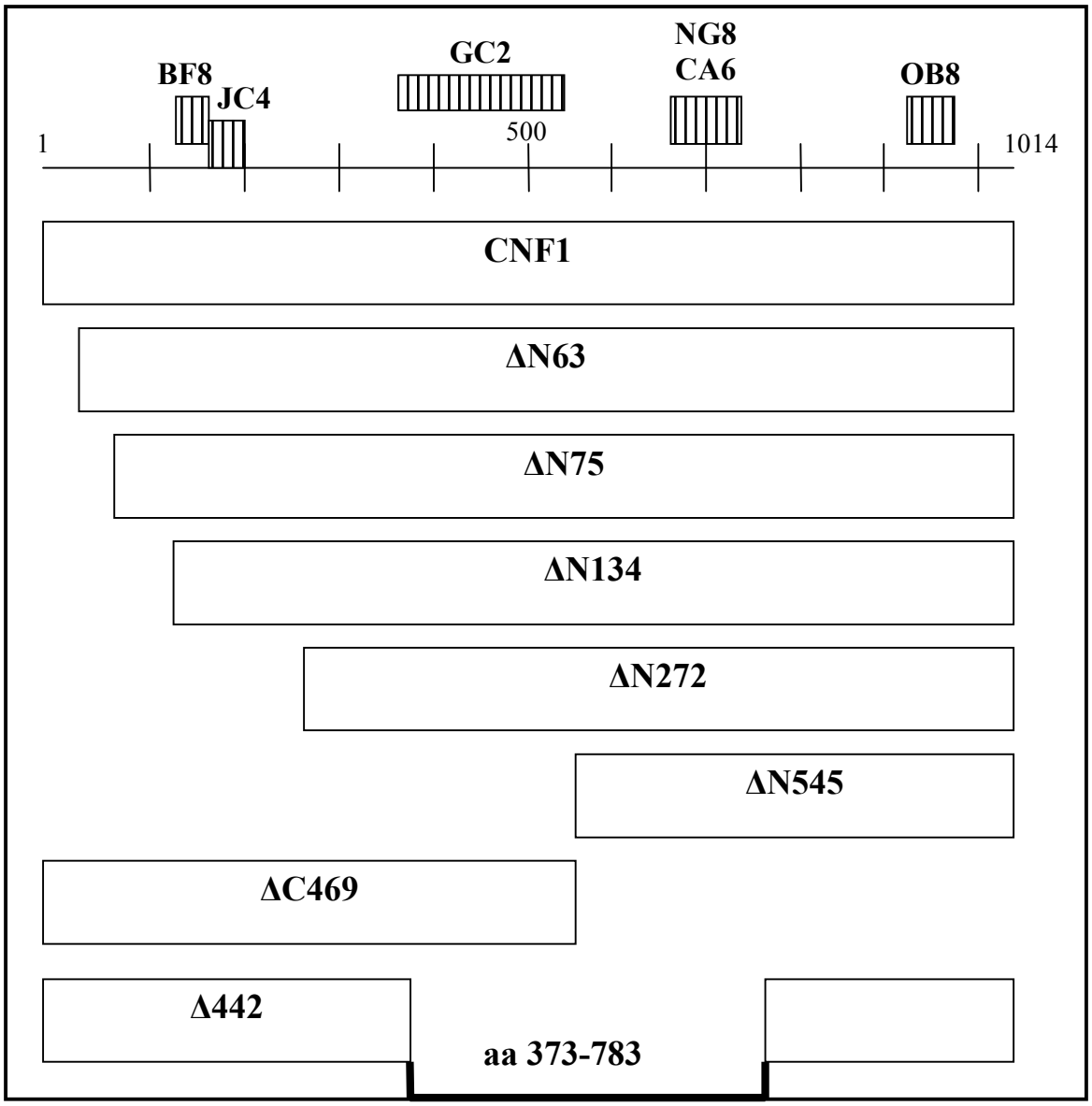
BF8
JC4
GC2
NG8
CA6
OB8
1
500
1014
CNF1
ΔN63
ΔN75
ΔN134
ΔN272
ΔN545
ΔC469
Δ442
aa 373-783

such a response (data not shown). Given that multinucleation reflects a series of steps that begins with toxin binding to the target cell and ends with deamidation of the small cytoplasmic GTPase targets, RhoA, Rac1, and Cdc42, the mutant toxins were evaluated for retention of enzymatic activity and structural conformation. To determine whether the mutants were enzymatically active *in vitro*, we tested the capacity of each protein to deamidate RhoA, Rac1 and Cdc42. As shown in Fig. 14A, toxins with various portions of the N-terminus deleted still retained the capacity to deamidate RhoA but not to the same extent as that demonstrated by wild-type CNF1 or CNF2. Similarly, these N-terminal truncation mutants also retained the capacity to deamidate Rac1 and Cdc42, but at levels below those obtained with wild-type toxins (data not shown). The ΔN75 and ΔN272 mutants were the least enzymatically active of the toxins (Fig. 14A); nevertheless, the extent to which these proteins deamidated RhoA was above that of background (reactivity of RhoA without toxin). The enzymatic activity of ΔC469 was not tested because this mutant toxin was devoid of the entire catalytic domain and therefore presumably inactive. Mutant toxin Δ442, which has a deletion of amino acids 320-783 but still harbors the putative binding and enzymatic regions, showed background levels of deamidation activity despite the presence of the catalytic domain (Fig. 14A).

To evaluate conformational structure and integrity, the truncated toxins were examined in native and denatured dot blots probed with a panel of anti-CNF monoclonal antibodies [(MAbs); (Meysick *et al.*, 2001)]. As shown in Figure 14B, CNF1 mutants ΔN63, ΔN75, ΔN134, ΔN545 and ΔC469 were detected by several of the anti-CNF MAbs under native conditions, but these reactivities were either partially reduced or

Figure 14: Enzymatic activity and conformation of CNF1 truncated toxins

A: Western blot analysis of RhoA incubated in the presence or absence of purified toxins. Membranes were probed with a monoclonal antibody against RhoA (top panel) or with antisera that only recognizes the deamidated form of the GTPase (bottom panel) and reactive proteins detected with appropriate HRP-conjugated secondary antibodies and ECL substrate. The pixel density of total and modified RhoA was used to calculate percent modification and is indicated below the blots. Background values from the RhoA control were subtracted from each of the sample values. *B*: Purified toxins (1 μg/well) were either applied directly to nitrocellulose membranes (upper panels) or denatured (SDS/DTT/boiling) prior to their application (lower panels). As indicated in the right hand column, blots were probed with either a monoclonal antibody against the 6x-His tag, CNF1 polyclonal antiserum, or a panel of CNF monoclonal antibodies and reactive proteins visualized with an HRP-conjugated secondary antibody and diaminobenzamidine (DAB) substrate.

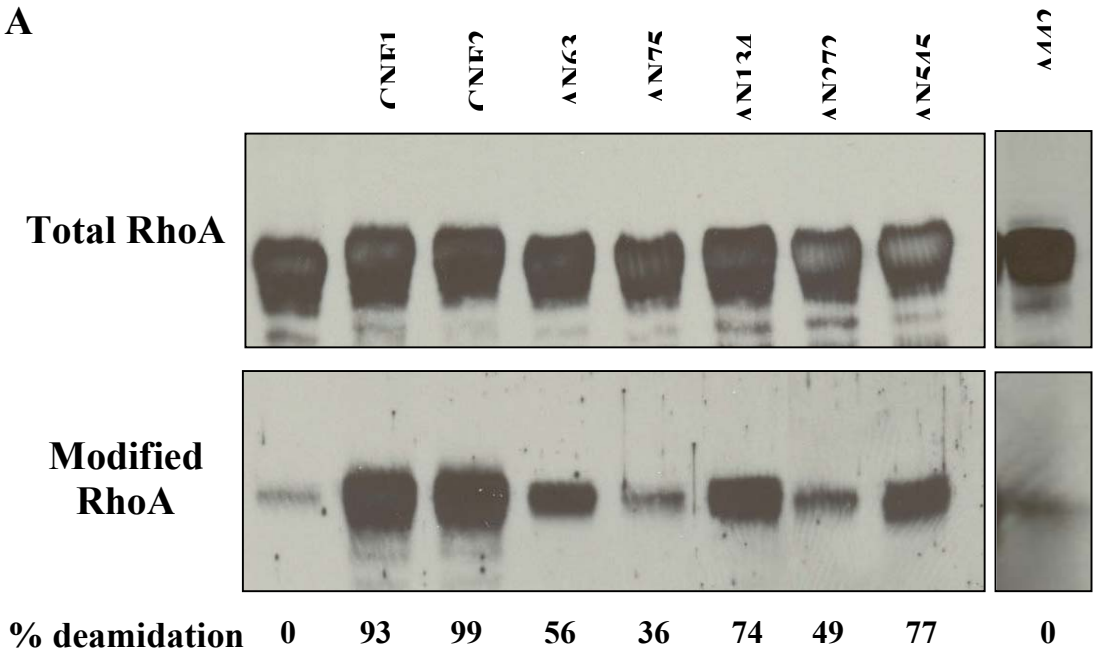
A
CNF1
CNF2
AN63
AN75
AN134
AN272
AN545
AA42
Total RhoA
Modified RhoA
% deamidation
0
93
99
56
36
74
49
77
0

B

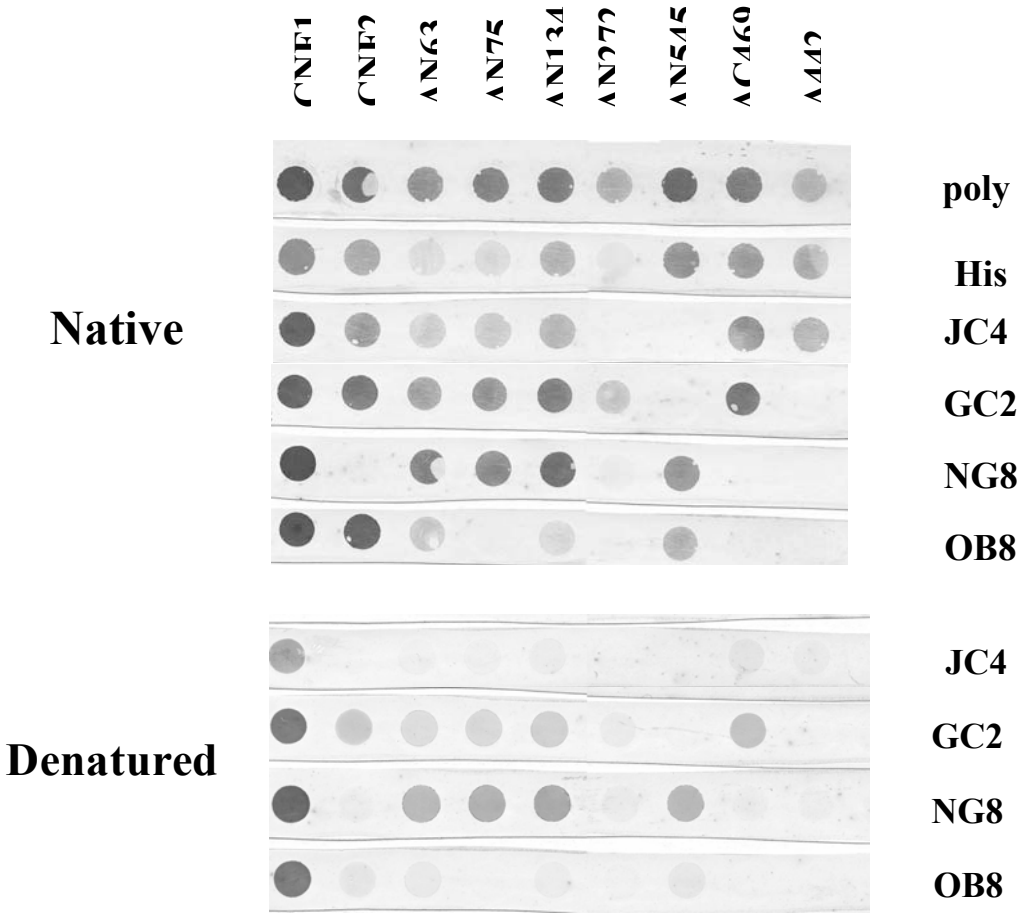
CNF1
CNF2
AN63
AN75
AN134
AN272
AN545
AC460
AA42
poly
His
JC4
GC2
NG8
OB8
Native
JC4
GC2
NG8
OB8
Denatured

completely abrogated after denaturation of the toxin. These results imply that the MAbs likely react with conformational epitopes, as previously reported (Meysick *et al.*, 2001), and that these epitopes remained conformationally intact in those truncated CNF1 toxins. In contrast, ΔN272 did not react with MAbs NG8 or OB8 under native or denatured conditions, but did react weakly with GC2 in native blots (Fig. 14B). From these results it appeared that mutant toxin ΔN272 did not maintain the same conformational structure in the C-terminus as wild-type CNF1. Interestingly, toxin ΔN75 was recognized by all MAbs except OB8, which suggests that the conformational integrity of the distal portion of the C-terminus of this toxin may be compromised. Finally, the structural integrity of mutant toxin Δ442 was also considered compromised based on the unexpected recognition pattern with MAbs JC4 and OB8, with reactivity only apparent under native conditions with MAb JC4. As expected, CNF2 reacted with JC4, GC2 and OB8, but not NG8, a finding that has been described previously (Meysick *et al.*, 2001). Taken together, the dot blot and enzyme analyses indicate that four (ΔN63, ΔN134, ΔN545, ΔC469) of the seven truncated mutants maintained proper structural folding and, with the exception of toxin ΔC469, retained enzymatic activity. The mutant toxins ΔN75 and ΔN272 were enzymatically active but exhibited disparate reactivity patterns in the C-terminal regions when analyzed by dot blots. The final toxin, Δ442, was only recognized in the N-terminal region by the CNF1 monoclonal antibodies and was not enzymatically active possibly due to conformational changes.

Binding of CNF1 and the CNF1 truncated mutants to HEp-2 cells

To address whether the truncated CNF1 toxins retained the capacity to bind to HEp-2 cells, a receptor binding ELISA was devised. In that assay, toxin was added to wells of fixed HEp-2 cell monolayers and bound toxin subsequently detected with anti-CNF1 polyclonal sera used at a dilution optimized to allow detection of CNF2 and all truncated forms of CNF1 at levels comparable to CNF1 itself. The standardization of toxin signal for the wild-type and mutant CNF toxins was used to permit comparisons of the relative binding of each of these proteins to HEp-2 cells and values were considered CNF-specific as no signal was detectable in the absence of toxin. As shown in Fig. 15A, wild-type and truncated toxins bound to fixed HEp-2 cells but with striking differences observed in the efficiency of binding. Notably, the degree of binding of ΔN134 and ΔN545 to fixed HEp-2 cells suggests that two distinct regions of CNF1, one between amino acids 135-272 and the second within the last 469 amino acids of the toxin are important for toxin binding. The greater degree of binding associated with ΔN545 suggests that a binding site within this region may be masked by the natural conformation of the holotoxin. The C-terminal truncation mutant ΔC469 adhered to HEp-2 cells at levels comparable to N-terminal mutants ΔN63 and ΔN75. This latter observation further supports the hypothesis that CNF1 harbors two HEp-2 cell binding regions between amino acids 135-272 and within the distal portion of the toxin. CNF2 was also found to adhere to HEp-2 cells but not to the extent observed with CNF1.

Localization of the region of CNF1 that binds LRP

To identify the region(s) of CNF1 that bound to LRP, a receptor binding ELISA was devised in which purified LRP, coated to the wells of an ELISA plate, was incubated

Figure 15: HEp-2 and LRP receptor binding ELISAs

A: Purified toxins (5 ug/well) were added to fixed HEp-2 cells for 1 hour and bound toxin was detected with CNF1 polyclonal antisera. Results shown are the average of two experiments done in triplicate. Error bars represent the standard deviation above and below the mean. Values from wells with toxin but no CNF1 antisera served as background controls and were subtracted from all sample readings. *B*: Purified toxins were incubated with LRP affixed to wells of an ELISA plate and bound toxin detected with anti-CNF1 polyclonal sera. Results shown are the average of two experiments done in triplicate. Error bars represent the standard deviation above and below the mean. Values from wells with toxin but no CNF1 antisera served as background controls and were subtracted from all sample readings.

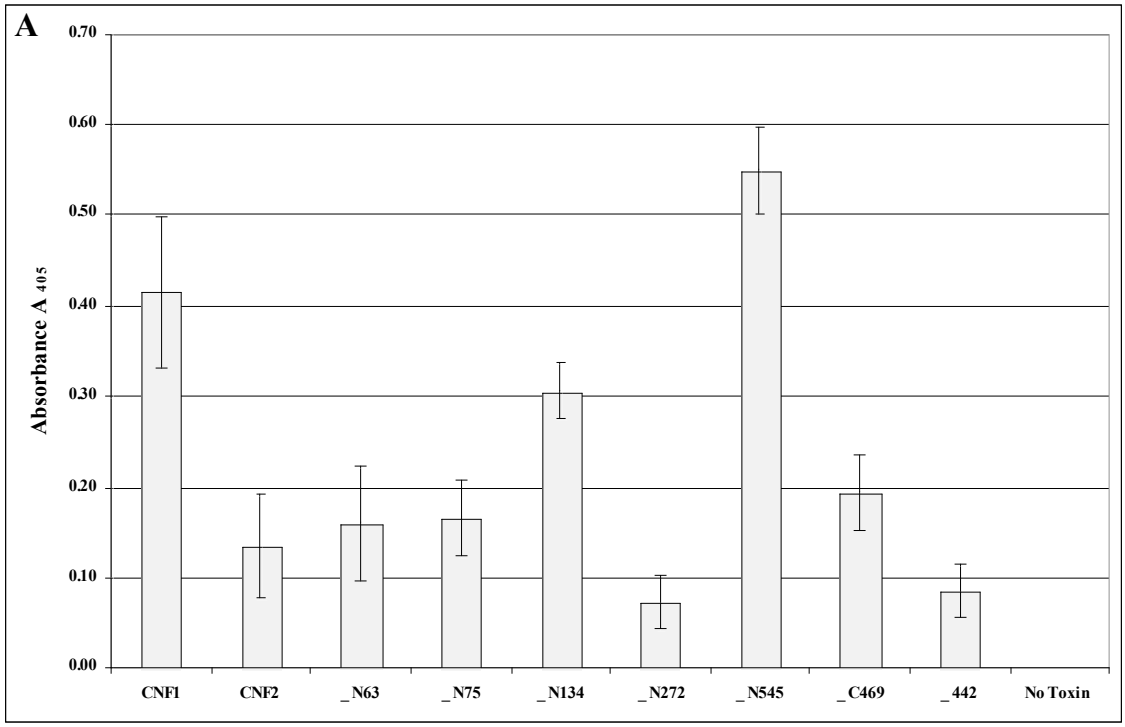
A
0.70
0.60
0.50
0.40
0.30
0.20
0.10
0.00
Absorbance A 405
CNF1
CNF2
_N63
_N75
_N134
_N272
_N545
_C469
_442
No Toxin

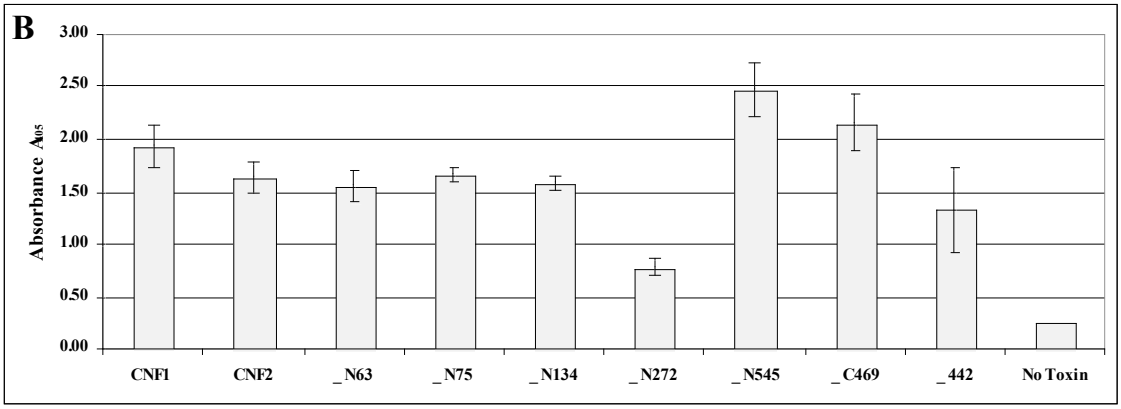
B
3.00
2.50
2.00
1.50
1.00
0.50
0.00
Absorbance A405
CNF1
CNF2
_N63
_N75
_N134
_N272
_N545
_C469
_442
No Toxin

with CNF1, CNF2 or the CNF1 truncated mutants, and bound toxin subsequently detected with anti-CNF1 polyclonal sera. All of the truncated toxins examined in this assay appeared to bind specifically to purified LRP with only low levels of signal observed in the absence of toxin (Fig. 15B). However, ΔN272 did not bind to LRP as well as the other truncated mutants, an observation which suggests the presence of a binding domain between amino acids 135-272. As was observed in HEp-2 receptor binding assays, truncated mutant ΔN545 showed the highest levels of binding to LRP which suggests the presence of a second binding region that is only exposed in the absence of the CNF1 N-terminus. Interestingly, mutants ΔC469 and Δ442 were also able to bind LRP. As ΔC469 is missing its entire C-terminus and Δ442 is without amino acids 373-783, binding by these two mutants correlates with a binding region between amino acids 135-272. In addition, it appears that CNF2 binds LRP at a level similar to CNF1, a finding which suggests that CNF2 may also use LRP as a receptor.

Inhibition of toxin binding to HEp-2 cells

To confirm the location of the CNF1 binding domains identified in HEp-2 cell and LRP-binding ELISAs, a series of competitive inhibition binding studies were carried out. Specifically, wild-type and truncated CNF1 toxins ΔN134 and ΔN545 were examined for the capacity to bind to HEp-2 cells in the presence of either anti-CNF MAbs or LRP. To appropriately compare the degree of binding of CNF1 and the truncated mutants ΔN134 and ΔN545 to HEp-2 cells, the concentration required to produce comparable absorbance signals in the HEp-2 receptor binding ELISA was first determined for each toxin (data not shown). Based on this information, appropriate amounts of each toxin were then

incubated with either CNF1 neutralizing MAbs BF8 and NG8, CNF1 non-neutralizing MAbs GC2 and CA6, or an irrelevant MAb (Shiga toxin type 1 (Stx1) MAb 13C4) prior to evaluation in the HEp-2 receptor binding ELISA. The regions recognized by these CNF1 MAbs have been previously mapped to amino acids 135-164 (BF8), 373-546 (GC2), and 683-730 (NG8 and CA6) [(Meysick *et al.*, 2001) and Fig. 13]. As shown in Fig. 16A and B, both MAbs BF8 and NG8 significantly reduced the extent of CNF1 binding to HEp-2 cells ($p = 0.0080$ and $p = 0.045$, respectively). Similarly, MAb BF8 almost completely blocked binding of truncated toxin ΔN134 ($p = 0.017$), and MAb NG8 significantly decreased binding of ΔN134 and ΔN545 to HEp-2 cells (Fig. 16B; $p = 0.028$ and 0.0070, respectively). Additionally, incubation of CNF1 and ΔN134 with equal concentrations of MAbs BF8 and NG8 led to decreased attachment of both toxins to fixed HEp-2 cells (Fig. 16C; $p<0.001$). No reduction in binding was noted when either CNF1, ΔN134 or ΔN545 were mixed with equivalent concentrations of two different non-neutralizing CNF MAbs, GC2 and CA6 [(Meysick *et al.*, 2001) and Fig. 13] or with the irrelevant Stx1 neutralizing MAb 13C4 (Fig. 17 and data not shown). The irrelevant MAb 13C4 blocks Stx1 from engagement with its cell receptor, globotriaosylceramide (Smith *et al.*, 2006). Furthermore, all binding was considered CNF1-specific as no signal was detected with any of the MAbs in the absence of toxin (data not shown). These data confirm the CNF1 binding regions identified in the earlier HEp-2 cells and LRP binding studies and further delineate these binding regions based on the epitopes recognized by MAbs BF8 and NG8. In addition, it was noted that the binding of CNF1 and ΔN134 to HEp-2 cells in the presence of both MAbs (Fig 16C), though markedly reduced, was not completely ablated. This observation suggests that there may be another site (or sites) on

Figure 16: Inhibition of toxin binding to HEp-2 cells by CNF1 monoclonal antibodies

A: Wild-type CNF1, CNF2, and ΔN134 were incubated with MAb BF8 and assessed for their capacity to bind HEp-2 cells in a receptor binding ELISA. The results shown are the average of two experiments performed in triplicate. *B*: Wild-type CNF1, ΔN134, and ΔN545 were incubated with MAb NG8 and assessed for their capacity to bind HEp-2 cells in a receptor binding ELISA. The results shown are the average of two experiments performed in triplicate. *C*: Equal concentrations of MAbs BF8 and NG8 were incubated with CNF1 and ΔN134 and toxins subsequently assessed for their capacity to bind HEp-2 cells. The results depicted are the average of one experiment performed in quadruplicate. For all experiments, error bars represent the standard deviation above and below the mean. Data were analyzed by paired, two-tailed t-tests with p-values indicated. Values from wells with toxin but no CNF1 antisera served as background controls and were subtracted from all sample readings.

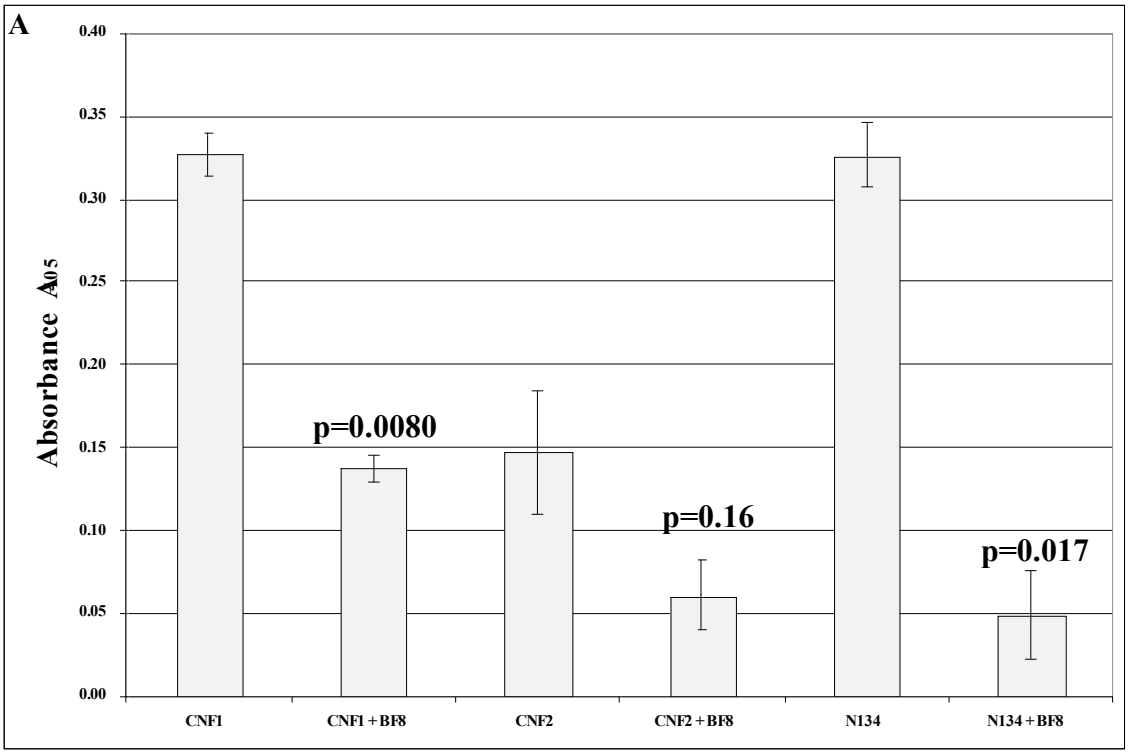
A
Absorbance A405
0.40
0.35
0.30
0.25
0.20
0.15
0.10
0.05
0.00
p=0.0080
p=0.16
p=0.017
CNF1
CNF1 + BF8
CNF2
CNF2 + BF8
N134
N134 + BF8

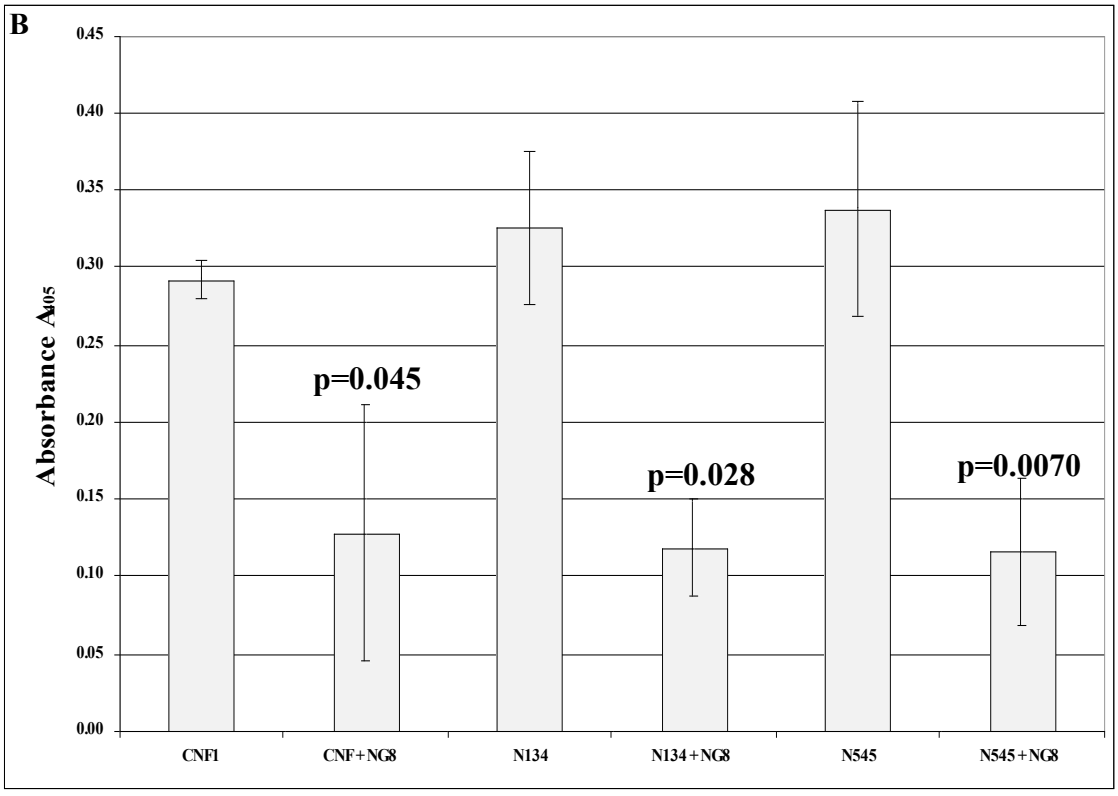
B
Absorbance A405
0.45
0.40
0.35
0.30
0.25
0.20
0.15
0.10
0.05
0.00
p=0.045
p=0.028
p=0.0070
CNF1
CNF + NG8
N134
N134 + NG8
N545
N545 + NG8

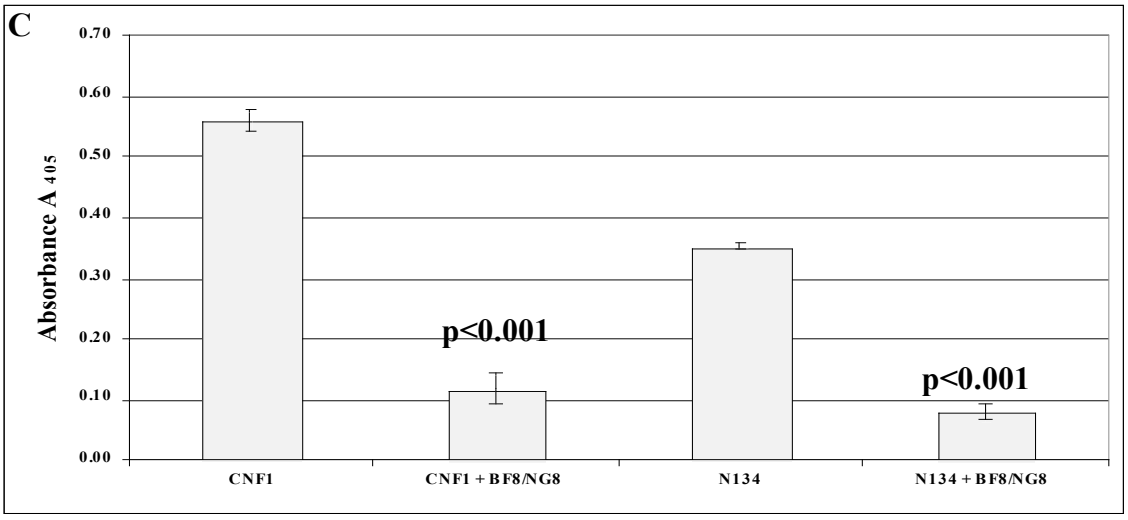
C
Absorbance A 405
0.70
0.60
0.50
0.40
0.30
0.20
0.10
0.00
p<0.001
p<0.001
CNF1
CNF1 + BF8/NG8
N134
N134 + BF8/NG8

Figure 17: Inhibition of toxin binding to HEp-2 cells by non-neutralizing CNF1 and irrelevant monoclonal antibodies

Wild-type CNF1 was incubated with non-neutralizing CNF1 monoclonal antibodies GC2 and CA6, or an irrelevant Shiga toxin type 1 neutralizing monoclonal antibody 13C4 and toxin subsequently assessed for its capacity to bind HEp-2 cells. The results shown are the average of two experiments performed in triplicate. Error bars represent the standard deviation above and below the mean. Data were analyzed by paired, two-tailed t-tests and p-values are indicated. Values from wells with toxin but no CNF1 antisera served as background controls and were subtracted from all sample readings.

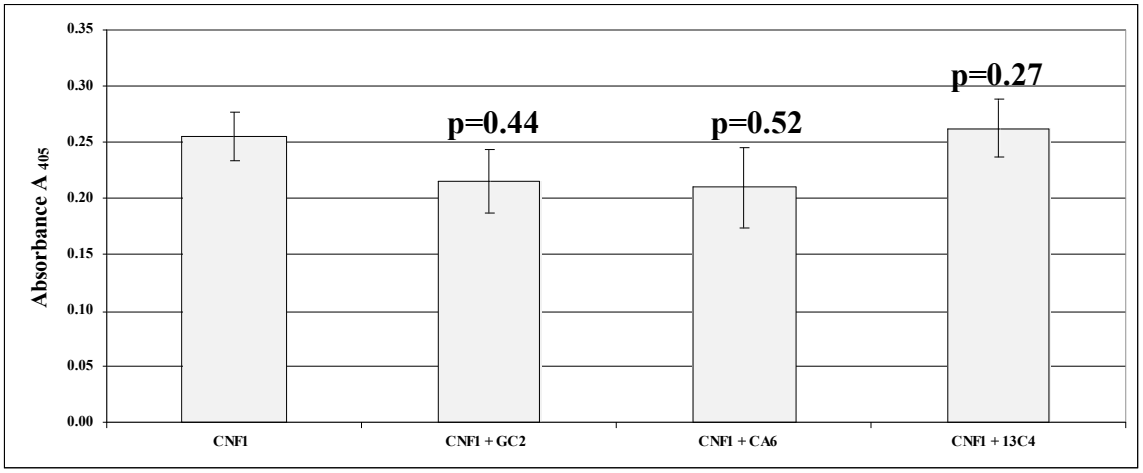
0.35
0.30
0.25
0.20
0.15
0.10
0.05
0.00
Absorbance A 405
p=0.44
p=0.52
p=0.27
CNF1
CNF1 + GC2
CNF1 + CA6
CNF1 + 13C4

the toxin that can participate to a minor extent in adherence to HEp-2 cells and that these amino acid sequences are distinct from those defined by reactivity with MAbs BF8 and NG8. Alternatively, the sensitivity of the assay might limit the full extent of binding inhibition observed with these neutralizing MAbs.

To establish whether the binding of CNF1 and the truncated toxins ΔN134 and ΔN545 to HEp-2 cells was through LRP, a second set of binding inhibition experiments was done. For these assays, toxins were incubated with exogenous LRP prior to addition to fixed HEp-2 cell monolayers. As expected, exposure to exogenous LRP significantly inhibited binding of CNF1, ΔN134 and ΔN545 to HEp-2 cells (Fig. 18, p values = 0.022, 0.033 and 0.0030, respectively). These findings indicate that the same regions of CNF1 shown to be necessary for HEp-2 cell-binding (*i.e.*, amino acids 135-272 and beyond 546) were also critical for interaction with LRP. Furthermore, because toxin binding was not completely abrogated by exogenous LRP, even when used in saturating concentrations (20 μg), the results also suggest the presence of an additional HEp-2 receptor for CNF1.

Our results indicate that CNF2 can bind and intoxicate HEp-2 cells but not to the same extent as CNF1 (Fig. 15A and K. Grande, S. Rasmussen, K. Meysick and A. O'Brien, unpublished data). To establish whether CNF1 and CNF2 share common binding regions, CNF2 was assessed in HEp-2 cell receptor binding ELISAs after pre-incubation with either MAb BF8, a CNF1 MAb that can cross-react with CNF2 and partially inhibit CNF2 activity (Meysick *et al.*, 2001), or exogenous LRP. CNF2 binding to HEp-2 cells was reduced both in the presence of MAb BF8 (Fig. 16A) and with LRP (Fig. 18); however, in neither case was the level of reduction in binding statistically

Figure 18: Inhibition of toxin binding to HEp-2 cells by exogenous LRP

Wild-type CNF1, CNF2, ΔN134 and ΔN545 were incubated with LRP prior to addition to HEp-2 cells. The results shown are the average of two experiments performed in triplicate. Error bars represent the standard deviation above and below the mean. Data were analyzed by paired, two-tailed t-tests with p-values indicated. Values from wells with toxin but no CNF1 antisera served as background controls and were subtracted from all sample readings.

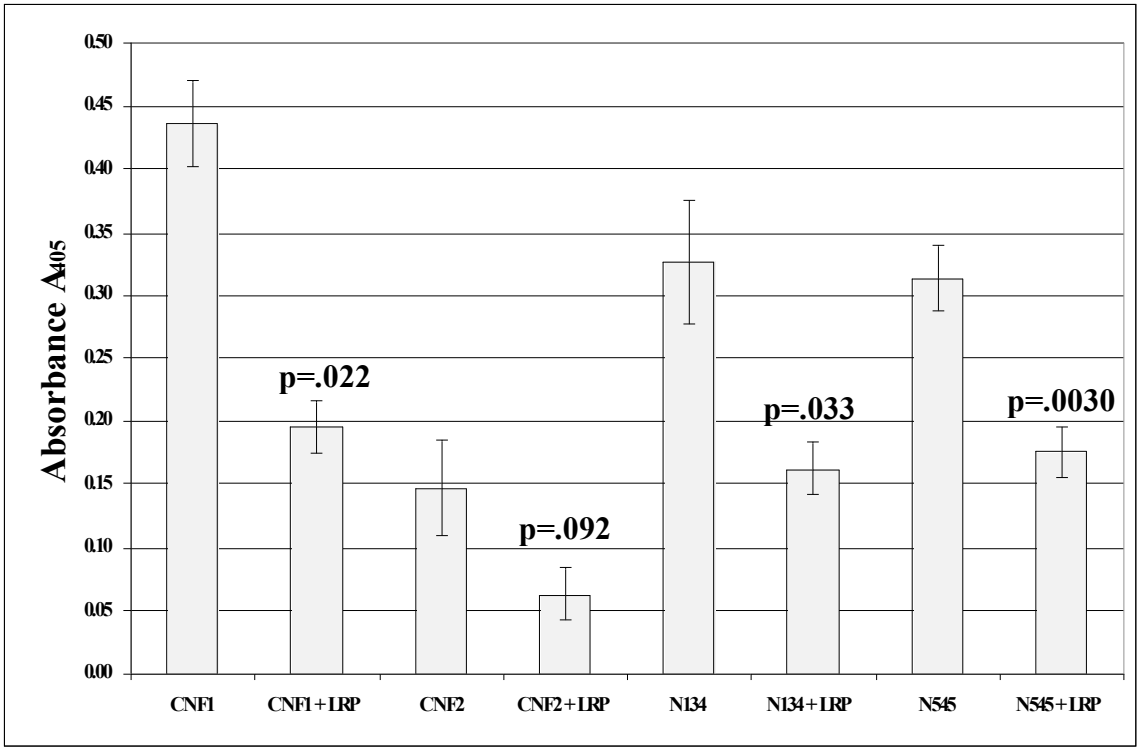
Absorbance A405
0.50
0.45
0.40
0.35
0.30
0.25
0.20
0.15
0.10
0.05
0.00
p=.022
p=.092
p=.033
p=.0030
CNF1
CNF1+LRP
CNF2
CNF2+LRP
N134
N134+LRP
N545
N545+LRP

significant compared to untreated toxin. Based on these results, it appears that the CNF2 epitope recognized by MAb BF8 can partially contribute to toxin binding and further suggests the presence of unique CNF2 binding sites or a secondary CNF2 receptor on HEp-2 cells in addition to LRP.

Co-localization of LRP and toxin on HEp-2 cells by immunofluorescence

As final confirmation of the delineation of the binding regions of CNF1, the truncated CNF1 toxins, ΔN134 and ΔN545 as well as CNF2, to LRP on HEp-2 cells, immunofluorescence co-localization experiments were performed. For these studies, toxins were allowed to bind to HEp-2 cells at 4°C prior to fixation and application of polyclonal anti-CNF1 and anti-LRP sera and differentially-labeled fluorescent secondary antibodies. As shown in Fig 19, CNF1, CNF2, ΔN134 and ΔN545 all co-localized with LRP (shown in merged panels with arrows). As toxins were not applied at saturating concentrations some unbound LRP on cells was also apparent in merged panels.

Figure 19: Co-localization of CNF1 and LRP on HEp-2 cells

CNF1, CNF2, ΔN134 and ΔN545 were bound to HEp-2 cells and cells subsequently stained with polyclonal anti-CNF1 and anti-LRP and the corresponding fluorescently-labeled secondary antibodies to allow visualization of toxin (green, Alexa 488) and LRP (red, Alexa 555). Confocal microscopy was used to demonstrate co-localization of the toxin and LRP receptor, as indicated by a yellow color (arrows) in merged panels. Images were taken at 100x magnification.

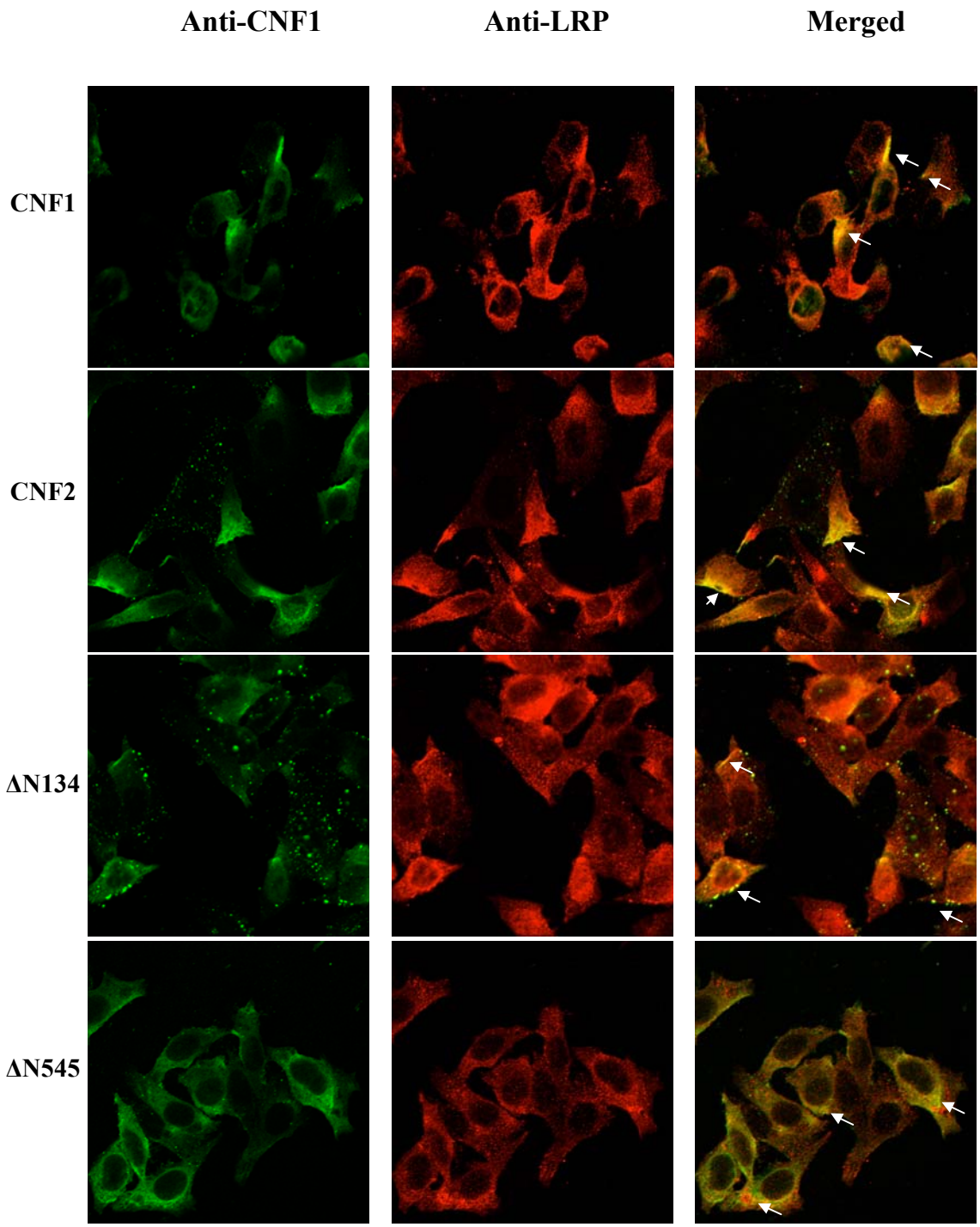
Anti-CNF1
Anti-LRP
Merged
CNF1
CNF2
ΔN134
ΔN545

Conclusions

Only one region of CNF1, its enzymatic C-terminal domain, has been crystallized (Buetow *et al.*, 2001). Thus, other functions attributed to the structure of this Rho GTPase-activating toxin have remained largely undefined. Prior to this work, only two published reports have focused on the identification of CNF1 domains required for eukaryotic cell binding (Fabbri *et al.*, 1999; Lemichez *et al.*, 1997). Furthermore, much of the earlier work on the delineation of CNF1 binding domains was hindered by the fact that the CNF1 receptor had not been identified. However, recent work which indicates that the 37 kDa laminin receptor precursor protein can serve as a receptor for CNF1 on HBMECs (Chung *et al.*, 2003) has provided new information that can be used in CNF1 structure-function analyses. In this study, recombinant LRP was used to help define the CNF1 cell-binding domains and here we report the involvement of two new regions of the toxin in binding to both LRP and HEp-2 cells.

The first CNF1 binding region specific for LRP is contained within the N-terminus of the toxin and resides between amino acids 135-272. The location of this LRP-binding site is consistent with a previous report which indicated that the first 190 amino acids of CNF1 were required for receptor binding (Fabbri *et al.*, 1999). However, in our studies, amino acids 53-75, the region proposed to be critical for cell binding, did not appear to be essential for toxin interaction with the target cell and as noted in the previous study, a peptide derived from this region could not inhibit binding (Fabbri *et al.*, 1999). In addition, a decrease in HEp-2 cell binding by mutants ΔN63 and ΔN75 was observed in our studies, which may suggest that removal of small portions of the N-terminus may alter the conformation of the toxin enough to hinder access to the binding

site that lies beyond amino acid 134. In fact, removal of the first 134 amino acids did not significantly affect the binding of CNF1 to LRP or HEp-2 cells as data presented here indicated that the N-terminal truncated CNF1 mutant, ΔN134, could bind to LRP, showed reduced binding to HEp-2 cells in the presence of exogenous LRP, and co-localized with LRP on the surface of HEp-2 cells. In addition, the results of toxin binding inhibition studies indicated that MAb BF8, a CNF1 neutralizing MAb that recognizes amino acids 135-164 (Meysick *et al.*, 2001), could significantly reduce the level of toxin binding to HEp-2 cells. Together, these data confirm the importance of amino acids 135-272 for effective toxin binding and strongly suggest that the first 30 amino acids of this region are critical in toxin-receptor interactions.

The second CNF1 eukaryotic cell-binding region identified in this study is contained within a region that lies beyond amino acid 546. Evidence which supports this conclusion includes the fact that truncated toxin ΔN545 exhibited strong binding to both HEp-2 cells and purified LRP. In addition, incubation of toxin ΔN545 with exogenous LRP prior to its application to HEp-2 cells significantly reduced toxin binding, an observation which suggests that this region can associate either directly or indirectly with surface-exposed LRP on HEp-2 cells. Finally, the presence of a receptor binding domain with this portion of CNF1 was substantiated by the fact that CNF1 neutralizing MAb NG8, whose epitope resides between residues 683-730 (Meysick *et al.*, 2001), could significantly reduce toxin binding to HEp-2 cells.

From the data presented here it appears that CNF1 contains two regions that are important for toxin binding, a finding that is particularly surprising given that one of these regions is located near the C-terminal catalytic domain of the toxin. Several

possibilities exist as to why CNF1 possesses two cellular binding domains. First, CNF may require two binding regions in order to permit maximal binding to surface-exposed LRP. As the crystal structure has only been resolved for amino acids 720-1014 of CNF1 (Buetow *et al.*, 2001), it is not clear how the N-terminus of the molecule folds or interacts with its putative receptor. Therefore, it is possible that amino acids 135-272 and those beyond 546 may fold in such a way so as to form an LRP-binding pocket. A second reason to explain why CNF1 possesses two binding domains is the presence of a second cellular receptor to which CNF1 can bind. This possibility is based on results which indicate that toxin binding can still occur even in the presence of high levels of exogenous LRP. Addition of exogenous LRP has also been shown to block CNF1 binding to the mature laminin receptor (Kim *et al.*, 2005). This putative second receptor may also serve as a co-receptor with LRP. The capacity of CNF1 to bind to other surface-exposed eukaryotic molecules, in addition to LRP, may also help to explain the wide range of tissue culture cell types that are susceptible to this toxin (Mills *et al.*, 2000). LRP is itself ubiquitous with humans possessing multiple copies of the gene (Mecham, 1991; Rieger *et al.*, 1999). Finally, the possibility exists that only the first binding region (amino acids 135-272) is required for interaction with LRP or other cellular receptors and that the second binding region is an artificial one created in truncated toxins by exposure of a portion of the molecule that is normally masked or inaccessible in the wild-type toxin. However, the results presented in this study do not appear to support this possibility as MAb NG8 not only recognized and blocked the binding of truncated toxin ΔN545 to HEp-2 cells but was equally effective in the inhibition of wild-type toxin binding as well as in the neutralization of toxic activity.

These data clearly indicate that the NG8 epitope is exposed and accessible in both ΔN545 and the holotoxin.

The fact that CNF1 and CNF2 share a high degree of amino acid homology also suggests that these two toxins could possess a common eukaryotic receptor, specifically LRP. From the binding and co-localization studies presented here, it does appear that CNF2 can bind to exogenous LRP as well as surface-bound LRP on HEp-2 cells but to a lesser extent than that observed with CNF1 (Fig 15A). Furthermore, neither the presence of neutralizing MAb BF8 nor exogenous LRP significantly affected the level of CNF2 bound to HEp-2 cells. Taken together, these data indicate that CNF2 can use LRP as its receptor ligand but also suggests that differences in affinity or avidity to LRP exist between these two toxins. This finding may also help to explain why CNF1 appears more potent than CNF2 in HEp-2 intoxication assays (K. Grande, S. Rasmussen, K. Meysick, and A. O'Brien, unpublished data).

In summary, two new regions of CNF1 have been identified that mediate toxin binding to purified preparations of the CNF1 receptor, LRP, as well as to LRP expressed on the surface of HEp-2 cells, amino acids 135-272 and the distal 468 amino acids of the toxin. In addition, we have found that CNF2 can also bind to exogenous LRP and co-localizes with LRP on the surface of HEp-2 cells. This latter result in particular suggests that LRP may also serve as the receptor for CNF2. Finally, it appears that two CNF1 MAbs, BF8 and NG8, mediate toxin neutralization by inhibiting binding of toxin to its LRP receptor.

CHAPTER 4: DISCUSSION AND FUTURE DIRECTIONS

Discussion

Overview of conclusions in context of the specific aims

In this study, I sought to accurately define regions of CNF1 that were responsible for the enzymatic, and receptor- binding activities of the toxin. Aim 1 was designed to define the segments within CNF1 that dictate the appearance of tissue culture cells after intoxication with CNF1. For this purpose, I evaluated the phenotypes on two different cell lines of CNF1/DNT chimeric toxins that had previously been constructed. I found that a 100 amino acid region of DNT that contained aa 1250-1314, the segment with the highest homology to CNF1, was sufficient to cause a DNT-like phenotype on a primarily CNF1 backbone. More specifically, CDHyb2, the chimeric toxin with the above noted region of DNT, had no effect on HEp-2 cells but evoked binucleation of Swiss 3T3 cells in a manner similar to that of wild-type DNT.

One major difference between CNF1 and DNT in the aa 1250-1314 region occurs within the catalytic site. CNF1 has two amino acids that are required for enzymatic activity, Cys^{866} and His^{881}. DNT also has those amino acids as part of its catalytic triad (Cys^{1292} and His^{1307}), but an additional residue, third, Lys^{1310}, is necessary for the toxin to function enzymatically. In the second aim, I hypothesized that Lys^{1310} DNT not only controls the phenotypes seen on HEp-2 and Swiss 3T3 cells but is also responsible for substrate preference (RhoA=Rac1>Cdc42) and the predilection of DNT for transglutamination over deamidation of Rho GTPases. Therefore, in the second aim, I derived site-directed mutations in CNF1 (T884K) and DNT (K1310T) to determine the role of Lys^{1310} in phenotypic and enzymatic assays. When lysine was substituted for threonine in CNF1, the CNF1 site-directed mutant acted more like DNT, in that CNF1

T884K lost the capacity to multinucleate HEp-2 cells and binucleated, but was not cytotoxic to, Swiss 3T3 cells. Conversely, a threonine to lysine switch in DNT caused this site-directed mutant to gain a CNF1-like phenotype, i.e., capacity to multinucleate HEp-2 cells and kill Swiss 3T3 cells. In spite of these CNF1-like effects on tissue culture cells that were in fact more striking than wild-type CNF1 at the same dose, DNT K1310T could not deamidate Rho GTPases. This latter observation suggests that the lysine residue in DNT is required for this enzymatic reaction to occur, a finding others have noted (Schmidt *et al.*, 1999). Nevertheless, DNT K1310T could still transglutaminate RhoA over time, although not as efficiently as wild-type DNT.

The experiments in the first two aims were focused on identification of the region and amino acids responsible for the differences in phenotypic effects on cells and enzymatic reactions of CNF1 and the related toxin, DNT. The third aim was designed to examine the region of CNF1 that binds to its receptor, laminin receptor precursor protein. In pursuit of that goal, I used previously constructed CNF1 truncated mutants in a newly-developed LRP binding assay. I found that CNF1 has two regions that bind LRP, one between amino acids 135-272 and the other after aa 546. To confirm that these regions were involved in interaction with the receptor, I incubated full-length CNF1 and truncated mutants that contain the above defined amino acid sequences with two antibodies previously described to neutralize CNF1, BF8 and NG8. The epitopes of these monoclonal antibodies lie within the two proposed binding regions, and the presence of these antibodies decreased adherence of CNF1 and truncated mutants ΔN134 and ΔN545 to HEp-2 cells. Incubation of CNF1, ΔN134 or ΔN545 with other non-neutralizing antibodies as well as an irrelevant anti-Stx antibody did not significantly attenuate the

level of binding of these toxins to HEp-2 cells. Furthermore, addition of exogenous LRP to CNF1, ΔN134, and ΔN545 prior to exposure of the mixtures to HEp-2 cells significantly diminished the amount of toxin that bound to the cells. However, that inhibition of binding was not complete, a finding that led to the conclusion that there may be an additional receptor or co-receptor of CNF1 on cells. I also found that CNF2 could bind to LRP both *in vitro* and on tissue culture cells, but the extent of this binding was reduced compared to CNF1. I speculated that CNF2 might use another receptor on HEp-2 cells in addition to LRP.

Toxin Structure as it Relates to Function

In 1998, Schmidt and colleagues identified Cys^{866} and His^{881} of CNF1 as essential for the enzymatic activity of the toxin through the creation and evaluation of site-specific alterations in these amino acids (Schmidt *et al.*, 1998). In 2001, Buetow *et al.*, reported the crystal structure of the C-terminus of CNF1 and described the positions of these two amino acids in the catalytic site of that toxin [(Buetow *et al.*, 2001); (Figure 20). Although the catalytic triad of DNT has been identified (Schmidt *et al.*, 1999), that toxin has not been crystallized. Therefore, the structural bases for the interactions between DNT and Rho GTPases remain subjects of speculation. That the exchange of a 100 amino acid region of DNT with the highest homology to CNF1 onto a CNF1 backbone can make this hybrid molecule evoke a phenotype like that of DNT (McNichol *et al.*, 2006) indicates that the DNT portion must fold appropriately within the context of the CNF1 molecule to elicit enzymatic activity. This finding, in turn, suggests that the two toxins have structural similarity in this region. Yet, the phenotypic and enzymatic

Figure 20: Crystal structure of the C-terminus of CNF1

The published crystal structure of the C-terminus of CNF1, representing amino acids 720-1014. In panel **A**, the stereo view of the C-terminus is represented. Panel **B** depicts the ribbon diagram. Alpha helices are shown in blue, beta sheets in red, and coils in green. The topology of the C-terminus is shown in panel **C**, with alpha helices represented with rectangles and beta sheets shown as arrows. The catalytic amino acids Cys^{866} and His^{881} are depicted.

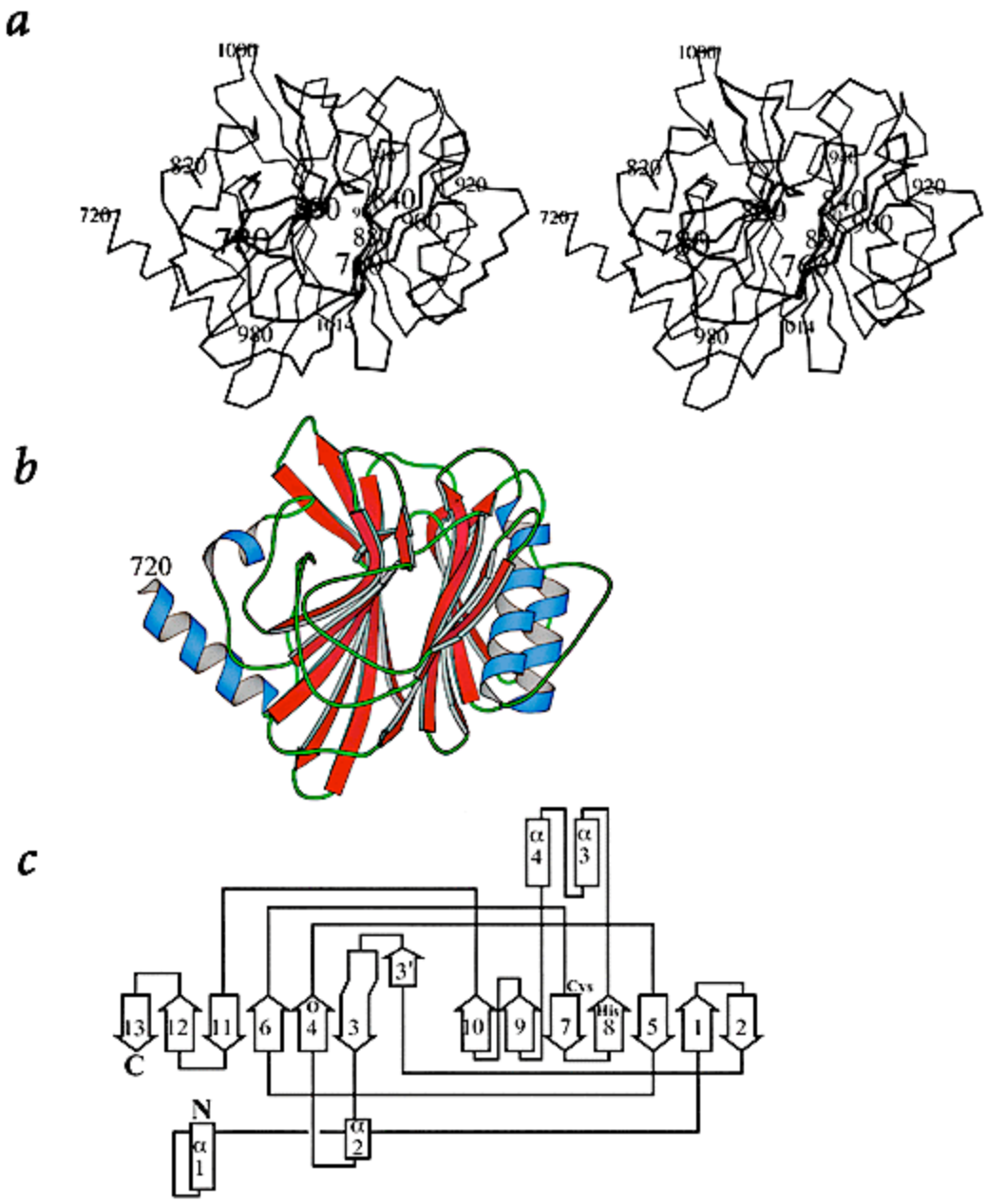

Courtesy of Dr. Partho Ghosh (Buetow *et al.*, 2001), used with permission

differences between the two toxins are striking. DNT can only intoxicate a few cell types and preferentially transglutaminates rather than deamidates Rho GTPases (Horiguchi, 2001), while CNF1 can intoxicate a wide variety of eukaryotic cells (Donelli and Fiorentini, 1992; Fiorentini *et al.*, 1988; McNichol *et al.*, 2006; Mills *et al.*, 2000) and preferentially deamidates, rather than transglutaminates RhoA, Rac1 and Cdc42 (Boquet, 2001). In addition, CNF1 favors RhoA and Cdc42 over Rac1 as substrates, while DNT targets RhoA and Rac1 over Cdc42 (Horiguchi, 2001).

The most surprising observation from my analysis of CNF1/DNT hybrids was that the lysine residue in the catalytic triad of DNT is sufficient to control the phenotype on cells. There are at least two explanations as to why this single amino acid could have an effect on phenotype and enzymatic activity of these toxins: the length of the amino acid side chain and/or the charge of the molecule. My theory on the possible impact of the long side chain of lysine is that it hinders the capacity of GTPases to bind tightly to the catalytic pocket, whereas threonine, the amino acid in the comparable position in CNF1, has a short side chain that may permit a closer interaction between CNF1 and RhoA, Rac1 or Cdc42. First, substitution of lysine for threonine in CNF1 resulted in a change to a DNT-like phenotype, whereas a threonine to lysine switch in DNT caused this site-directed mutant to act more like CNF1. The following information favors the idea of side chain length altering the strength of the interaction between enzyme and substrate; a hypothetical ribbon diagram of the CNF1 catalytic pocket, specifically amino acids 866, 881 and 884, is depicted in Figure 21 (J. Sinclair, unpublished data). One could argue, based on the decrease in multinucleation activity of CNF1 T884K that making a

Figure 21: Hypothetical ribbon structure of the catalytic pocket of CNF1 and the site-directed mutant CNF1 T884K

Hypothetical ribbon diagram of wild-type CNF1 and CNF1 T884K. Panel **A**: Wild-type CNF1 with the active Cys^{866} and His^{881} residues highlighted, as well as Thr^{884}. Panel **B**: CNF1 T884K shown with the threonine to lysine amino acid change. Ribbon structures were generated with Protein Explorer (http://proteinexplorer.org) (Martz, 2002).

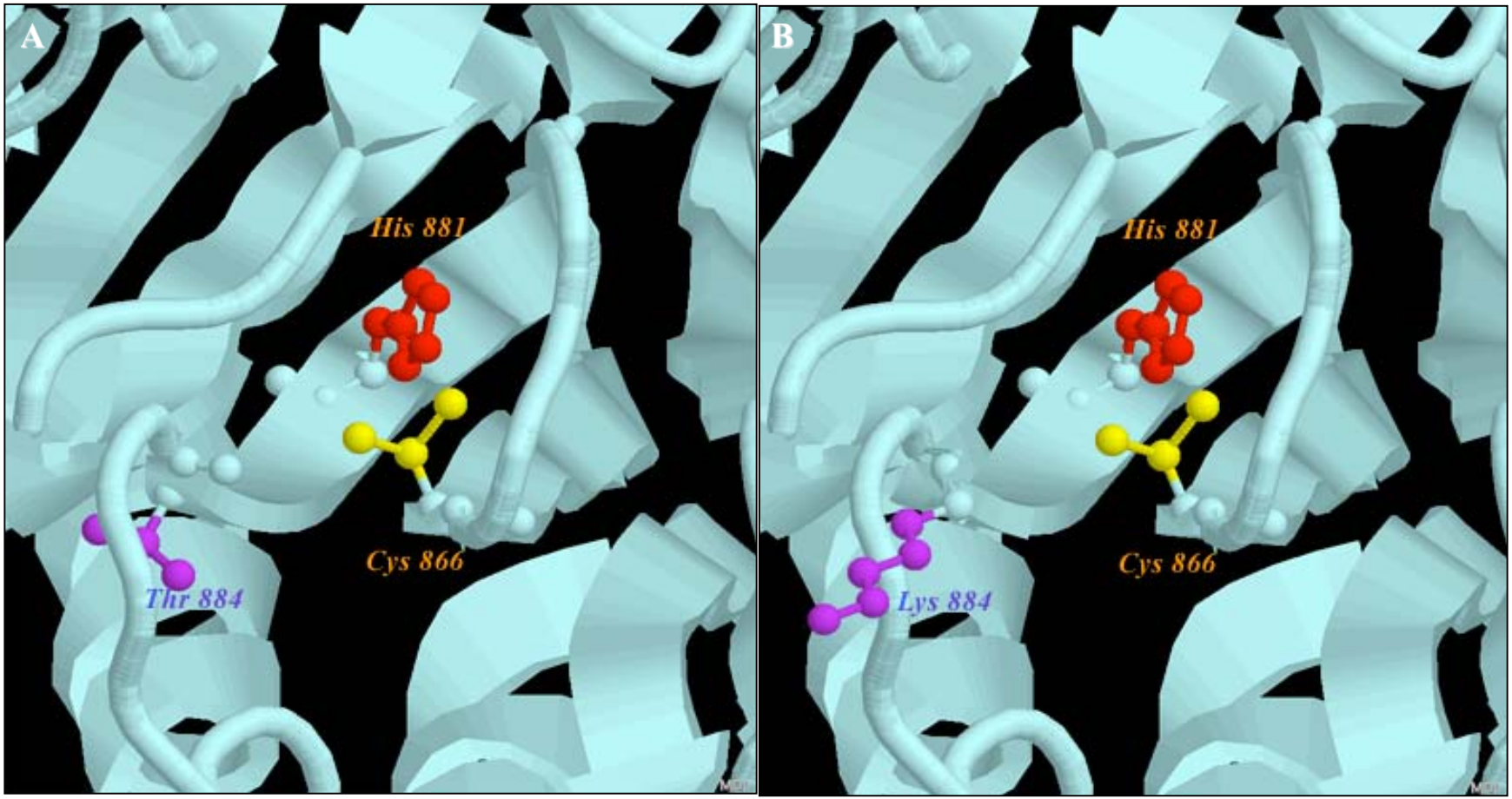

CNF1 Wild-type **CNF1 T884K**

Courtesy of Dr. James Sinclair (used with permission)

substitution in the active site of CNF1 might result in an inactive toxin. However, the CNF1 site-directed mutant toxin binucleated Swiss 3T3 cells in a DNT-like manner. Second, removal of lysine from DNT and CDHyb2 led to multinucleation of HEp-2 cells by two toxins that lacked this phenotype in their native states. Third, the substitution of threonine for lysine at position 1310 of DNT resulted in a toxin that was more cytotoxic to Swiss 3T3 cells than wild-type CNF1. In aggregate, these data support the theory that the lysine residue interferes with a strong association between the toxin and substrate.

The other factor associated with the presence of the lysine residue in DNT versus a threonine at the comparable position in CNF1 is that a different charge is created in the catalytic pocket. The mode of action preferred by DNT is transglutamination in which Rho GTPases are cross-linked to a co-substrate (Barbieri *et al.*, 2002). A number of primary amines, such as putrescine, spermidine and cadaverine, can serve as co-substrates for DNT (Schmidt *et al.*, 2001). Lysine carries a negative charge that could attract the positively-charged amines to the catalytic pocket and thus permit modification of the GTPases. However, this residue must not be the only factor important for transglutamination because the DNT site-directed mutant was still capable of transglutaminating RhoA, albeit at a slower rate than wild-type DNT. Similarly, CNF1 T884K did not demonstrate increased efficiency for transglutamination as expected. Further modification of amino acids in the catalytic pocket may answer more questions regarding the preference of DNT for transglutamination over deamidation.

In the N-terminal binding domain of CNF1, we sought to determine the region of the toxin that bound to LRP, its cellular receptor. What we actually found, however, was that there are two regions of CNF1 that interact with LRP, one in the N-terminus between

amino acids 135-272 and the other in the C-terminus, after amino acid 546. This finding was not predicted because the dogma in current literature is that the binding site is contained within the first 190 amino acids of the toxin (Fabbri *et al.*, 1999). That there might be more than one region of CNF1 important for binding was a surprising observation based on the paradigms of other single chain toxins.

There is no crystal structure of the N-terminus of CNF1 so we cannot definitively predict where the toxin might come in contact with the receptor. However, hypothetical molecular modeling suggests that the two regions defined above may, in fact, come together to bind LRP on the eukaryotic cell surface (J. Sinclair, unpublished data; figure 22). In the model, the N-terminus, as well as the region between the proposed transmembrane segment and C-terminus, has homology to ATPase domains that function to move substances across the cell membrane. One possibility based on this model is that upon binding of the two regions of CNF1 to LRP, a conformational change occurs that facilitates the insertion of the transmembrane domain into the eukaryotic cell. This insertional event could in turn, trigger internalization of the toxin.

Another important inference from the results of the binding studies with CNF1 and HEp-2 cells is that there may be a second receptor or co-receptor present on those cells with which CNF1 interacts. Specifically, addition of exogenous LRP, which will inhibit binding to both the 37 kDa precursor and 67 kDa mature forms of LRP/LR (Kim *et al.*, 2005), did not completely block the association of toxin with HEp-2 cells. Of note, LRP can serve as a receptor for other pathogens, including viruses and prions (Gauczynski *et al.*, 2001; Hundt *et al.*, 2001; Ludwig *et al.*, 1996; Rieger *et al.*, 1999; Wang *et al.*, 1992), and Hundt *et al*. suggested that the cellular prion protein binds to LRP via two regions.

Figure 22: Probable structure of CNF1

A hypothetical diagram of how CNF1 may fold to interact with LRP. Model: the two ATPase-like domains that encompass amino acids 1-250 and 450-700, come together and cause the proposed transmembrane segment to protrude outward. When the ATPase-like domains of CNF1 bind to the receptor on the eukaryotic cell surface, a conformational change in the toxin occurs in which the transmembrane domain flips and inserts into the cell. This latter step facilitates internalization of the toxin.

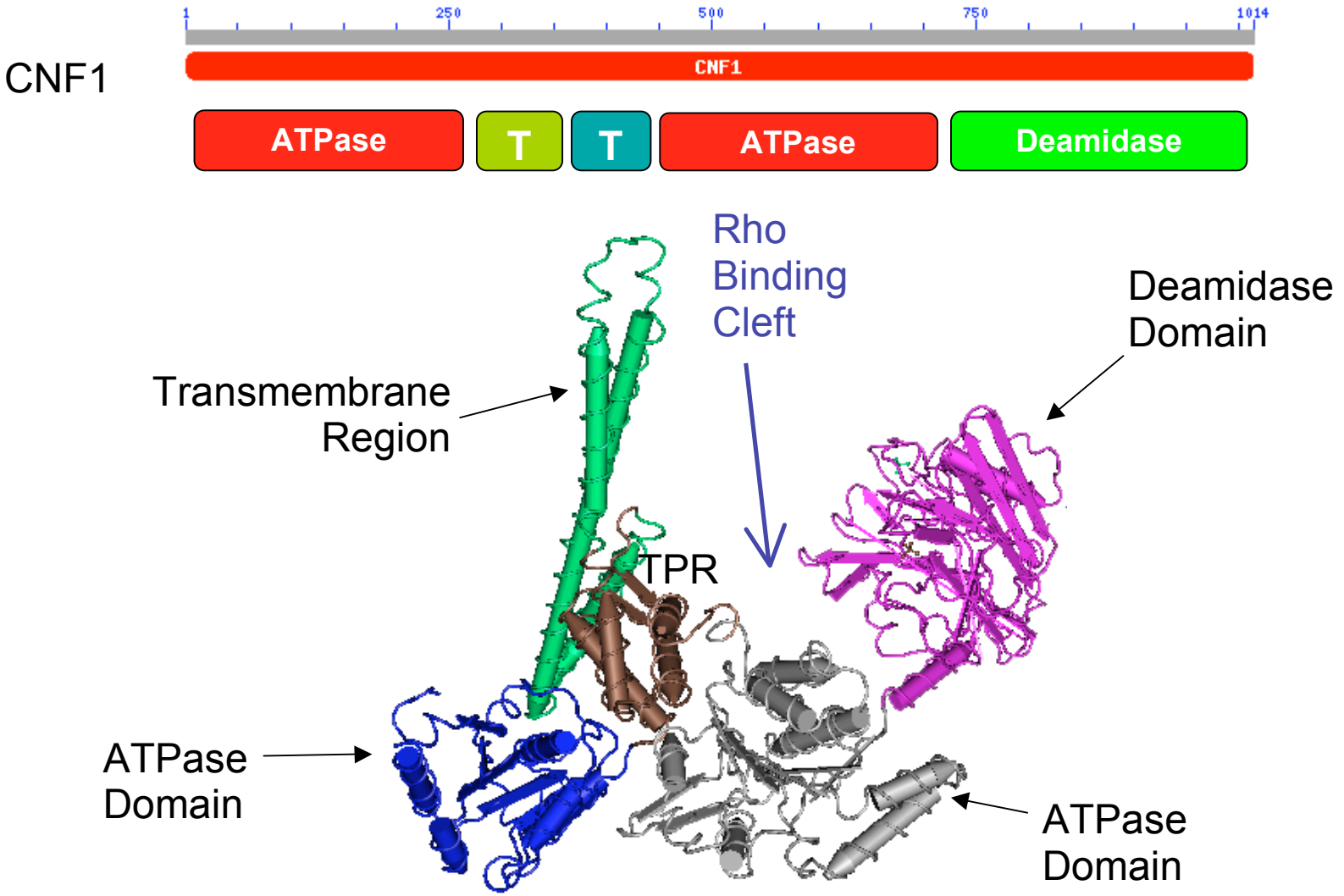

Courtesy of Dr. James Sinclair (used with permission)

The second region on the cellular prion protein interacts with LRP through a heparin sulfate side chain of a heparin sulfate proteoglycan (HSPG) molecule (Gauczynski *et al.*, 2001; Hundt *et al.*, 2001). While I do not suggest that CNF1 uses HSPG as its second receptor, I made this point to illustrate that a precedent of a second receptor has already been set for another infectious agent that also engages LRP as its receptor. It is possible that CNF1 is acting like the prion protein, in that it uses a co-receptor to bind and, subsequently, intoxicate the cell.

Future Directions

While significant insight about the enzymatic functions of CNF1 and the related DNT was gained from our published studies with the CNF1/DNT hybrids, there are still several questions that remain to be answered. First, we would like to know whether the same region of CNF1 that was replaced by DNT, corresponding to amino acids 824-925, could transfer a CNF1-like phenotype on to a DNT backbone. To address this question, I constructed this hybrid by using splicing by overlap extension PCR and then purified the toxin by FPLC. However, the chimeric toxin, DCHyb2, was not active on either HEp-2 or Swiss 3T3 cells. Moreover, DCHyb2 appeared to be just barely capable of deamidating RhoA and Rac1. Because there are no monoclonal antibodies against DNT available, I could not ascertain by the approach of probing the chimera with conformationally-reactive monoclonal antibodies whether the toxin was relatively inactive because it was folding improperly.

Another question we would like to answer is whether the CNF1 and DNT site-directed mutants behave like the opposite toxin regarding substrate preference. Because

our data only represented two points in time, it would be interesting to observe the kinetics of modification of GTPases. This could be done *in vivo* in HEp-2 or HeLa cells with fluorescently-labeled antibodies against RhoA, Rac1 and Cdc42 to visualize the cellular modifications caused after intoxication with the toxins. Tracking a time course of intoxication might help to better understand exactly how the residues of the catalytic diad/triad of CNF1 and DNT, respectively, contribute to substrate preference.

The results of the binding studies raised several other issues that can be addressed. First, the binding data reinforced the need for a crystal structure of the CNF1 holotoxin to facilitate interpretation of results. At this point, we can only speculate about how the two regions of CNF1 that we identified as binding sites for LRP come together to make contact with the receptor. Work is currently underway through a collaboration with our laboratory to accomplish the goal of solving the crystal structure of CNF1. Not only will such a crystal structure provide insight about the binding regions of CNF1, it will also delineate where the putative transmembrane domains lie. This latter information is crucial to understand how the toxin becomes internalized within its eukaryotic target cell. Second, our studies indirectly imply that CNF1 may interact with more than one receptor to gain entry into eukaryotic cells. Because CNF1 intoxicates so many cell types, the presence of a second receptor/co-receptor is quite plausible. To investigate this bi-receptor theory, a yeast two-hybrid system could be applied in a manner similar to that used by Chung *et al.*, 2003 to identify LRP as a receptor for CNF1 (Chung *et al.*, 2003). Another approach to identify a second receptor might be to prepare tryptic digests of CNF1-intoxicated HEp-2 cell lysates and analyze them by mass spectrometry.

REFERENCES

Agace, W., Connell, H., and Svanborg, C. (1996) Host Resistance to Urinary Tract Infection. In *Urinary Tract Infections: Molecular Pathogenesis and Clinical Management*. Mobley, H.L. and Warren, J.W. (eds). Washington, D.C.: ASM Press, pp. 221-243.

Aktories, K. (1997) Rho proteins: targets for bacterial toxins. *Trends Microbiol* **5**: 282-288.

Aktories, K. (2003) Glucosylating and Deamidating Bacterial Protein Toxins. In *Bacterial Protein Toxins*. Burns, D., Barbieri, J.T., Iglewski, B.H. and Rappouli, R. (eds). Washington, D. C.: ASM Press, pp. 229-243.

Aktories, K., and Barbieri, J.T. (2005) Bacterial cytotoxins: targeting eukaryotic switches. *Nat Rev Microbiol* **3**: 397-410.

Andreu, A., Stapleton, A.E., Fennell, C., Lockman, H.A., Xercavins, M., Fernandez, F., and Stamm, W.E. (1997) Urovirulence determinants in *Escherichia coli* strains causing prostatitis. *J Infect Dis* **176**: 464-469.

Aspenstrom, P. (1999) Effectors for the Rho GTPases. *Curr Opin Cell Biol* **11**: 95-102.

Baldwin, M.R., Lakey, J.H., and Lax, A.J. (2004) Identification and characterization of the *Pasteurella multocida* toxin translocation domain. *Mol Microbiol* **54**: 239-250.

Barbieri, J.T., Riese, M.J., and Aktories, K. (2002) Bacterial toxins that modify the actin cytoskeleton. *Annu Rev Cell Dev Biol* **18**: 315-344.

Bishop, A.L., and Hall, A. (2000) Rho GTPases and their effector proteins. *Biochem J* **348 Pt 2**: 241-255.

Blanco, J., Blanco, M., Alonso, M.P., Blanco, J.E., Gonzalez, E.A., and Garabal, J.I. (1992) Characteristics of haemolytic *Escherichia coli* with particular reference to production of cytotoxic necrotizing factor type 1 (CNF1). *Res Microbiol* **143**: 869-878.

Boquet, P. (1998) Cytotoxic necrotizing factor 1 from *Escherichia coli*: a toxin with a new intracellular activity for eukaryotic cells. *Folia Microbiol (Praha)* **43**: 285-289.

Boquet, P. (2000) The cytotoxic necrotizing factor 1 (CNF1) from uropathogenic *Escherichia coli*. *Adv Exp Med Biol* **485**: 45-51.

Boquet, P. (2001) The cytotoxic necrotizing factor 1 (CNF1) from *Escherichia coli*. *Toxicon* **39**: 1673-1680.

Boquet, P., and Lemichez, E. (2003) Bacterial virulence factors targeting Rho GTPases: parasitism or symbiosis? *Trends Cell Biol* **13**: 238-246.

Bower, J.M., Eto, D.S., and Mulvey, M.A. (2005) Covert operations of uropathogenic *Escherichia coli* within the urinary tract. *Traffic* **6**: 18-31.

Brockmeier, S.L., Register, K.B., Magyar, T., Lax, A.J., Pullinger, G.D., and Kunkle, R.A. (2002) Role of the dermonecrotic toxin of *Bordetella bronchiseptica* in the pathogenesis of respiratory disease in swine. *Infect Immun* **70**: 481-490.

Buetow, L., Flatau, G., Chiu, K., Boquet, P., and Ghosh, P. (2001) Structure of the Rho-activating domain of *Escherichia coli* cytotoxic necrotizing factor 1. *Nat Struct Biol* **8**: 584-588.

Buetow, L., and Ghosh, P. (2003) Structural Elements Required for Deamidation of RhoA by Cytotoxic Necrotizing Factor 1. *Biochemistry* **42**: 12784-12791.

Busch, C., Orth, J., Djouder, N., and Aktories, K. (2001) Biological activity of a C-terminal fragment of *Pasteurella multocida* toxin. *Infect Immun* **69**: 3628-3634.

Caprioli, A., Falbo, V., Roda, L.G., Ruggeri, F.M., and Zona, C. (1983) Partial purification and characterization of an *Escherichia coli* toxic factor that induces morphological cell alterations. *Infect Immun* **39**: 1300-1306.

Caprioli, A., Falbo, V., Ruggeri, F.M., Baldassarri, L., Bisicchia, R., Ippolito, G., Romoli, E., and Donelli, G. (1987) Cytotoxic necrotizing factor production by hemolytic strains of *Escherichia coli* causing extraintestinal infections. *J Clin Microbiol* **25**: 146-149.

Chung, J.W., Hong, S.J., Kim, K.J., Goti, D., Stins, M.F., Shin, S., Dawson, V.L., Dawson, T.M., and Kim, K.S. (2003) 37-kDa laminin receptor precursor modulates cytotoxic necrotizing factor 1-mediated RhoA activation and bacterial uptake. *J Biol Chem* **278**: 16857-16862.

Contamin, S., Galmiche, A., Doye, A., Flatau, G., Benmerah, A., and Boquet, P. (2000) The p21 Rho-activating toxin cytotoxic necrotizing factor 1 is endocytosed by a clathrin-independent mechanism and enters the cytosol by an acidic-dependent membrane translocation step. *Mol Biol Cell* **11**: 1775-1787.

D'Orazio, S.E., and Collins, C.M. (1998) Molecular pathogenesis of urinary tract infections. *Curr Top Microbiol Immunol* **225**: 137-164.

Davis, J.M., Rasmussen, S.B., and O'Brien, A.D. (2005) Cytotoxic necrotizing factor type 1 production by uropathogenic *Escherichia coli* modulates polymorphonuclear leukocyte function. *Infect Immun* **73**: 5301-5310.

Davis, J.M., Carvalho, H.M., Rasmussen, S.B., and O'Brien A, D. (2006) Cytotoxic Necrotizing Factor Type 1 (CNF1) Delivered by Outer Membrane Vesicles of Uropathogenic *Escherichia coli* Attenuates Polymorphonuclear Leukocyte Antimicrobial Activity and Chemotaxis. *Infect Immun* **In press**.

De Rycke, J., Guillot, J.F., and Boivin, R. (1987) Cytotoxins in non-enterotoxigenic strains of *Escherichia coli* isolated from feces of diarrheic calves. *Vet Microbiol* **15**: 137-150.

De Rycke, J., Oswald, E., and Boivin, R. (1989) An in vivo assay for the detection of cytotoxic strains of *Escherichia coli*. *Ann Rech Vet* **20**: 39-46.

De Rycke, J., Gonzalez, E.A., Blanco, J., Oswald, E., Blanco, M., and Boivin, R. (1990) Evidence for two types of cytotoxic necrotizing factor in human and animal clinical isolates of *Escherichia coli*. *J Clin Microbiol* **28**: 694-699.

De Rycke, J., Milon, A., and Oswald, E. (1999) Necrotoxic *Escherichia coli* (NTEC): two emerging categories of human and animal pathogens. *Vet Res* **30**: 221-233.

Donelli, G., and Fiorentini, C. (1992) Cell injury and death caused by bacterial protein toxins. *Toxicol Lett* **64-65 Spec No**: 695-699.

Donnenberg, M.S., and Welch, R.A. (1996a) Virulence Determinants of Uropathogenic *Escherichia coli*. In *Urinary Tract Infections: Molecular Pathogenesis and Clinical Management*. Mobley, H.L.T. and Warren, J.W. (eds). Washington, D. C.: ASM Press, pp. 439.

Donnenberg, M.S., and Welch, R.A. (1996b) Virulence determinants of uropathogenic *Escherichia coli*. In *Urinary Tract Infections: Molecular Pathogenesis and*

Clinical Management. Mobley, H.L.T. and Warren, J.W. (eds). Washington, D. C.: American Society of Microbiology Press, pp. 135-174.

Emody, L., Kerenyi, M., and Nagy, G. (2003) Virulence factors of uropathogenic *Escherichia coli*. *Int J Antimicrob Agents* **22 Suppl 2**: 29-33.

Fabbri, A., Gauthier, M., and Boquet, P. (1999) The 5' region of *cnf1* harbours a translational regulatory mechanism for CNF1 synthesis and encodes the cell-binding domain of the toxin. *Mol Microbiol* **33**: 108-118.

Falbo, V., Pace, T., Picci, L., Pizzi, E., and Caprioli, A. (1993) Isolation and nucleotide sequence of the gene encoding cytotoxic necrotizing factor 1 of *Escherichia coli*. *Infect Immun* **61**: 4909-4914.

Falkow, S., Isberg, R.R., and Portnoy, D.A. (1992) The interaction of bacteria with mammalian cells. *Annu Rev Cell Biol* **8**: 333-363.

Falnes, P.O., and Sandvig, K. (2000) Penetration of protein toxins into cells. *Curr Opin Cell Biol* **12**: 407-413.

Falzano, L., Fiorentini, C., Donelli, G., Michel, E., Kocks, C., Cossart, P., Cabanie, L., Oswald, E., and Boquet, P. (1993) Induction of phagocytic behaviour in human epithelial cells by *Escherichia coli* cytotoxic necrotizing factor type 1. *Mol Microbiol* **9**: 1247-1254.

Fiorentini, C., Arancia, G., Caprioli, A., Falbo, V., Ruggeri, F.M., and Donelli, G. (1988) Cytoskeletal changes induced in HEp-2 cells by the cytotoxic necrotizing factor of *Escherichia coli*. *Toxicon* **26**: 1047-1056.

Fiorentini, C., Fabbri, A., Flatau, G., Donelli, G., Matarrese, P., Lemichez, E., Falzano, L., and Boquet, P. (1997) *Escherichia coli* cytotoxic necrotizing factor 1 (CNF1), a toxin that activates the Rho GTPase. *J Biol Chem* **272**: 19532-19537.

Flatau, G., Lemichez, E., Gauthier, M., Chardin, P., Paris, S., Fiorentini, C., and Boquet, P. (1997) Toxin-induced activation of the G protein p21 Rho by deamidation of glutamine. *Nature* **387**: 729-733.

Flatau, G., Landraud, L., Boquet, P., Bruzzone, M., and Munro, P. (2000) Deamidation of RhoA glutamine 63 by the *Escherichia coli* CNF1 toxin requires a short sequence of the GTPase switch 2 domain. *Biochem Biophys Res Commun* **267**: 588-592.

Foxman, B., Zhang, L., Tallman, P., Palin, K., Rode, C., Bloch, C., Gillespie, B., and Marrs, C.F. (1995) Virulence characteristics of *Escherichia coli* causing first urinary tract infection predict risk of second infection. *J Infect Dis* **172**: 1536-1541.

Foxman, B., Gillespie, B., Koopman, J., Zhang, L., Palin, K., Tallman, P., Marsh, J.V., Spear, S., Sobel, J.D., Marty, M.J., and Marrs, C.F. (2000) Risk factors for second urinary tract infection among college women. *Am J Epidemiol* **151**: 1194-1205.

Foxman, B. (2002) Epidemiology of urinary tract infections: incidence, morbidity, and economic costs. *Am J Med* **113 Suppl 1A**: 5S-13S.

Franco, A.V. (2005) Recurrent urinary tract infections. *Best Pract Res Clin Obstet Gynaecol* **19**: 861-873.

Frankel, G., Candy, D.C., Everest, P., and Dougan, G. (1994) Characterization of the C-terminal domains of intimin-like proteins of enteropathogenic and

enterohemorrhagic *Escherichia coli*, *Citrobacter freundii*, and *Hafnia alvei*. *Infect Immun* **62**: 1835-1842.

Fukui, A., and Horiguchi, Y. (2004) *Bordetella* dermonecrotic toxin exerting toxicity through activation of the small GTPase Rho. *J Biochem (Tokyo)* **136**: 415-419.

Gauczynski, S., Peyrin, J.M., Haik, S., Leucht, C., Hundt, C., Rieger, R., Krasemann, S., Deslys, J.P., Dormont, D., Lasmezas, C.I., and Weiss, S. (2001) The 37-kDa/67-kDa laminin receptor acts as the cell-surface receptor for the cellular prion protein. *Embo J* **20**: 5863-5875.

Hall, A. (1994) Small GTP-binding proteins and the regulation of the actin cytoskeleton. *Annu Rev Cell Biol* **10**: 31-54.

Hall, A. (1998) Rho GTPases and the actin cytoskeleton. *Science* **279**: 509-514.

Hofman, P., Flatau, G., Selva, E., Gauthier, M., Le Negrate, G., Fiorentini, C., Rossi, B., and Boquet, P. (1998) *Escherichia coli* cytotoxic necrotizing factor 1 effaces microvilli and decreases transmigration of polymorphonuclear leukocytes in intestinal T84 epithelial cell monolayers. *Infect Immun* **66**: 2494-2500.

Horiguchi, Y., Nakai, T., and Kume, K. (1989) Purification and characterization of *Bordetella bronchiseptica* dermonecrotic toxin. *Microb Pathog* **6**: 361-368.

Horiguchi, Y., Nakai, T., and Kume, K. (1991) Effects of *Bordetella bronchiseptica* dermonecrotic toxin on the structure and function of osteoblastic clone MC3T3-e1 cells. *Infect Immun* **59**: 1112-1116.

Horiguchi, Y., Sugimoto, N., and Matsuda, M. (1993) Stimulation of DNA synthesis in osteoblast-like MC3T3-E1 cells by *Bordetella bronchiseptica* dermonecrotic toxin. *Infect Immun* **61**: 3611-3615.

Horiguchi, Y., Okada, T., Sugimoto, N., Morikawa, Y., Katahira, J., and Matsuda, M. (1995a) Effects of *Bordetella bronchiseptica* dermonecrotizing toxin on bone formation in calvaria of neonatal rats. *FEMS Immunol Med Microbiol* **12**: 29-32.

Horiguchi, Y., Senda, T., Sugimoto, N., Katahira, J., and Matsuda, M. (1995b) *Bordetella bronchiseptica* dermonecrotizing toxin stimulates assembly of actin stress fibers and focal adhesions by modifying the small GTP-binding protein rho. *J Cell Sci* **108 (Pt 10)**: 3243-3251.

Horiguchi, Y., Inoue, N., Masuda, M., Kashimoto, T., Katahira, J., Sugimoto, N., and Matsuda, M. (1997) *Bordetella bronchiseptica* dermonecrotizing toxin induces reorganization of actin stress fibers through deamidation of Gln-63 of the GTP-binding protein Rho. *Proc Natl Acad Sci U S A* **94**: 11623-11626.

Horiguchi, Y. (2001) *Escherichia coli* cytotoxic necrotizing factors and *Bordetella* dermonecrotic toxin: the dermonecrosis-inducing toxins activating Rho small GTPases. *Toxicon* **39**: 1619-1627.

Horton, R.M. (1993) In Vitro Recombination and Mutagenesis of DNA: SOEing Together Tailor-Made Genes. In *PCR Protocols: Current Methods and Applications*. Vol. 15. White, B.A. (ed). Totowa, NJ: Humana Press, pp. 251-261.

Houdouin, V., Bonacorsi, S., Brahimi, N., Clermont, O., Nassif, X., and Bingen, E. (2002) A uropathogenicity island contributes to the pathogenicity of *Escherichia coli* strains that cause neonatal meningitis. *Infect Immun* **70**: 5865-5869.

Hundt, C., Peyrin, J.M., Haik, S., Gauczynski, S., Leucht, C., Rieger, R., Riley, M.L., Deslys, J.P., Dormont, D., Lasmezas, C.I., and Weiss, S. (2001) Identification of

interaction domains of the prion protein with its 37-kDa/67-kDa laminin receptor. *Embo J* **20**: 5876-5886.

Jaseja, M., Mergen, L., Gillette, K., Forbes, K., Sehgal, I., and Copie, V. (2005) Structure-function studies of the functional and binding epitope of the human 37 kDa laminin receptor precursor protein. *J Pept Res* **66**: 9-18.

Kaashoek, J.G., Mout, R., Falkenburg, J.H., Willemze, R., Fibbe, W.E., and Landegent, J.E. (1991) Cytokine production by the bladder carcinoma cell line 5637: rapid analysis of mRNA expression levels using a cDNA-PCR procedure. *Lymphokine Cytokine Res* **10**: 231-235.

Kashimoto, T., Katahira, J., Cornejo, W.R., Masuda, M., Fukuoh, A., Matsuzawa, T., Ohnishi, T., and Horiguchi, Y. (1999) Identification of functional domains of *Bordetella* dermonecrotizing toxin. *Infect Immun* **67**: 3727-3732.

Khan, N.A., Wang, Y., Kim, K.J., Chung, J.W., Wass, C.A., and Kim, K.S. (2002) Cytotoxic necrotizing factor-1 contributes to *Escherichia coli* K1 invasion of the central nervous system. *J Biol Chem* **277**: 15607-15612.

Kim, K.J., Chung, J.W., and Kim, K.S. (2005) 67-kDa laminin receptor promotes internalization of cytotoxic necrotizing factor 1-expressing *Escherichia coli* K1 into human brain microvascular endothelial cells. *J Biol Chem* **280**: 1360-1368.

Kleman, J.P., Aeschlimann, D., Paulsson, M., and van der Rest, M. (1995) Transglutaminase-catalyzed cross-linking of fibrils of collagen V/XI in A204 rhabdomyosarcoma cells. *Biochemistry* **34**: 13768-13775.

Kouokam, J.C., Wai, S.N., Fallman, M., Dobrindt, U., Hacker, J., and Uhlin, B.E. (2006) Active Cytotoxic Necrotizing Factor 1 Associated with Outer Membrane Vesicles from Uropathogenic *Escherichia coli*. *Infect Immun* **74**: 2022-2030.

Kucheria, R., Dasgupta, P., Sacks, S.H., Khan, M.S., and Sheerin, N.S. (2005) Urinary tract infections: new insights into a common problem. *Postgrad Med J* **81**: 83-86.

Landowski, T.H., Dratz, E.A., and Starkey, J.R. (1995) Studies of the structure of the metastasis-associated 67 kDa laminin binding protein: fatty acid acylation and evidence supporting dimerization of the 32 kDa gene product to form the mature protein. *Biochemistry* **34**: 11276-11287.

Landraud, L., Gauthier, M., Fosse, T., and Boquet, P. (2000) Frequency of *Escherichia coli* strains producing the cytotoxic necrotizing factor (CNF1) in nosocomial urinary tract infections. *Lett Appl Microbiol* **30**: 213-216.

Landraud, L., Gibert, M., Popoff, M.R., Boquet, P., and Gauthier, M. (2003) Expression of cnf1 by *Escherichia coli* J96 involves a large upstream DNA region including the hlyCABD operon, and is regulated by the RfaH protein. *Mol Microbiol* **47**: 1653-1667.

Lax, A.J., Chanter, N., Pullinger, G.D., Higgins, T., Staddon, J.M., and Rozengurt, E. (1990) Sequence analysis of the potent mitogenic toxin of *Pasteurella multocida*. *FEBS Lett* **277**: 59-64.

Lemichez, E., Flatau, G., Bruzzone, M., Boquet, P., and Gauthier, M. (1997) Molecular localization of the *Escherichia coli* cytotoxic necrotizing factor CNF1 cell-binding and catalytic domains. *Mol Microbiol* **24**: 1061-1070.

Lerm, M., Schmidt, G., Goehring, U.M., Schirmer, J., and Aktories, K. (1999a) Identification of the region of rho involved in substrate recognition by *Escherichia coli* cytotoxic necrotizing factor 1 (CNF1). *J Biol Chem* **274**: 28999-29004.

Lerm, M., Selzer, J., Hoffmeyer, A., Rapp, U.R., Aktories, K., and Schmidt, G. (1999b) Deamidation of Cdc42 and Rac by *Escherichia coli* cytotoxic necrotizing factor 1: activation of c-Jun N-terminal kinase in HeLa cells. *Infect Immun* **67**: 496-503.

Lerm, M., Pop, M., Fritz, G., Aktories, K., and Schmidt, G. (2002) Proteasomal degradation of cytotoxic necrotizing factor 1-activated rac. *Infect Immun* **70**: 4053-4058.

Lockman, H.A., Gillespie, R.A., Baker, B.D., and Shakhnovich, E. (2002) *Yersinia pseudotuberculosis* produces a cytotoxic necrotizing factor. *Infect Immun* **70**: 2708-2714.

Ludwig, G.V., Kondig, J.P., and Smith, J.F. (1996) A putative receptor for Venezuelan equine encephalitis virus from mosquito cells. *J Virol* **70**: 5592-5599.

Madaule, P., Eda, M., Watanabe, N., Fujisawa, K., Matsuoka, T., Bito, H., Ishizaki, T., and Narumiya, S. (1998) Role of citron kinase as a target of the small GTPase Rho in cytokinesis. *Nature* **394**: 491-494.

Marrs, C.F., Zhang, L., and Foxman, B. (2005) *Escherichia coli* mediated urinary tract infections: are there distinct uropathogenic *E. coli* (UPEC) pathotypes? *FEMS Microbiol Lett* **252**: 183-190.

Martz, E. (2002) Protein Explorer: easy yet powerful macromolecular visualization. *Trends Biochem Sci* **27**: 107-109.

Masuda, M., Betancourt, L., Matsuzawa, T., Kashimoto, T., Takao, T., Shimonishi, Y., and Horiguchi, Y. (2000) Activation of rho through a cross-link with polyamines catalyzed by *Bordetella* dermonecrotizing toxin. *Embo J* **19**: 521-530.

Masuda, M., Minami, M., Shime, H., Matsuzawa, T., and Horiguchi, Y. (2002) In vivo modifications of small GTPase Rac and Cdc42 by *Bordetella* dermonecrotic toxin. *Infect Immun* **70**: 998-1001.

Matsuzawa, T., Kashimoto, T., Katahira, J., and Horiguchi, Y. (2002) Identification of a receptor-binding domain of *Bordetella* dermonecrotic toxin. *Infect Immun* **70**: 3427-3432.

McNichol, B.A., Rasmussen, S.B., Meysick, K.C., and O'Brien, A.D. (2006) A single amino acid substitution in the enzymatic domain of cytotoxic necrotizing factor type 1 of *Escherichia coli* alters the tissue culture phenotype to that of the dermonecrotic toxin of *Bordetella spp*. *Mol Microbiol* **60**: 939-950.

Mecham, R.P. (1991) Receptors for laminin on mammalian cells. *Faseb J* **5**: 2538-2546.

Menard, S., Tagliabue, E., and Colnaghi, M.I. (1998) The 67 kDa laminin receptor as a prognostic factor in human cancer. *Breast Cancer Res Treat* **52**: 137-145.

Meysick, K.C., Mills, M., and O'Brien, A.D. (2001) Epitope mapping of monoclonal antibodies capable of neutralizing cytotoxic necrotizing factor type 1 of uropathogenic *Escherichia coli*. *Infect Immun* **69**: 2066-2074.

Mills, M., Meysick, K.C., and O'Brien, A.D. (2000) Cytotoxic necrotizing factor type 1 of uropathogenic *Escherichia coli* kills cultured human uroepithelial 5637 cells by an apoptotic mechanism. *Infect Immun* **68**: 5869-5880.

Mitsumori, K., Terai, A., Yamamoto, S., Ishitoya, S., and Yoshida, O. (1999) Virulence characteristics of *Escherichia coli* in acute bacterial prostatitis. *J Infect Dis* **180**: 1378-1381.

Mobley, H.L.T. (2000) Virulence of the two primary uropathogens. In *ASM News*. Vol. 66, pp. 403-410.

Nicolle, L.E. (2001) Epidemiology of Urinary Tract Infection. *Infect Med* **18**: 153-162.

Nicolle, L.E. (2002) Epidemiology of urinary tract infection. In *Clinical Microbiology Newsletter*. Vol. 24, pp. 135-141.

O'Hanley, P., Lalonde, G., and Ji, G. (1991) Alpha-hemolysin contributes to the pathogenicity of piliated digalactoside-binding *Escherichia coli* in the kidney: efficacy of an alpha-hemolysin vaccine in preventing renal injury in the BALB/c mouse model of pyelonephritis. *Infect Immun* **59**: 1153-1161.

Oelschlaeger, T.A., Dobrindt, U., and Hacker, J. (2002) Virulence factors of uropathogens. *Curr Opin Urol* **12**: 33-38.

Orenstein, R., and Wong, E.S. (1999) Urinary tract infections in adults. *Am Fam Physician* **59**: 1225-1234, 1237.

Oswald, E., and De Rycke, J. (1990) A single protein of 110 kDa is associated with the multinucleating and necrotizing activity coded by the Vir plasmid of *Escherichia coli*. *FEMS Microbiol Lett* **56**: 279-284.

Oswald, E., Sugai, M., Labigne, A., Wu, H.C., Fiorentini, C., Boquet, P., and O'Brien, A.D. (1994) Cytotoxic necrotizing factor type 2 produced by virulent Escherichia coli modifies the small GTP-binding proteins Rho involved in assembly of actin stress fibers. *Proc Natl Acad Sci U S A* **91**: 3814-3818.

Oswald, E., Nougayrede, J.P., Taieb, F., and Sugai, M. (2005) Bacterial toxins that modulate host cell-cycle progression. *Curr Opin Microbiol* **8**: 83-91.

Pei, S., Doye, A., and Boquet, P. (2001) Mutation of specific acidic residues of the CNF1 T domain into lysine alters cell membrane translocation of the toxin. *Mol Microbiol* **41**: 1237-1247.

Pullinger, G.D., Adams, T.E., Mullan, P.B., Garrod, T.I., and Lax, A.J. (1996) Cloning, expression, and molecular characterization of the dermonecrotic toxin gene of *Bordetella spp*. *Infect Immun* **64**: 4163-4171.

Pullinger, G.D., Sowdhamini, R., and Lax, A.J. (2001) Localization of functional domains of the mitogenic toxin of *Pasteurella multocida*. *Infect Immun* **69**: 7839-7850.

Rao, C.N., Castronovo, V., Schmitt, M.C., Wewer, U.M., Claysmith, A.P., Liotta, L.A., and Sobel, M.E. (1989) Evidence for a precursor of the high-affinity metastasis-associated murine laminin receptor. *Biochemistry* **28**: 7476-7486.

Ridley, A.J. (2001a) Rho family proteins: coordinating cell responses. *Trends Cell Biol* **11**: 471-477.

Ridley, A.J. (2001b) Rho GTPases and cell migration. *J Cell Sci* **114**: 2713-2722.

Rieger, R., Lasmezas, C.I., and Weiss, S. (1999) Role of the 37 kDa laminin receptor precursor in the life cycle of prions. *Transfus Clin Biol* **6**: 7-16.

Rippere-Lampe, K.E., Lang, M., Ceri, H., Olson, M., Lockman, H.A., and O'Brien, A.D. (2001a) Cytotoxic necrotizing factor type 1-positive *Escherichia coli* causes increased inflammation and tissue damage to the prostate in a rat prostatitis model. *Infect Immun* **69**: 6515-6519.

Rippere-Lampe, K.E., O'Brien, A.D., Conran, R., and Lockman, H.A. (2001b) Mutation of the gene encoding cytotoxic necrotizing factor type 1 (*cnf1*) attenuates the virulence of uropathogenic *Escherichia coli*. *Infect Immun* **69**: 3954-3964.

Rozengurt, E., Higgins, T., Chanter, N., Lax, A.J., and Staddon, J.M. (1990) *Pasteurella multocida* toxin: potent mitogen for cultured fibroblasts. *Proc Natl Acad Sci U S A* **87**: 123-127.

Russo, T.A., and Johnson, J.R. (2003) Medical and economic impact of extraintestinal infections due to *Escherichia coli*: focus on an increasingly important endemic problem. *Microbes Infect* **5**: 449-456.

Sandvig, K., Spilsberg, B., Lauvrak, S.U., Torgersen, M.L., Iversen, T.G., and van Deurs, B. (2004) Pathways followed by protein toxins into cells. *Int J Med Microbiol* **293**: 483-490.

Schilling, J.D., Mulvey, M.A., and Hultgren, S.J. (2001) Dynamic interactions between host and pathogen during acute urinary tract infections. *Urology* **57**: 56-61.

Schmidt, G., Sehr, P., Wilm, M., Selzer, J., Mann, M., and Aktories, K. (1997) Gln 63 of Rho is deamidated by *Escherichia coli* cytotoxic necrotizing factor-1. *Nature* **387**: 725-729.

Schmidt, G., Selzer, J., Lerm, M., and Aktories, K. (1998) The Rho-deamidating cytotoxic necrotizing factor 1 from *Escherichia coli* possesses transglutaminase activity. Cysteine 866 and histidine 881 are essential for enzyme activity. *J Biol Chem* **273**: 13669-13674.

Schmidt, G., Goehring, U.M., Schirmer, J., Lerm, M., and Aktories, K. (1999) Identification of the C-terminal part of *Bordetella* dermonecrotic toxin as a transglutaminase for rho GTPases. *J Biol Chem* **274**: 31875-31881.

Schmidt, G., Goehring, U.M., Schirmer, J., Uttenweiler-Joseph, S., Wilm, M., Lohmann, M., Giese, A., Schmalzing, G., and Aktories, K. (2001) Lysine and polyamines are substrates for transglutamination of Rho by the *Bordetella* dermonecrotic toxin. *Infect Immun* **69**: 7663-7670.

Self, A.J., and Hall, A. (1995) Purification of recombinant Rho/Rac/G25K from Escherichia coli. *Methods Enzymol* **256**: 3-10.

Shime, H., Ohnishi, T., Nagao, K., Oka, K., Takao, T., and Horiguchi, Y. (2002) Association of *Pasteurella multocida* toxin with vimentin. *Infect Immun* **70**: 6460-6463.

Smith, H.W. (1974) A search for transmissible pathogenic characters in invasive strains of *Escherichia coli*: the discovery of a plasmid-controlled toxin and a plasmid-controlled lethal character closely associated, or identical, with colicine V. *J Gen Microbiol* **83**: 95-111.

Smith, M.J., Carvalho, H.M., Melton-Celsa, A.R., and O'Brien A, D. (2006) The 13C4 Monoclonal Antibody That Neutralizes Shiga Toxin Type 1 (Stx1) Recognizes Three Regions on the Stx1 B Subunit and Prevents Stx1 from Binding to Its Eukaryotic Receptor Globotriaosylceramide. *Infect Immun* **74**: 6992-6998.

Sorokin, A.V., Mikhailov, A.M., Kachko, A.V., Protopopova, E.V., Konovalova, S.N., Andrianova, M.E., Netesov, S.V., Kornev, A.N., and Loktev, V.B. (2000) Human

recombinant laminin-binding protein: isolation, purification, and crystallization. *Biochemistry (Mosc)* **65**: 546-553.

Sugai, M., Hatazaki, K., Mogami, A., Ohta, H., Peres, S.Y., Herault, F., Horiguchi, Y., Masuda, M., Ueno, Y., Komatsuzawa, H., Suginaka, H., and Oswald, E. (1999) Cytotoxic necrotizing factor type 2 produced by pathogenic *Escherichia coli* deamidates a gln residue in the conserved G-3 domain of the rho family and preferentially inhibits the GTPase activity of RhoA and rac1. *Infect Immun* **67**: 6550-6557.

Swenson, D.L., Bukanov, N.O., Berg, D.E., and Welch, R.A. (1996) Two pathogenicity islands in uropathogenic *Escherichia coli* J96: cosmid cloning and sample sequencing. *Infect Immun* **64**: 3736-3743.

Takai, Y., Sasaki, T., and Matozaki, T. (2001) Small GTP-binding proteins. *Physiol Rev* **81**: 153-208.

Teel, L.D., Melton-Celsa, A.R., Schmitt, C.K., and O'Brien, A.D. (2002) One of two copies of the gene for the activatable shiga toxin type 2d in *Escherichia coli* O91:H21 strain B2F1 is associated with an inducible bacteriophage. *Infect Immun* **70**: 4282-4291.

U.S. Department of Health and Human Services, N.I.o.D.a.D.a.K.D., National Institutes of Health (2003) Urinary tract infections in adults. Bethesda, MD.

U.S. Department of Health and Human Services, N.I.o.D.a.D.a.K.D., National Institutes of Health (2004) Kidney and urologic diseases statistics for the United States. Bethesda, MD.

Vojtek, A.B., and Cooper, J.A. (1995) Rho family members: activators of MAP kinase cascades. *Cell* **82**: 527-529.

Walker, K.E., and Weiss, A.A. (1994) Characterization of the dermonecrotic toxin in members of the genus *Bordetella*. *Infect Immun* **62**: 3817-3828.

Wandersman, C., and Delepelaire, P. (1990) TolC, an *Escherichia coli* outer membrane protein required for hemolysin secretion. *Proc Natl Acad Sci U S A* **87**: 4776-4780.

Wang, K.S., Kuhn, R.J., Strauss, E.G., Ou, S., and Strauss, J.H. (1992) High-affinity laminin receptor is a receptor for Sindbis virus in mammalian cells. *J Virol* **66**: 4992-5001.

Ward, P.N., Miles, A.J., Sumner, I.G., Thomas, L.H., and Lax, A.J. (1998) Activity of the mitogenic *Pasteurella multocida* toxin requires an essential C-terminal residue. *Infect Immun* **66**: 5636-5642.

Warren, J.W. (1996) Clinical presentations and epidemiology of urinary tract infections. In *Urinary Tract Infections: Molecular Pathogenesis and Clinical Management*. Mobley, H.L.T. and Warren, J.W. (eds). Washington, D.C.: American Society of Microbiology Press, pp. 3-27.

Weiss, A.A., and Goodwin, M.S. (1989) Lethal infection by *Bordetella pertussis* mutants in the infant mouse model. *Infect Immun* **57**: 3757-3764.

Welch, R.A., Burland, V., Plunkett, G., 3rd, Redford, P., Roesch, P., Rasko, D., Buckles, E.L., Liou, S.R., Boutin, A., Hackett, J., Stroud, D., Mayhew, G.F., Rose, D.J., Zhou, S., Schwartz, D.C., Perna, N.T., Mobley, H.L., Donnenberg, M.S., and Blattner, F.R. (2002) Extensive mosaic structure revealed by the complete

genome sequence of uropathogenic *Escherichia coli*. *Proc Natl Acad Sci U S A* **99**: 17020-17024.

Wilhelm, B., Meinhardt, A., and Seitz, J. (1996) Transglutaminases: purification and activity assays. *J Chromatogr B Biomed Appl* **684**: 163-177.

Wilson, B.A., Ponferrada, V.G., Vallance, J.E., and Ho, M. (1999) Localization of the intracellular activity domain of *Pasteurella multocida* toxin to the N terminus. *Infect Immun* **67**: 80-87.

Yamamoto, S., Tsukamoto, T., Terai, A., Kurazono, H., Takeda, Y., and Yoshida, O. (1995) Distribution of virulence factors in *Escherichia coli* isolated from urine of cystitis patients. *Microbiol Immunol* **39**: 401-404.

Zhang, L., and Foxman, B. (2003) Molecular epidemiology of *Escherichia coli* mediated urinary tract infections. *Front Biosci* **8**: e235-244.